UNIVERSITY OF CALIFORNIA, SAN DIEGO

Calcium Isotopic Variation in Marine Evaporites and Carbonates: Applications to Late Miocene Mediterranean Brine Chemistry and Late Cenozoic Calcium Cycling in the Oceans

A dissertation submitted in partial satisfaction of the requirements for the degree

Doctor of Philosophy

in Earth Sciences

by

Tabitha Michele Hensley

Committee in Charge:

J. Douglas Macdougall, Chair
Chris Charles
Miriam Kastner
Kurt Marti
Jeff Severinghaus

2006

The dissertation of Tabitha Michele Hensley is approved, and it is acceptable in quality and form for publication on microfilm:

_____

_____

_____

_____

_____
Chair

University of California, San Diego

2006

To my parents, Eddy and Brenda Hensley

TABLE OF CONTENTS

LIST OF FIGURES

LIST OF TABLES

ACKNOWLEDGEMENTS

I would first like to thank my advisor, J. Douglas Macdougall. He accepted me as a graduate student in my first year at SIO even though he had not planned to do so and allowed me to work on what would be his last research project at UCSD. Doug has allowed me to actively pursue other academic interests, specifically various teaching projects associated with the university, as I found that I greatly enjoyed the teaching aspects of being a graduate student. He has allowed me the freedom to pursue any research ideas that I wanted to explore and has always been willing to talk with me about research problems and pitfalls. Doug retired in 2005 and moved to Scotland to pursue his other career passion, writing, and even though he was overseas for long portions of my time as a graduate student, he has always been available to help me with all aspects of my research.

I would also like to thank my committee members, Chris Charles, Miriam Kastner, Kurt Marti, and Jeff Severinghaus. I have benefited from their knowledge, suggestions, and encouragement throughout my time at SIO. Specifically, I would like to thank Miriam Kastner for her willingness to take me along on four different cruises even though I had no research projects on board. By including me in these oceanographic experiences, she helped to broaden my earth science background and taught me how to be a tireless scientist by example. Thanks also to Chris MacIsaac, who provided limitless support and instruction in the lab, without which I would never have been able to complete my research on time. Special thanks to the Ocean Drilling Program for providing samples for data contained in Chapter III and IV.

Many friends have supported me throughout this long and unique process. I have greatly benefited from discussions with fellow graduate students Evan Solomon, Wei Wei, Jenna Munson, and Melissa Headley, Brian Hopkinson and Henry Ruhl regarding various aspects of my dissertation. Thanks to Christine Whitcraft who has been an unfailing friend and lent a sympathetic ear throughout our time at Scripps. Sondra Bilben, one of my best friends in San Diego and favorite bartender, has been a true friend and in every case has always looked after me as I wondered through tough times. Dominic Moreau has taught me the importance of unity and unconditional love.

Lastly, I would like to thank my parents, Eddy and Brenda Hensley, who have never failed to answer the phone, listen to my insecurities and triumphs, and love me without judgment as only parents can.

VITA

1979	Born, Atlanta Georgia, USA
2000	B.S. Geology, University and Departmental Honors University of New Orleans
2001-2006	Graduate Student Researcher Scripps Institution of Oceanography University of California, San Diego
2002, 2003, 2004	Teaching Assistant, Department of Earth Sciences University of California, San Diego
2005	Instructor of Record, Department of Earth Sciences University of California, San Diego
2006	Ph.D. University of California, San Diego

Publications

Luckow, H., Pavlis, T., Serpa, L., Guest, B., Wagner, D., Snee, L., Hensley, T., Korjenkov, A. 2005. Late Cenozoic sedimentation and volcanism during transtensional deformation in Wingate Wash and the Owlshead Mountains, Death Valley. Earth Science Reviews 73 pp. 177-219

Hensley, T.M. and Macdougall, J.D. 2003. Calcium isotope fractionation in Ca-bearing phases of marine evaporites. In American Geophysical Union Fall 2003 meeting abstracts

Hensley, T.M., Webber, K.L., Falster. A.U., Simmons, W.B. 2002. Biotite trace element chemistry in the anorogenic Wausau Syenite Complex, Wisconsin. Rocks and Minerals 77 (3) pp.173

Hensley, T.M. 2000. Regional geochemical variation of the Central American Volcanic Arc: tectonic parameters affecting magma chemistry. Abstracts with Programs Geological Society of America 32 (7) pp.271

FIELDS OF STUDY

Major Field: Geochemistry

Studies in Isotope Geology
Professors J. Douglas Macdougall, Devendra Lal, Pat Castillo and David Hilton

Studies in Marine Chemistry
Professors Lihini Aluwihare and Kathy Barbeau

Studies in Paleoceanography
Professors Chris Charles, Miriam Kastner, Jeff Severinghaus, and Dick Norris

Studies in Marine Geology
Professors Neal Driscoll, James Hawkins, Peter Lonsdale, and Steve Cande

Studies in Marine Geophysics
Professors LeRoy Dorman and John Hildebrand

Studies in Physical Oceanography
Professors Myrl Hendershott and Paul Robbins

ABSTRACT OF THE DISSERTATION

Calcium Isotopic Variation in Marine Evaporites and Carbonates: Applications to Late Miocene Mediterranean Brine Chemistry and Late Cenozoic Calcium Cycling in the Oceans

by

Tabitha Michele Hensley

Doctor of Philosophy in Earth Sciences

University of California, San Diego, 2006

Professor J. Douglas Macdougall, Chair

This dissertation uses calcium isotopes to examine two major geochemical processes: sequestration of Ca in the late Miocene Mediterranean evaporites and Ca cycling in the late Cenozoic oceans. Each chapter focuses on a different part of this work. Chapter I contains information regarding calcium isotope systematics and analytical methods, reproducibility of standard data, double spiking theory, and methods for sample extraction and loading of Ca.

Chapter II explores the idea of large evaporite deposits (Saline Giants) as potential sinks for Ca in the oceans. These may record significant isotopic fractionation effects, which could expand the limited range of Ca isotopes on Earth. No past Ca isotope studies have addressed the range of isotopic variation in Ca-

bearing phases of marine, hydrothermal, or continental evaporites. Ca isotope data was obtained for various gypsum and anhydrite samples and an experiment was performed to determine the fractionation factor of inorganically precipitated anhydrite.

In Chapter III, evaporites from ODP Site 654 in the Tyrrhenian Basin were analyzed for Ca and Sr isotopes. This saline giant did not sequester enough Ca to affect global calcium cycling in the late Miocene, and the average isotopic composition overlaps with the average carbonate value. Ca data exhibit a total range of 1.43 per mil, and little correlation between the Ca and Sr isotope systems is apparent. Several samples show significant disagreement, suggesting that Ca isotopes in evaporite deposits may be overprinted by a reservoir effect at times of rapid deposition, whereas Sr isotopes record true brine composition.

Calcium isotopes could shed light on the balance between continental weathering and carbonate sedimentation, and few high resolution records of seawater Ca isotopic variation exist for the late Neogene. Chapter IV reports Ca isotope data for bulk carbonates from ODP Site 850 for the past 12 Ma. Additionally, Ca concentrations were calculated from the isotopic data. The data show no consistent trend towards increasing or decreasing $\delta^{44}Ca$ for the past 12 Ma, in contrast to other isotope systems such as Os and Sr. Short term fluctuations on the order of 1-2 Ma occur, but these excursions are not uniquely correlated to known paleoceanographic events.

Chapter I Introduction and Ca Isotope Background

1.1 Calcium Isotope Systematics

Calcium is the fifth most abundant element in the earth's crust (3.6%) and is a major component in sedimentary rocks. It is comprised of 6 stable isotopes: masses 40, 42, 43, 44, 46, and 48 with the two most abundant isotopes being masses 40 and 44. Russell et al. (1978) gives the abundances in both ratios and in terms of percentage of total calcium as 96.98% ^{40}Ca, 0.642% ^{42}Ca, 0.133% ^{43}Ca, 2.056% ^{44}Ca, 0.003% ^{46}Ca, and 0.182% ^{48}Ca (^{40}Ca/^{44}Ca = 47.153 ± 3 can vary due to radiogenic ^{40}Ca, ^{42}Ca/^{44}Ca = 0.31221 ± 2, ^{43}Ca/^{44}Ca = 0.06486 ± 1, ^{46}Ca/^{44}Ca = 0.001518 ± 2, ^{48}Ca/^{44}Ca = 0.088727 ± 9, ^{44}Ca/^{40}Ca = 0.0212076 ± 13). Its ubiquity in geochemical processes and isotopic variability in nature has the potential to shed light on a variety of geochemical problems.

The calcium isotopic composition of a sample depends on several factors both organic and inorganic. The lightest isotope, ^{40}Ca, is produced abundantly during nucleosynthesis; however, ^{40}Ca is also the primary radiogenic daughter product of ^{40}K β- decay. Therefore old rocks and minerals (the half-life of ^{40}K is 1.25 billion years, Steiger and Jaeger 1977) with very high K/Ca will have considerable accumulations of ^{40}Ca. Using the average age of crustal rocks on Earth as 2 Ga, a typical upper crustal K/Ca = 0.9, and a typical bulk continental crust K/Ca = 0.35, DePaolo (2004) calculated enrichment of ^{40}Ca due to radiogenic decay as $\varepsilon_{Ca} = 0.8$ for average continental crust and $\varepsilon_{Ca} = 2.0$ for upper continental rocks where ε_{Ca} is

$$10000 * \{ (^{40}Ca/^{42}Ca)_{sample} / (^{40}Ca/^{42}Ca)_{std}) - 1\}$$

For most samples, enrichments in ^{40}Ca due to radiogenic decay of ^{40}K will be minimal and probably limited to less than the range of current analytical uncertainty of 0.1 to 0.2 per mil (DePaolo 2004). Because of the wide mass range of calcium isotopes (8 mass units, representing a 20% mass difference), there is potential for significant mass-dependent fractionation effects in terrestrial materials (Hirt and Epstein 1964, Stahl and Wendt 1968, Russell et al. 1978). The currently known range of calcium isotope fractionation in nature is around 4-5 per mil, mostly accounted for by biologic processes. Studies into the behavior of calcium isotopes have ranged from rock dating techniques to foraminifera paleothermometry, as both radiogenic and mass-dependent fractionation effects are found in natural samples (DePaolo 2004).

Initial research on the thermodynamic behavior of calcium isotopes during mass-dependant fractionation identified only a kinetic fractionation effect due to diffusion and chemical exchange reactions (O'Neil et al. 1969, Gussone et al. 2003). Calcium isotope kinetic fractionation during temperature dependent processes causes enrichments of the heavy isotope (^{44}Ca) in a precipitate as temperature increases. This is the opposite of the equilibrium fractionation controlled oxygen isotope system, where the light isotope (^{16}O) is preferentially incorporated at warmer temperatures. There is a lack of studies considering equilibrium fractionation effects for calcium isotopes, but there is the possibility that both kinetic and equilibrium fractionation occurs during calcification as asserted by Lemarchand et al. (2004).

1.2 Calcium Isotope Notation and Common Standards

Calcium isotopic variations are usually reported using the familiar delta notation, as used in other stable isotope systems such as C, O, N, and S. Most commonly data are reported for the $^{44}Ca/^{40}Ca$ isotope pair. $\delta^{44}Ca$ is defined as:

$$[(^{44}Ca/^{40}Ca)_{sample} / (^{44}Ca/^{40}Ca)_{standard} - 1] * 1000$$

The standards used for reference vary by study. Modern seawater (Zhu and Macdougall 1998a, Schmitt et al. 2003a), Ultrapure $CaCO_3$ (Skulan et al. 1997), National Institute of Standards (NIST) carbonate reference standard SRM 915a (Schmitt et al 2003b), CaF_2 standard solutions and CaF_2 natural samples (Russell et al. 1978, Heuser et al.2002) have all been used in published papers. At this point, laboratories use one of these standards, but there is no common standard for ease of inter-laboratory comparison.

All samples in this study will be compared relative to modern seawater as a standard. Because seawater is well mixed with respect to the long residence time of calcium in the oceans (approx. 1 million years), the calcium isotopic composition of modern seawater is the same in all regions of the ocean (Zhu and Macdougall 1998a). The two main sources of calcium to seawater are dissolved riverine Ca and hydrothermal fluids enriched in Ca from the alteration of Mid-Ocean Ridge Basalt during new crust formation. Seawater is made isotopically heavy relative to carbonates because of biological fractionation during calcification. Organisms discriminate against the heavy isotope and preferentially incorporate the light isotope into their shells, thus causing the remaining pool of calcium in the oceans to become

enriched in the heavy isotope. Most materials measured in this study are enriched in the light isotope relative to seawater and therefore have negative $\delta^{44}Ca$ values.

During the course of this study two different spiking methods were used for determination of Ca isotopic compositions. Different spiking methods are discussed in more detail in following sections. The first method employed a ^{42}Ca-^{48}Ca double spike, the second a ^{42}Ca-^{43}Ca double spike. 'Absolute' isotopic compositions measured for standards using these two spikes differ slightly, most likely because of uncertainties in the spike composition that propagate through the iterative procedure used to calculate sample isotopic compositions. These differences have no effect on the data reported using the delta notation as long as reference and sample values used were determined using the same double spike.

Our laboratory seawater reference value used in calculation of $\delta^{44}Ca$ values for the 42-48 double spiking method is 0.0217434 ± 13; this defines the $\delta^{44}Ca$ value of seawater as zero per mil. This value was determined by 10 measurements on 5 different seawater samples located in the Atlantic, Pacific, and Indian Ocean's (Zhu 1999). Table 1.2.1a and Figure 1.2.1 contain the data for 19 runs, analyzed over a period of 2 years, of a North Atlantic seawater to demonstrate that the reproducibility of results using the 42-48 double spike is $\pm$ 0.20 per mil. The $^{44}Ca/^{40}Ca$ seawater reference value for the 42-43 spiking method is 0.0217227 and was obtained by 14 measurements of the same North Atlantic seawater over a period of one year. Reproducibility is $\pm$ 0.09 per mil. The NIST SRM915a standard was also measured 12 times with reproducibility of $\pm$ 0.08 per mil. Data for these runs are in Tables

Table 1.2.1a Calcium isotopic composition of North Atlantic seawater using the 42-48 double spike.

Run Number	$^{44}Ca/^{40}Ca$	$\delta^{44}Ca$ (per mil)
1	0.0217446	0.06
2	0.0217473	0.18
3	0.0217436	0.01
4	0.0217369	-0.30
5	0.0217427	-0.03
6	0.0217438	0.02
7	0.0217484	0.23
8	0.0217492	0.27
9	0.0217428	-0.03
10	0.0217483	0.22
11	0.0217404	-0.14
12	0.0217412	-0.10
13	0.0217491	0.26
14	0.0217438	0.02
15	0.0217483	0.22
16	0.0217454	0.09
17	0.0217360	-0.34
18	0.0217354	-0.37
19	0.0217419	-0.07
MEAN	0.0217436	0.01 ± 0.20

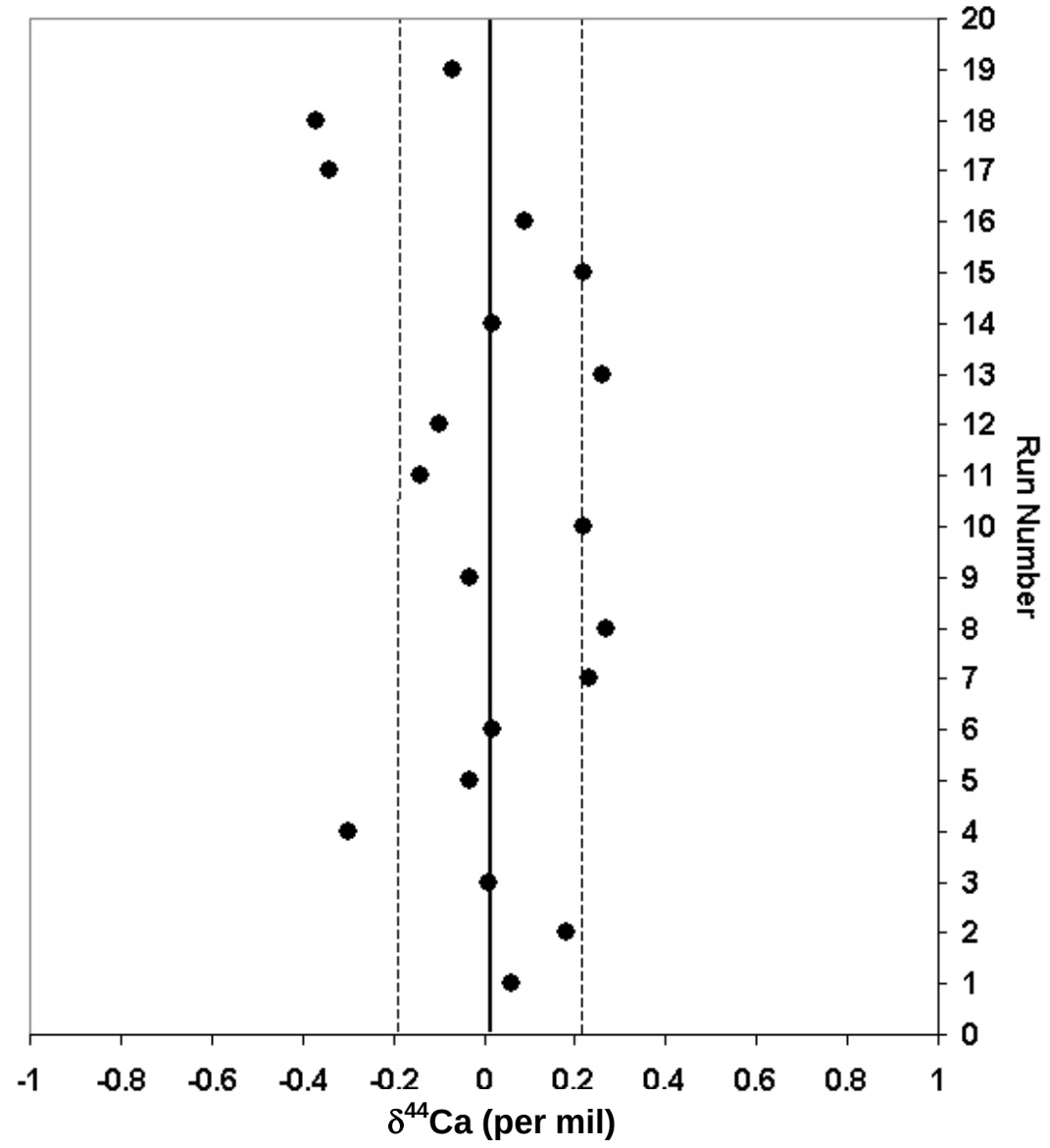

Figure 1.2.1a δ^{44}Ca vs. run number for a North Atlantic seawater using the 42-48 double spike. The mean of 19 runs is 0.01 ± 0.20 per mil ($2\sigma_m$).

Table 1.2.1b Calcium isotopic composition for a North Atlantic seawater using the 42-43 double spike

Run Number	$^{44}Ca/^{40}Ca$	$\delta^{44}Ca$ (per mil
1	0.0217223	-0.02
2	0.0217244	0.08
3	0.0217212	-0.07
4	0.0217245	0.08
5	0.0217196	-0.14
6	0.0217242	0.07
7	0.0217227	0.00
8	0.0217240	0.06
9	0.0217235	0.04
10	0.0217255	0.13
11	0.0217234	0.03
12	0.0217228	0.00
13	0.0217186	-0.19
14	0.0217211	-0.08
MEAN	0.0217227	0.00 ± 0.09

Table 1.2.1c Calcium isotopic composition for the NIST SRM915a carbonate standard using the 42-43 double spike

Run Number	$^{44}Ca/^{40}Ca$	$\delta^{44}Ca$ (per mil)
1	0.0216804	-1.95
2	0.0216803	-1.95
3	0.0216822	-1.86
4	0.0216836	-1.80
5	0.0216804	-1.95
6	0.0216795	-1.99
7	0.0216798	-1.98
8	0.0216788	-2.02
9	0.0216771	-2.10
10	0.0216783	-2.04
11	0.0216816	-1.89
12	0.0216798	-1.98
MEAN	0.0216802	-1.96 ± 0.08

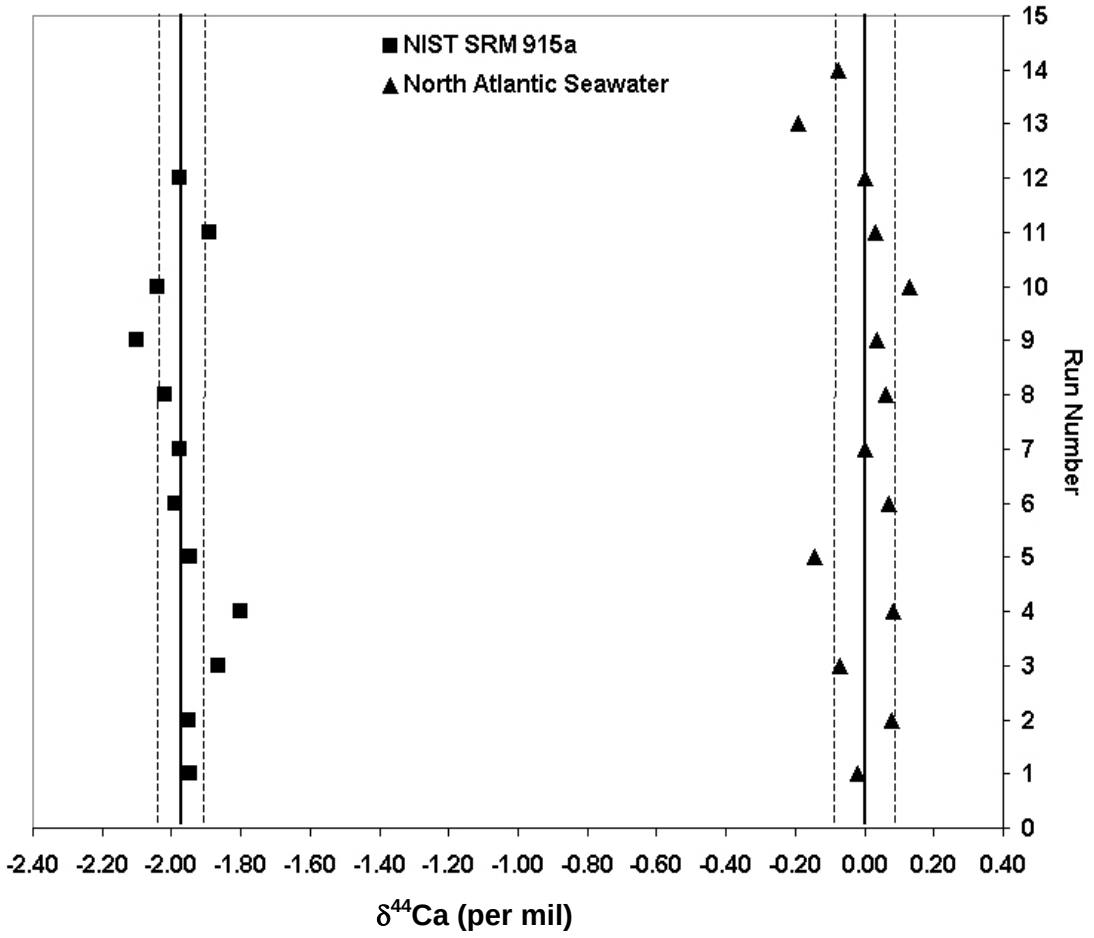

Figure 1.2.1b δ^{44}Ca vs. run number for the NIST SRM915a carbonate standard (12 runs) and North Atlantic seawater (14 runs) for the 42-43 double spike. The mean for the NIST standard is –1.96 ± 0.08 per mil ($2\sigma_m$) and the mean for the seawater is 0.00 ± 0.09 per mil ($2\sigma_m$).

1.2.1b and 1.2.1c and Figure 1.2.1. Because absolute $^{44}Ca/^{40}Ca$ ratios vary from lab to lab and with different measurement methods even within one lab, only the $\delta^{44}Ca$ difference between average values for different standards (for example seawater and the SRM 915a NIST standard) is important for inter-lab comparison and consistency. In order to compare calcium isotope values between labs, all $\delta^{44}Ca$ values from other studies will be compared to their stated $\delta^{44}Ca$ seawater value, as is done for sample values in this study.

1.3 Double Spiking and TIMS Measurement

Because of isotopic variability in nature there is no pair of Ca isotopes with a fixed ratio that can be used to correct for machine-induced fractionation, and samples undergoing calcium isotope analysis must be double spiked (Russell et al. 1978). The principals behind double spiking are well established (Compston and Oversby 1969, Eugster et al. 1969, Gale 1970, Russell 1971), and the method has been used for several heavier elements such as barium, lead, neodymium, and calcium. Throughout the course of a mass spectrometer analysis, fractionation between heavy and light isotopes occurs as the sample is ionized. Light isotopes ionize before heavy isotopes and thus machine-induced fractionation can obscure natural fractionation effects. This is particularly true for calcium isotopes, which have a large mass range over which machine-induced fractionation may occur.

A correction must be applied to the data in order to account for these effects. Russell et al. (1978) investigated the best approach to correct calcium isotope data for

fractionation and utilized an exponential law, which progressively applies smaller correction factors as the mass of the target isotope increases. For this study, the exponential correction scheme is applied and the true $^{44}Ca/^{40}Ca$ is found with an iterative method based on the procedure originally used by Compston and Oversby (1969) for lead isotopes. The correction method follows the same principles for both the ^{42}Ca-^{48}Ca and ^{42}Ca-^{43}Ca spikes. Further details are found in the 1999 Ph.D. dissertation by Zhu (Zhu 1999) and the paper by Gopalan et al. (2006).

Existing double spike mixtures (^{42}Ca-^{48}Ca and ^{42}Ca-^{43}Ca) prepared from precisely weighed, isotopically enriched calcium salts were used in this dissertation. The isotopic compositions of these spikes, important for the calculation of true sample isotopic compositions, were determined by a combination of direct measurements of spike-laboratory standard mixtures and gravimetry (Zhu 1999, Gopalan et al. 2006).

Spike-sample mixtures typically had 95% of ^{42}Ca and ^{48}Ca coming from the spike and 97% of ^{40}Ca and ^{44}Ca from the sample. For the 42-43 spike, a solution containing calcium precisely enriched in ^{43}Ca was added to the 42-48 stock solution producing a triply spiked mixture so that 90% of the ^{43}Ca was contributed by the spike (Gopalan et al. 2006). The spike was then calibrated against the calcium NIST SRM 915a (at NGRI, India) and La Jolla standards (SIO) for exact determination of the normalizing ratio $^{42}Ca/^{43}Ca$. The uncertainty in the $^{42}Ca/^{43}Ca$ ratio in the double-spike relative to standards is less than 0.2% (Gopalan et al. 2006). Uncertainty in the $^{42}Ca/^{48}Ca$ ratio is approximately ± 1%, however it is important to mention that all of these uncertainties affect the samples equally when they are measured using the same

double spike, therefore sample to sample differences are unaffected (Zhu and Macdougall 1998a).

Calcium isotopes were measured using a VG Sector 54 Thermal Ionization Mass Spectrometer (TIMS) at Scripps Institution of Oceanography. The procedure for running calcium samples on the TIMS is detailed in Zhu (1999) and below for the 42-48 double spike. Chapters II and III contain data that were obtained using the 42-48 double spike and measured using a single collector. Data in Chapter IV utilize a 42-43 spike and a multicollector procedure as described in Gopalan et al. (2006) and below.

The different spiking schemes have different measurement conditions and parameters. The older 42-48 spike and dynamic single collector analysis was extremely time consuming and less precise than the newer 42-43 spike and static multicollector analysis. These differences in speed and precision can be attributed to collecting data over a shortened mass range and simultaneously using several collectors. Since the target isotopes are ^{40}Ca and ^{44}Ca, it is only necessary to measure the isotopes from 40-44. If the middle isotopes 42 and 43 are used as spiking isotopes, fractionation corrections can still be applied, and optimally the corrections will be smaller and better approximate fractionation conditions between the two isotopes of interest because the average mass of the two spiking isotopes is only 0.5 mass units different than the targets isotopes average mass. The procedure uses four collectors, each always collecting the same isotope, which reduces uncertainties from fractionation drift and results in a quicker analysis time. For the 42-43 spike measurement procedure the ^{40}Ca current was maintained between 8 and 12 * 10^{-11} A

and was measured using the L4 collector with a 10^{10} Ohm resistor. All isotopes 40-44 were collected simultaneously with an integration time of 5s (Gopalan et al. 2006). For the single collector 42-48 spike measurement procedure, the ^{40}Ca current was maintained between 5.4-6.6 $*10^{-11}$ A with baseline measurements taken at 46.5. Integration times were 5s for all masses except ^{40}Ca, which was measured for only 3s followed by a 2s magnet settling time. The sequence of measurement was 46.5-40-43-48-42-44-46.5 (Zhu and Macdougall 1998a). Possible interference from ^{39}K was negligible, as the intensity was always observed to be less than $1.5 * 10^{-14}$ A.

1.4 Sample Preparation

There were two mineral phases sampled for calcium isotopes in this dissertation, gypsum ($CaSO_4 * 2H_2O$) or anhydrite ($CaSO_4$) and calcium carbonate ($CaCO_3$). For samples from the Ocean Drilling Program, a small rock chip was cut from the larger sample rock for either direct dissolution or powdering and then dissolution. For the bulk carbonate oozes of Leg 138 Site 850 (Chapter IV) the sample was disaggregated in Millipore water and then sonicated for 10 minuets to dislodge any clay minerals from the carbonate. The water was decanted off and fresh Millipore water added; the process was repeated a total of three times to ensure that mostly carbonate was left in the beaker and the sample was washed clean of contaminates. The sample was then transferred to a centrifuge tube where 500 μl of 1.8 N HCl was added for dissolution, then centrifuged to further separate any

remaining clays from the calcium rich sample fluid. The fluid was then pipetted into a clean Teflon beaker.

The evaporitic sediments (gypsum, anhydrite, and dolomites) of ODP Leg 107 and DSDP Leg 13 (chapters 2 and 3) had to be powdered before dissolution. A small mineral chip was taken and then rinsed in Millipore water, dried by a low temperature heat lamp, and powered with a mortar and pestle. After powdering, about 1-3 milligrams of sample powder was weighed out and added to a clean Teflon beaker for dissolution in 500 μl of 4.5 N HCl. The samples were left for several days and sometimes sonicated with low heat to ensure all powder went into solution. Anhydrite that was precipitated in the lab was simply dissolved in 500 μl of 4.5 N HCl and did not need powdering due to the very small crystal size.

For isotope analysis, all samples must be processed through a cation exchange resin (Mitsubishi Cation Exchange Resin CK08P 75-150 μm) in order to separate calcium from other elements in a sample such as K, Mg, Al, and Sr. Approximately 30 μg of calcium was loaded onto the columns for data in Chapters II and III. Since all samples are in solution form at this point, a volume representing 30 μg was dried down to a crust then brought back to a solution by addition of 50 μl of a low normality HCl. Various amounts of acid are then added to elute all other elements before and after the calcium cut.

Careful calibration of the columns ensured that almost 100% of the calcium contained in the sample was captured in the calcium cut. This is important because there is a strong possibility that fractionation can occur within the resin, up to 3 per

mil per mass unit (Russell et al. 1978). The resin tends to hold the lighter isotopes longer than the heavier ones, and even if only a small percentage (20%) of the total cut is excluded, the bias may be up to 0.5 per mil. If all of the calcium is collected in the cut, this fractionation problem is resolved. Therefore special care was taken to calibrate the columns such that all calcium was recovered.

Column fractionation can also be accounted for by spiking the sample before elution through the columns. In this case the iterative procedure used to correct for fractionation during the mass spectrometer run also corrects for any fractionation that occurs in the column. This approach was used for the analyses reported in Chapter IV. For each sample, 400 μl of the double spike mixture (^{42}Ca-^{43}Ca) was added in careful proportion to approximately four micrograms of Ca, then dried down to a crust and reconstituted with 50 μl of a low normality HCl acid before loading on the columns. This provides enough sample for four mass spectrometer runs.

Calcium cuts from the column procedure were measured on an ICP-OES to obtain concentrations. For samples that had not yet been spiked, 1μg of Ca was mixed with 100 μl of ^{42}Ca-^{48}Ca double spike, and for samples that had been pre-spiked, exactly 1 μg was set aside for loading onto a filament. The sample was dried down to a small volume, about 1-3 μl, and a sandwich loading technique was used to load the sample onto the filament; four drops of mélange, the total sample in a series of drops, then two more drops of mélange. The mélange mixture is a solution of tantalum oxide in HF and concentrated nitric acid modified after Birck (1986). Each drop of mélange

was dried at 1.4 A and each drop of sample at 1.5A. Once the sample was loaded, the whole sandwich was oxidized at a dull red heat (3.4A) for 20 seconds.

Standard ion exchange column chemistry was also used to separate strontium for the strontium isotope analyses used to supplement the Ca isotope data reported in Chapter III. Special care had to be taken with the Sr cut for these high-Ca samples because residual calcium in the Sr cut can seriously suppress Sr emission during mass spectrometry. About 40 ng of strontium was loaded onto a tungsten filament with the same mélange and sandwich technique for loading as calcium. No spiking is needed for strontium analysis on the TIMS, as there is a natural fixed normalizing ratio available for strontium. Machine induced fractionation of $^{87}Sr/^{86}Sr$ is corrected using the natural ratio $^{86}Sr/^{88}Sr = 0.1194$ since both these isotopes are non-radiogenic and produced only by nucleosynthesis.

1.5 Summary of Calcium Isotope Research

This dissertation will only focus on mass-dependent fractionation effects in low temperature inorganic and biologic processes. The first half of the work deals with calcium-sulfate minerals and inorganic fractionation within brines, and the last half focuses on calcium cycling in the oceans for the Neogene and Pleistocene using bulk carbonate oozes as a monitor. A brief summary of calcium isotope studies to date on this subject follows in the next sections. DePaolo (2004) published a concise history of calcium isotope studies, which includes all aspects of this system and is a

very good secondary reference for the reader interested in a broader view of calcium isotope research.

1.5.1 Temperature dependent fractionation in foraminifera

Calcium isotope temperature dependent fractionation is perhaps the most widely contested subject within calcium research simply because it *could be* an ideal paleothermometer for ancient oceans. The commonly used oxygen isotopes have a built in evaporation/precipitation and ice volume effect in addition to an equilibrium temperature fractionation effect in biologically mediated calcite precipitation. The two effects can be untangled successfully, but it is preferable to find another isotopic or chemical proxy that can directly record calcification temperature, such as the incorporation of minor elements (Nurnbuerg et al 1996).

Several studies have investigated the extent of calcium isotope fractionation in both lab cultured foraminifera and core-top sediments (Skulan et al. 1997, Zhu and Macdougall 1998a, De La Roche and Depalao 2000, Nagler et al. 2000, Gussone et al. 2003, Sime et al. 2005). Although these studies at times express conflicting results, there are some common findings on temperature dependent fractionation, such as the data for abiogenic calcite and the formainifera species O. *universa*. For inorganically precipitated aragonite the slope of $\delta^{44}Ca$ with temperature is 0.015 per mil/°C and for the foraminifera O. *universa* the slope is 0.019 per mil/°C (Gussone et al. 2003), which represent a very weak relationship with temperature in regard to the limited precision of calcium isotopes and agrees with other work (Sime et al. 2005). The

slope for foraminifera species G. *sacculifer* is 0.24 per mil/°C, representing a much stronger fractionation with temperature. Based on this data, Gussone et al (2003) claim that G. *sacculifer* would be a good species to use in paleotemperature reconstructions.

Sime et al. (2005) questions this strong temperature dependent relationship in his study of core top planktonic foraminifera. He found absolutely no temperature relationship in 12 species of foraminifera, and for G. *sacculifer* in particular there was a 0.1 per mil variation uncorrelated with temperature. The discrepancy between cultured and core-top data indicates that the controlled conditions in the laboratory do not adequately describe the actual calcification or diagenetic conditions in the ocean. Biological processes, sometimes species specific, may overprint calcium isotope temperature dependent signatures in foraminifera and cocolithophores (Sime et al. 2005).

Some researchers even question the generally accepted notion that calcium isotopes are solely controlled by a kinetic fractionation effect. Lemarchand et al. (2004) propose that calcium isotope fractionation in synthetically precipitated calcite is controlled by an equilibrium effect dependent on calcification rate. According to these authors, isotope shifts in calcium isotopes are dictated by the availability of calcium in the vicinity of the crystal-solution interface. They find an equilibrium fractionation factor of –1.5 per mil as the primary process for observed fractionation effects in carbonates; however, if supersaturation of calcium is maintained close to the crystal-solution interface and precipitation is fast, the equilibrium fractionation will be

overprinted or even canceled out by kinetic effects related to temperature controlled equilibrium constants.

Their experiments do not address the specific biological conditions that control saturation state at the crystal-solution interface; therefore the results are not directly applicable to the variable behavior of calcium isotopes and temperature in foraminifera. However they do soundly reject the ideas of Gussone et al. (2003) who explain the different temperature dependent slopes of G. *sacculifer* and O. *universa* by invoking aquacomplexes ($Ca[H_2O]_n^{2+} * mH_2O$ with hydration numbers of 25-33 for O *universa*). They propose that G. *sacculifer* actively dehydrates Ca aquacomplexes before calcification, which leads to a larger temperature dependent fractionation effect, while O. *universa* does not dehydrate the Ca aquacomplexes and is therefore less susceptible to temperature dependent kinetic fractionation effects. Lemarchand et al. (2004) conclude that the Ca aquacomplexes suggested by Gussone et al. (2003) would have to be unrealistically large to account for the fractionation effects.

The temperature-$\delta^{44}Ca$ relationship is a complicated one, but it will not be addressed in this dissertation. The calcium budget study of chapter 4 deals with bulk carbonate values instead of a single species of foraminifera for this very reason. Bulk values may not be as accurate as using a single species of foraminifera that has a small temperature-$\delta^{44}Ca$ effect, but given the unsettled state of debate on temperature dependence and its mechanisms, it is best to use a bulk sample. Since the goal of the measurements is to obtain data on the average $\delta^{44}Ca$ of seawater, a bulk sample will

theoretically represent an average composition of carbonate produced during a particular time interval.

1.5.2 Global calcium cycling

Another interesting application of calcium isotope variation in nature concerns the global weathering of calcium in rocks, cycling through the oceans, and subsequent deposition as new carbonate or evaporite sediments. Several studies have conducted geochemical budgets of calcium by measuring the $\delta^{44}Ca$ of bulk carbonate samples as an indicator of changes in the $\delta^{44}Ca$ of seawater through geologic time (Skulan et al. 1997, Zhu and Macdougall 1998a, De La Rocha and DePaolo 2000, Schmitt et al. 2003a and 2003b, Fantle and DePaolo 2005). These studies have measured calcium isotope data for most sources and sinks of calcium in the oceans, such as river water, hydrothermal inputs, groundwater, and various carbonates.

Because the residence time of calcium in the oceans is ≈ one million years, changes in the $\delta^{44}Ca$ of seawater cannot be resolved for time periods much less than this time interval. Therefore geochemical budgets involving calcium isotopes will be long term quantifications that will average out shorter term events such as ice-age cycles but will record longer duration events like tectonic reorganizations or gradual changes in the rate of source and sink functions.

Rivers and hydrothermal alteration of basalts at spreading ridges are the two main sources of calcium to the oceans. There are no published pore water data for calcium isotopes, however the diagenetic flux (slightly less than the hydrothermal

flux) is expected to have a δ^{44}Ca value very close to the average carbonate value of –1.3 per mil (DePaolo 2004). River water and hydrothermal fluids have been measured for calcium isotopes by several researchers. Schmitt et al. (2003b) adds new work and summarizes previous studies showing that both rivers and hydrothermal fluids have similar δ^{44}Ca values, -0.96 ± 0.19 for hydrothermal fluids and –1.07 per mil for a weighted average of 8 world rivers. The hydrothermal fluids are not much isotopically different than MORB basalts, which have an average δ^{44}Ca value of –0.81 ± 0.26, suggesting little to no fractionation occurs during high temperature alteration of basalt (Schmitt et al. 2003b).

Although river water δ^{44}Ca values have a significant range of values (-1.71 ± 0.17 to –0.63 ± 0.07), the difference between silicates and carbonates is only about 0.40 per mil, limiting variations in the δ^{44}Ca of runoff/rivers to 0.20 per mil. The larger range of values seen in world rivers might be explained by biological activity in the surficial soil horizon, which enriches the soil in the heavy isotope (Schmitt et al. 2003b). The average δ^{44}Ca seawater value may change significantly through geologic time, as it may have during rapid uplift of the Tibetan Plateau shown through strontium isotopes (Raymo et al. 1988), but Schmitt et al. (2003b) contend that the average values will stay the same and only the strength of the fluxes will determine changes in δ^{44}Ca of seawater. The current average input δ^{44}Ca value (river and hydrothermal) is –1.1 per mil according to Schmitt et al. (2003b).

The primary modern sink for calcium in the oceans is carbonate deposition, although at different geologic periods evaporites and phosphates may also act as sinks

Table 1.5.2 Selected summary of previously published $\delta^{44}Ca$ values for carbonate sediments, foraminifera, and cocolithophorid oozes. All $\delta^{44}Ca$ values have been adjusted to the seawater scale.

Sample Type	$\delta^{44}Ca$	$2\sigma_m$	Data Source*
Holocene carbonate ooze	-0.86	0.14	1
Miocene carbonate ooze	-1.29	0.15	1
Eocene chalk	-1.04	0.21	1
Jurassic chalk, Italy	-1.04	0.26	1
Jurassic chalk, Itlay	-0.83	0.08	1
Intertidal foraminifera (average)	-1.2	---	2
Cultured cocolithophorid (16°C)	-1.3	0.05	2
Average carbonate (0-80 Ma)	-1.36	19 samples range 0.9 per mil	2
Holocene Pacific cocco. ooze	-2.61	0.11	3
Holocene Atlantic carbonate ooze	-1.93	0.06	3
Holocene Carribean cocolith. ooze	-2.21	0.09	3
Holocene Atlantic carbonate ooze	-1.93	0.13	3
Holocene Atlantic cocolith. ooze	-2.64	0.07	3
Holocene Atlantic cocolith. ooze	-1.88	0.23	3
Holocene tropical coral	-1.84	0.22	3
74 Ma carbonate ooze	-1.89	0.03	4
22 Ma carbonate ooze	-1.92	0.18	4
Average carbonate (0-20Ma)	-1.45	36 samples range 0.70 per mil	5

*** Data sources and standards used:**

1 = Skulan et al. 1997, ultrapure CaCO3

2 = De La Rocha and DePaolo 2000, ultrapure CaCO3

3 = Zhu and Macdougall 1998a, seawater

4 = Zhu and Macdougall 1998b, seawater

5 = Fantle and DePaolo 2005, bulk earth

for Ca in the ocean. Many studies have measured carbonates of various ages and types (e.g. single forams, coccolithophorids, and bulk oozes). Table 1.5.2 shows the published data for these carbonate sediments. The average value is –1.63 per mil, however the data from Zhu and Macdougall (1998a) are significantly more negative as compared to the other studies, and if the analyses lighter than –2.0 per mil are taken out of consideration the average becomes –1.45 per mil. This discrepancy makes a significant difference in the question of whether steady state conditions currently exist for calcium isotopes in the ocean. Zhu and Macdougall (1998a) concluded that the system is not in steady state, as the calcium δ^{44}Ca output (carbonate sedimentation -2.15 per mil) does not equal the calcium δ^{44}Ca input (river, hydrothermal –0.95 per mil) to the oceans. This offset could be brought to equality if there was a large calcium sink with characteristic δ^{44}Ca values that were heavier than the carbonate values measured in the Zhu and Macdougall study.

Alternatively, the system could be in steady state if the carbonate value was significantly heavier than these initial estimates. De La Rocha and DePaolo (2000) publish different carbonate δ^{44}Ca values that are much heavier than Zhu and Macdougall (1998a) at –1.3 per mil. If this value is used, calcium cycling in the ocean is currently close to a steady-state mode. However, it is not expected that the ocean remain in steady-state conditions throughout geologic time. Sustained changes in the strength of Ca fluxes may push the oceans to a temporary non-steady-state condition that could last longer than the residence time of Ca in the oceans. Fantle and DePaolo (2005) found the marine cycle of Ca in the oceans is rarely in a steady-state mode

from their study of carbonates over the last 20 Ma. If δ^{44}Ca of seawater changes through time, these changes will be reflected in the δ^{44}Ca values of carbonate sediments. The residence time of calcium may have varied from its current one million years to a number five or ten times different depending on the concentration of calcium in seawater and changes in the magnitude of calcium fluxes to the oceans (DePaolo 2004). Based on fluid inclusions in evaporites, Hardie (1996) suggests a range of Ca concentration from 10mM to 40mM during the Phanerozoic. Fantle and DePaolo (2005) calculated a range of concentration from 0.5 to 1.7 times present concentration for the last 20 Ma.

Data from this study found in Chapter IV also confirms the range and average of carbonate values listed in Schmitt et al. (2003b) and De La Rocha and DePaolo (2000). The average of 22 bulk carbonate samples in this study is -1.26 ± 0.22 per mil with a total range of 0.86 per mil. This also agrees well with the average value of 36 nannofossil oozes measured by Fantle and DePaolo (2005) of -1.45 ± 0.10 per mil with a total range of 0.70 per mil. Schmitt et al. (2003a) used marine phosphates (eleven samples) to investigate changes in the δ^{44}Ca of seawater, and found that over the past twenty-five million years the δ^{44}Ca of marine phosphates and thus seawater did indeed vary considerable (ranging from –0.53 to –1.12 per mil). They found that the fractionation factor for calcium isotopes in phosphates is steady regardless of diagenetic, temperature, or local variations. The difference between δ^{44}Ca values of carbonates and phosphates remains the same, indicating that the δ^{44}Ca of marine phosphates reflected actual changes in the δ^{44}Ca of seawater. Early Miocene samples

show a positive excursion in the $\delta^{44}Ca$ of seawater, while the last nineteen million years show a relatively steady calcium isotope composition. Only seven samples were used to support the idea of a steady isotopic composition for the last 19 Ma, and the samples are not evenly spaced, so the record may have a sampling bias. Further studies of the $\delta^{44}Ca$ of seawater will be limited to a resolution that is determined by the long residence time of calcium in the oceans. However there is a lack of detailed studies of bulk carbonate values for the past fifteen million years. The last chapter of this dissertation takes up this task and focuses on the last twelve million years with a regular 500,000-year spacing between samples.

1.6 Calcium Isotopes and Evaporites: Fractionation Effects in Massive Ca-Salt Deposits

The only known calcium isotope measurements of gypsum are found in Russell et al. (1978), who measured two samples, one from the Lower Cambrian and the other from the Middle Jurassic. Their $\delta^{44}Ca$ values are –1.5 and –2.1 per mil relative to their seawater value. Both Skulan et al. (1997) and Russell et al. (1978) state that the evaporation-distillation conditions inherent in precipitation of gypsum or anhydrite could produce significant mass-fractionation effects, larger than any previously measured fractionation. The first half of this dissertation focuses on evaporitic sediments, specifically marine gypsums and anhydrites, as another previously unmeasured sink of calcium in the oceans. It is important to fit the range and characteristic values of these sediments into a survey of calcium isotopes in nature

regardless of their role in global calcium cycling. Various gypsum and anhydrite samples were analyzed for calcium isotopes, with the majority of samples coming from Late Messinian sediments from the Mediterranean. The fractionation factor for lab-precipitated anhydrite was also established in order to interpret the calcium isotopic changes that occur in an evaporating brine.

The Messinian Salinity Crisis presented an ideal, geologically recent and large body of evaporitic sediments to test the additional sink hypothesis. The Messinian Salinity Crisis (MSC) sequestered 6% of the ocean's salt content in only 200,000 years (Ryan 1973) starting at 5.96 Ma. Repeated desiccation and re-filling events occurred during this time period, and complete evaporation of the Mediterranean and Red Seas was a common phenomenon. In the Balearic Basin alone, over one million cubic kilometers of evaporitic salts with a thickness of up to two kilometers was deposited (Ryan 1973).

The resulting deposits show cyclical patterns of gypsum and anhydrite beds with intercalated dolomitic oozes. This dissertation not only looked at the global influence of evaporites on calcium cycling in the ocean, but also at the calcium isotopic changes that occur in an evaporating brine. One exploratory site in the Tyrrhenian Basin of the Mediterranean was chosen to investigate fluctuating brine chemistry, and both calcium and strontium isotopic analyses were preformed in order to better understand processes that cause calcium isotopes to fractionate in extreme geochemical conditions.

Chapter II Calcium Isotopes in Evaporitic Sediments

2.1. Mineralogy of evaporitic deposits and mineral stability

When seawater naturally evaporates, a known assemblage of evaporite minerals precipitate. The resulting group of minerals is not only interesting and important for chemical studies, but also for economic utilization as both gypsum ($CaSO_4*2H_2O$)/anhydrite ($CaSO_4$) and halite (NaCl) have critical uses in society as components in building materials, industrial chemicals, and also for human consumption in the case of halite.

Harvie et al. (1980) calculated evaporite mineral assemblages and then compared these assemblages to observed distributions in one particularly large evaporite body, the Permian Zechstein deposits of Germany. Their model better predicts the ratio of anhydrite to halite in natural deposits than did earlier calculations by Van't Hoff described in Eugster (1971), which had generally predicted lower ratios than actually occur in nature. According to Harvie et al. (1980), in order to account for natural distributions calcium-bearing phases remain in equilibrium with the brine, rather than undergo fractionation crystallization where they would not react further with the evaporating brine. In this condition, anhydrite precipitates at all stages of brine concentrations, mainly at lower concentrations. However, as the brine moves toward very high concentration, anhydrite may partially dissolve supplying additional calcium to the brine, in which case numerous other, more obscure calcium-bearing evaporite minerals may precipitate at anhydrite's expense. Back reactions involving

this recycled Ca can then continue to produce more anhydrite at very high brine concentrations. Thus, evaporation of seawater and the study of evaporative minerals are both extremely complicated.

Natural deposits tend not to show the mineralogical variability seen either in chemical models or in the laboratory under controlled conditions. Rather, the minerals gypsum or anhydrite, halite, glauberite ($Na_2Ca(SO_4)_2$), polyhalite ($K_2MgCa_2(SO_4)_4$), carnallite ($KMgCl_3*6H_2O$), and kieserite ($MgSO_4*H_2O$) are more commonly observed in seawater derived evaporitic bodies, with gypsum/anhydrite and halite accounting for the large majority of evaporitic minerals by volume. All of these later phase evaporite minerals are highly soluble, including halite, which after precipitation can be dissolved by an influx of seawater or rainwater. Also, halite may not even precipitate from a brine and accumulate if the atmospheric humidity is high, greater than about 76%. At this level the activity of water is higher in the atmosphere than it is in the brine, and water will transfer from the atmosphere to the brine, decreasing the salinity and preventing precipitation (Kinsman 1976).

Upon evaporation of seawater, the first phase to precipitate is aragonite ($CaCO_3$) at twice the total salt concentration of seawater (40-60 per mil). Next comes gypsum or anhydrite (see below) at five times the concentration of seawater (130-160 per mil). At ten to twelve times concentration (340-360 per mil) halite precipitates and at seventy to ninety times the concentration of seawater the bittern salts (Mg and K sulfates and chlorides) fall out of solution (Warren 1999). Most brines rarely get to the bittern salt stage because recharge from seawater, groundwater, or continental

runoff occurs both lowering salinity and re-dissolving any accumulation of late stage salts. High atmospheric humidity may also tend to prevent the brine from reaching concentrations of seventy to ninety times seawater (Kinsman 1976).

The occurrence of gypsum or anhydrite in an evaporite deposit depends on temperature and salinity at the time of precipitation. Below 40°C gypsum is the stable phase and above that anhydrite is the stable phase (Braitsch 1971). Gypsum can only alter to anhydrite if the temperature is at least 40°C. For NaCl concentrations above five times seawater, anhydrite is the stable phase at 30°C. The release of two water molecules upon dehydration of gypsum serves only to slow salt precipitation as long as communication of pore spaces with the overlying brine occurs and evaporation is continuous (Braitsch 1971).

2.2. Determination of a Fractionation Factor for Calcium Isotopes in Precipitated Anhydrite

2.2.1 Introduction

Investigation into the behavior of calcium isotopes in evaporite deposits requires the determination of a fractionation factor, in this case a number which describes the extent of discrimination of one isotope in favor of another isotope during precipitation of a mineral in equilibrium with the source brine. For inorganically precipitated aragonite this fractionation factor is very weakly temperature dependent (δ^{44}Ca 0.015 per mil/°C) and is -1.79 ± 0.12 for aragonite at 10°C and -1.23 ± 0.12 at 50°C (Gussone et al. 2003). Precipitation of aragonite discriminates against the heavy

isotope ^{44}Ca and favors the light isotope ^{40}Ca, and as temperature increases this fractionation is very slightly reduced. As described in Chapter I, the nature of fractionation is complicated when a marine organism secretes a carbonate shell. Biological or species specific effects cloud the weak temperature dependent fractionation and no clear relationship with temperature is seen at all (Sime et al. 2005). However, during calcification by organisms the light isotope as well is always preferred, it is only the degree of this preference that is variable and subject to debate.

Gypsum and anhydrite are only inorganically precipitated and biological vital effects never enter the equation. The determination of a fractionation factor to describe most geochemical circumstances is therefore much clearer. One task for this dissertation was to find the calcium isotope composition of the very first crystals of anhydrite that form in an evaporating brine (the fractionation factor) and take subsequent anhydrite samples as the brine concentrated through halite saturation to see if the brine followed an isotopic Rayleigh fractionation path.

2.2.2 Experiment design

The fractionation factor was determined for two temperatures, 30°C and 40°C. For the 40°C experiment the path of evaporation was followed to halite saturation and anhydrite samples were taken at four other times during the experiment. In the 40°C experiment 400 ml of 0.2 μm filtered north Pacific seawater collected at a water depth of 250 m was evaporated using a heat lamp. In the 30°C scenario a warm bath was used to raise the temperature of the seawater and only 200 ml were evaporated.

Temperature was carefully monitored during these experiments and every attempt was made to hold a constant temperature. These temperatures were chosen because they are common temperatures of shallow water evaporating brines as seen in typical sabkah environments.

Retrieval of precipitated crystals was accomplished by filtering the brine through 0.2 μm filters, and the mineralogy was confirmed using a petrographic microscope. Corresponding samples of brine were taken in order to know the isotopic composition of the solution from which the crystals precipitated. The samples were processed through the column and loading procedures described in Chapter I. The data in the 30°C experiment was processed using the 42-43 spiking and measurement procedure, whereas the data in the 40°C experiment were processed with the 42-48 spiking procedure.

2.2.3 δ^{44}Ca data for precipitated anhydrite

Data for the evaporation experiments are listed in Table 2.2.3 and in Figure 2.2.3b. Figure 2.3.2a illustrates the ideal Rayleigh fractionation path if the fractionation factor is –1 per mil. The δ^{44}Ca value for starting seawater is zero and throughout concentration eventually evolves to a heavy value of +2.07 per mil after 90% of the starting seawater volume has been lost to evaporation. The corresponding precipitated anhydrite crystals will start out at –1 per mil and progress to a value of +1.07 per mil when only 10% of the initial volume remains. Precipitation of anhydrite in the laboratory in a closed system should follow this idealized path. No new Ca is

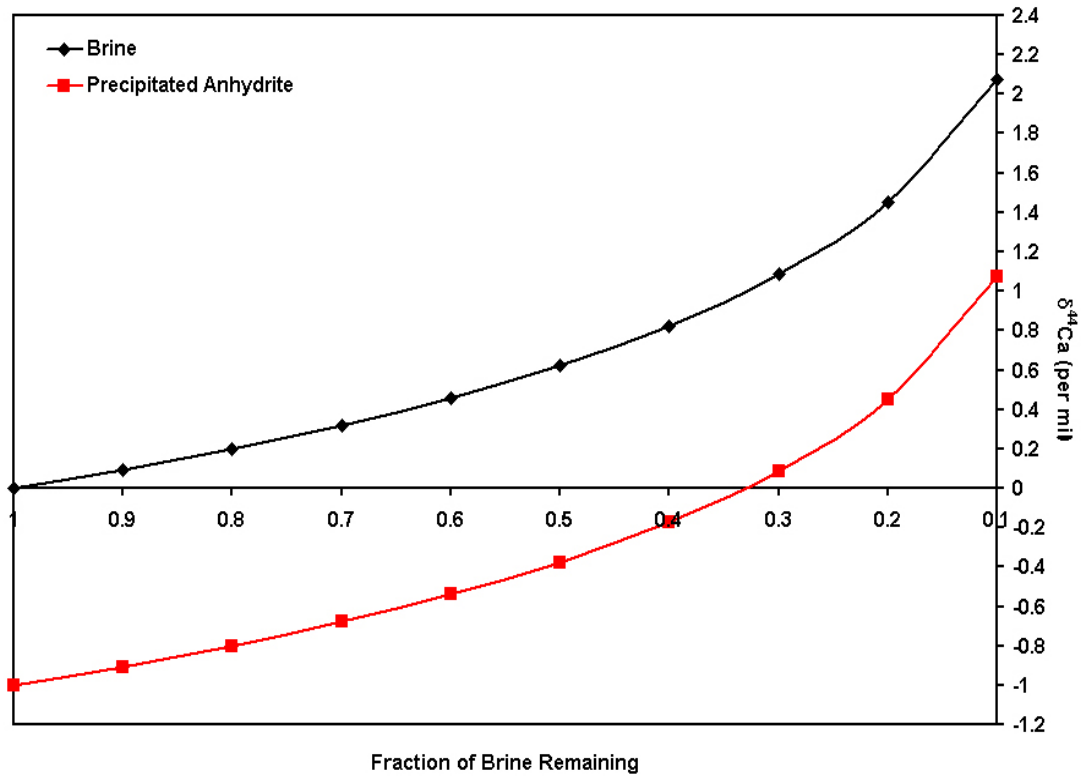

Figure 2.2.3a Idealized Rayleigh fractionation path for calcium isotopes in a closed system. A fractionation factor of –1 per mil is used and the starting $\delta^{44}Ca$ of seawater is set to zero per mil. The total range of values for the brine and precipitated anhydrite crystals is 2 per mil.

Table 2.2.3 $\delta^{44}Ca$ data for the evaporation experiments. Fractionation factor is determined by subtracting the value for the first anhydrite crystals from the corresponding brine value.

Sample	Run	Temp.	Time (hr)	$^{44}Ca/^{40}Ca$	$\delta^{44}Ca$	Average $\delta^{44}Ca$	$2\sigma_m$	Fractionation Factor
Starting SW	run a	30	0	0.02172287	0	-0.01	0.01	
	run b	30	0	0.02172233	-0.02			
Anhydrite 1	run a	30	124	0.02170003	-1.04	-0.97	0.10	0.86
	run b	30	124	0.02170309	-0.9			
Brine 1	run a	30	124	0.02172122	-0.07	-0.11	0.06	
	run b	30	124	0.02171952	-0.15			
Sample	**Run**	**Temp.**	**Time (hr)**	**$^{44}Ca/^{40}Ca$**	**$\delta^{44}Ca$**	**Average $\delta^{44}Ca$**	**$2\sigma_m$**	**Fractionation Factor**
Starting SW	run a	40	0	0.02173591	-0.34	-0.35	0.01	
	run b	40	0	0.02173581	-0.35			
Anhydrite 1	run a	40	25	0.02172463	-0.86	-0.93	0.09	1.035
	run b	40	25	0.02172184	-0.99			
Brine 1	run a	40	25	0.02174667	0.15	0.11	0.06	
	run b	40	25	0.02174502	0.07			
Anhydrite 2	run a	40	26	0.02173446	-0.41	-0.50	0.12	
	run b	40	26	0.02173083	-0.58			
Brine 2	run a	40	26	0.02175248	0.42	0.53	0.16	
	run b	40	26	0.02175729	0.64			
Anhydrite 3	run a	40	27	0.02173388	-0.44	-0.42	0.03	
	run b	40	27	0.02173476	-0.4			
Brine 3	run a	40	27	0.02175549	0.56	0.55	0.01	
	run b	40	27	0.02175504	0.54			
Anhydrite 4	run a	40	28	0.0217433	0	0.10	0.13	
	run b	40	28	0.02174753	0.19			
Brine 4	run a	40	28	0.02176389	0.94	1.04	0.14	
	run b	40	28	0.02176816	1.14			
Brine 5	run a	40	29	0.02176601	1.04	1.15	0.15	
	run b	40	29	0.02177051	1.25			

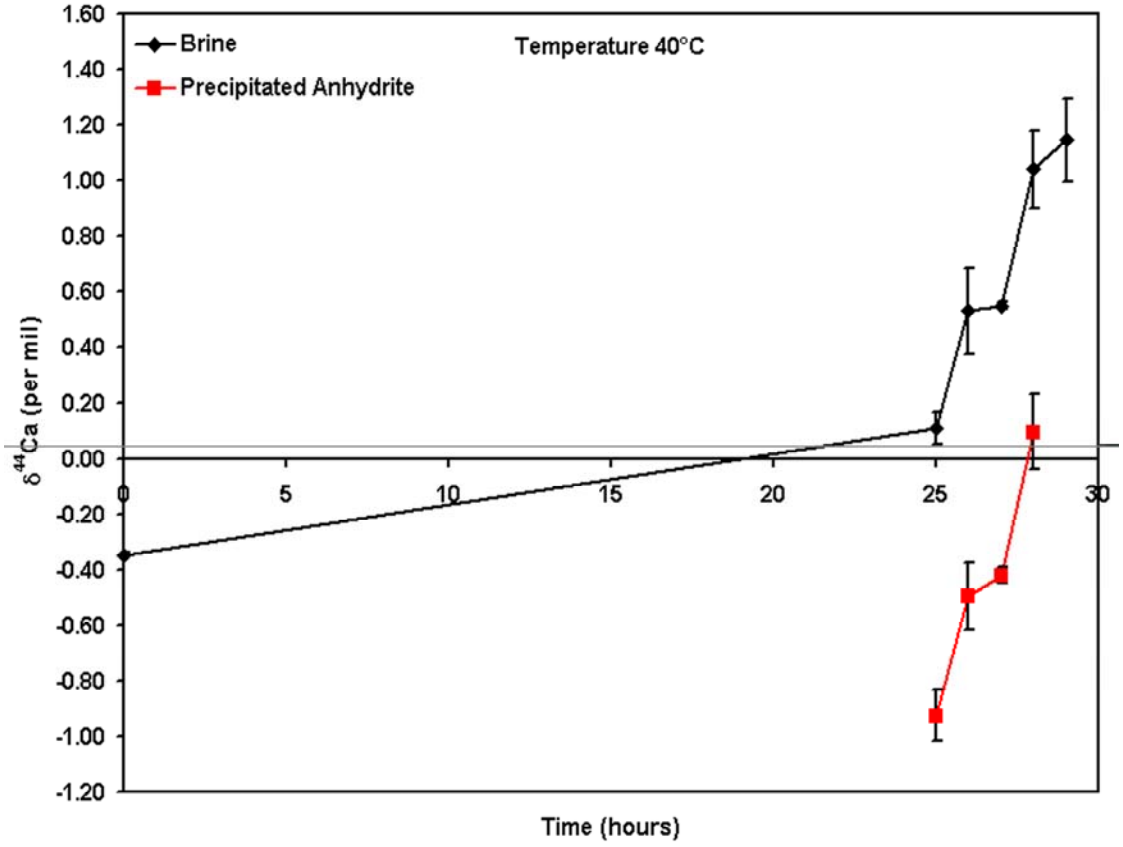

Figure 2.2.3b Data for the 40°C evaporation experiment followed to halite saturation. The first crystals appear at t=25 hours and have a value of –0.93 per mil. The brine at t=25 has evolved to a δ^{44}Ca value of 0.11 per mil. The last anhydrite crystals before halite almost exclusively precipitates (t=29 hours) are 0.10 per mil representing a total fractionation of 1.03 per mil. The brine shows a total fractionation of 1.15 per mil. The last brine sample does not have a corresponding crystal sample because the anhydrite content of the crystal sludge at this point is very low and a sample could not be retrieved.

added to the system and Ca is only removed by anhydrite precipitation within the evaporation vessel.

Figure 2.2.3b shows the calcium isotope data for the 40°C experiment. The fractionation factor is –1.04 per mil and the total fractionation after 29 hours of evaporation is 1.5 per mil for the brine and 1.03 for the precipitated crystals. The total fractionation is higher for the brine than the crystals because one additional sample was taken for the brine. The amount of anhydrite present in the crystal sludge at 29 hours was very small and a significant amount of co-precipitating halite made retrieval of a sample difficult. The full range of fractionation predicted by Figure 2.2.3a was not seen in the 40°C experiment. This is because anhydrite continues to co-precipitate with other later phase evaporative minerals all the way to complete initial volume loss, and samples of this very late stage anhydrite are extremely difficult to retrieve and separate from other minerals. Only two-thirds of the total fractionation predicted is seen in the experimental data for this reason. The overall trend of the data is very similar to the idealized Rayleigh fractionation path in Figure 2.2.3a, however this is a controlled laboratory experiment where no new sources of Ca are added to the brine. Therefore natural evaporative ponds will probably experience a larger range of isotopic conditions as re-concentration and rejuvenation of the brine occurs seasonally or with geographic changes that may restrict highly saline outflow.

The 30°C experiment was performed only to obtain the very first crystals precipitated for determination of a fractionation factor. The first crystals to precipitate had a δ^{44}Ca value of -0.93 ± 0.10 per mil and the brine was -0.11 ± 0.06 per mil. This

fractionation factor of –0.86 per mil is slightly less than the 40°C fractionation factor but the analyses are within error of each other. It is reasonable to assume an average of the two numbers for later studies on evaporites (-0.95 ± 0.10 per mil).

2.3 Range of Calcium Isotope Values in Evaporitic Deposits

2.3.1 Required conditions for evaporite formation and types of evaporites

Evaporitic deposits will accumulate whenever there is an excess of evaporation over precipitation in a body of water, either fresh or marine. These conditions are met in numerous places throughout the world, but primarily between the latitudes of 15° to 45° north and south of the equator. These so-called Horse latitudes have arid to semi-arid climates (<25 mm rainfall per year) because they lie beneath the cold and dry descending air of the Hadley Cells (Warren 1999). The position of these arid latitudinal belts has changed throughout geologic time, even on the relatively short timescales of ice ages. Other geographic conditions can cause a localized arid region, such as in deserts that form in the rain shadow of a mountain range (Patagonia on the lee side of the Andes mountains and Death Valley, California on the lee side of the Sierra Nevada range) or adjacent to cold upwelling ocean currents (Baja California). Regardless of geography, the end result and one condition that must always be achieved for the formation of evaporitic bodies is an excess of evaporation over precipitation.

The predominant types of evaporites forming in nature today are associated with coastal environments, specifically bays and lagoons in the subtropics. These

shallow depressions, which are sometimes inundated with marine incursions, are called sabkahs. Terms synonymous with sabkahs vary by culture, but in the English speaking world the words pans, saline lakes, alkali flats, salt plains, dry lakes, salt flats, and salinas are all interchangeably used to denote a sabkha type environment, whether it be continental or marine (Yechieli and Wood 2002). Modern examples of sabkahs occur in the Arabian Gulf, West Texas, and the Dead Sea.

Continental evaporites are distributed throughout the horse latitudes, and are different from marine sabkah environments only in the fact that their primary solute source is continental runoff or groundwater instead of seawater, although depending on location it is possible for seawater incursions to temporarily fill a continental basin. Continental evaporites may be fed by ephemeral or perennial streams with varying contributions of fault fed springs or hydrothermally heated groundwater. Local tectonics dictates where these evaporating water bodies will be located because fault bounded mountain ranges isolate basins where water can then accumulate.

During certain geologic periods such as the Permian or Miocene, much larger accumulations of evaporitic sediments have been deposited as basin-wide evaporites. Evaporite deposition sequestered significant amounts of sulfur, enough to drive the sedimentary Sulfur-Oxygen-Carbon system and control the flux of organic carbon to sediments (Garrels and Lerman 1981). Some of these ancient basin-wide evaporites are two to three orders of magnitude larger than modern deposits. These units, which are usually greater than 50m thick, exhibit both shallow and deep water depositional features and are mostly composed of anhydrite and halite beds with minor

accumulations of late stage salts (Warren 1999). Simple, constant evaporation is not the only requirement in formation of basinwide evaporites. For example, if the entire volume of the Mediterranean Sea were to evaporate today, only 1.5-2.0m of gypsum/anhydrite would precipitate even though water depths in the region are in excess of 1450m (Sonnenfeld 1984).

In order for large volumes of evaporites to accumulate over time, a semi-continuous supply of seawater is required, an excess of evaporation over precipitation, and a restricted or absent outlet for highly saline waters to leave the basin. Examples of basinwide evaporites, also known as "saline giants", are the Late Miocene deposits of the Mediterranean and Red Seas, the Permian Zechstein evaporites of Eastern Europe, and the Permian basins of West Texas. The formation of these large evaporites is a complicated interplay of changes in brine level, tectonics, and climate and there is no unique way to form thick and continuous basinwide evaporites. As long as salt is pumped into the basin and there is restricted outflow, the brine will inevitably concentrate with time; the rate will only be a matter of groundwater exchange (leakage), evaporation, and precipitation (Sonnenfeld 1984).

2.3.2 Calcium in evaporite deposits

Calcium is abundant in both seawater and continental runoff. Therefore accumulating calcium in a concentrating brine leads to the precipitation of calcium-bearing minerals (predominately gypsum or anhydrite), as discussed in Section 2.3.1 one of this chapter. One goal of this dissertation was to survey the calcium isotopic

composition of various gypsums and anhydrites found in all types of evaporitic deposits. Continental gypsums, hydrothermal anhydrites, marine gypsum/anhydrite, and laboratory-precipitated anhydrite were all sampled for calcium isotopes. As discussed in the seawater evaporation experiment, calcium isotopes in an evaporating brine appear to follow a Rayleigh fractionation path, where the light isotope is preferentially incorporated into precipitated calcium minerals and the heavy isotope is relegated to the concentrating brine. If no new sources of calcium are available to the brine, all of the calcium will be sequestered in precipitated gypsum/anhydrite, and the last crystals to precipitate are isotopically the heaviest.

The simplified laboratory experiment does not wholly describe conditions in natural evaporative brines. Brines are constantly recharged with calcium from groundwater, seawater, or continental runoff. Ultimately, the steady-state solute concentration depends on the transportation rates of solute back to the ocean (or some other outlet), evaporation rates, thermodynamic equilibrium with precipitated minerals, and water and solute flux to the basin (Yechieli and Wood 2002). It logically follows that the steady-state isotopic composition of the brine will be affected by the same parameters. Therefore the generalized survey of calcium isotopes in evaporites that is discussed in the next section approximates the range of $\delta^{44}Ca$ values that may be found in these extreme geochemical environments.

2.3.3 $\delta^{44}Ca$ data for evaporites and hydrothermal anhydrites

Table 2.3.3 lists the $\delta^{44}Ca$ values for 12 different gypsum or anhydrite samples both modern and ancient, and Figure 2.3.3 groups the data by type of evaporite. Three oceanic hydrothermal anhydrites are included. The gypsum from the Anza Borrego desert east of San Diego (5 Ma) and the sample from the evaporative rim of Lake Meade in Nevada (modern) are classified as continental evaporites. The gypsum from the San Diego South Bay Saltworks and the anhydrite precipitated in the lab are samples derived from modern seawater. All of the hydrothermal anhydrites are from the East Pacific Rise from deep-sea chimneys located within 200 m of the ridge axis. The 9N Stockwork (9º 50.6'N) anhydrite sample is from the northern East Pacific Rise from the vein system underneath the "Tubeworm Barbecue" site (Haymon et al. 1993), and the Sylvester (21º 25.9'S) and Sojourn (18º 24.3'S) samples are from these respective hydrothermal chimneys on the southern East Pacific Rise (personal communication Rachel Haymon). All of the late Miocene samples from the Red Sea and Mediterranean are anhydrites from the massive Messinian evaporitic bodies deposited during the late Miocene Salinity Crisis in that region. They are marine evaporites, but may have a riverine influence, as the connection with Atlantic seawater during the salinity crisis was not continuous.

The entire range of $\delta^{44}Ca$ values for these evaporites is 2.18 per mil, considerable for calcium isotopes since the known range in all terrestrial materials is on the order of 4-5 per mil. The lightest samples are from the hydrothermal anhydrites (-2.48 to –1.61 per mil) and the continental gypsums (-1.91 to –1.45 per mil).

Table 2.3.3 Mean δ^{44}Ca values for 12 gypsums and anhydrites. Errors represent 2σ of the mean with 2 runs for each sample, except for the Sylvester Anhydrite.1 and the Saltworks Gypsum, which have only 1 run each. The hydrothermal anhydrites were processed twice in order to test external precision. Agreement between the splits is within measurement error. The Red Sea (Leg 23) and Balearic Basin (Leg 13) samples are from the DSDP.

Sample	Mean δ^{44}Ca	$2\sigma_m$	n
Anza Borrego Gypsum	-1.45	0.06	2
Lake Meade Gypsum	-1.91	0.07	2
Saltworks Gypsum	-0.30	--	1
Lab Precipitated Anhydrite	-0.93	0.09	2
9NStockwork Anhydrite.1	-1.85	0.36	2
9NStockwork Anhydrite.2	-1.80	0.17	2
Sojourn Anhydrite.1	-1.61	0.01	2
Sojourn Anhydrite.2	-1.79	0.19	2
Sylvester Anhydrite.1	-2.48	--	1
Sylvester Anhydrite.2	-2.42	0.24	2
Red Sea Site 225 Anhydrite	-0.86	0.02	2
Red Sea Site 225 Anhydrite	-0.28	0.04	2
Red Sea Site 227 Anhydrite	-0.46	0.04	2
Red Sea Site 227 Anhydrite	-0.97	0.01	2
Balearic Basin Site 124 Anhydrite	-0.80	0.16	2

Anhydrite is precipitated at deep-sea chimneys where superheated seawater rich in calcium from alteration of Mid-ocean Ridge Basalt (MORB) meets very cold ambient seawater. No evaporation is required for precipitation of these anhydrites, however the parent fluid is still seawater but with addition of calcium from surrounding sediments and basalts. The average δ^{44}Ca value for MORB is –0.81 ± 0.26 per mil and for hydrothermal fluids is –0.96 ± 0.19 per mil (Schmitt et al. 2003b). It is unknown if the fractionation factor for calcium isotopes in high temperature anhydrite is the same as for low temperature evaporative precipitation (-1 per mil), but clearly the chimney anhydrites are isotopically lighter than the average MORB values. For sake of discussion in this study, the low temperature fractionation factor is assumed. The hydrothermal anhydrites were processed in two separate splits in order to test external precision. The data between splits are within measurement error confirming that the dissolution, column elution, and filament loading steps between samples are reproducible.

The other possible source of calcium to altered seawater for these hydrothermal anhydrites is deep-sea carbonates. The average value for 19 bulk carbonate samples in De La Rocha and DePaolo (2000) is –1.36 per mil with a range 0.90 per mil, and a compiled average of other published carbonate values is –1.45 per mil if Zhu and Macdougall (1998a) values above –2.0 per mil are excluded. The lightest value is from the Sylvester chimney at –2.48 per mil (only 1 run), followed by the 9N Stockwork anhydrite at –1.80 ± 0.17, and then the Sojourn sample at –1.61 ± 0.01 per mil. If we assume the low temperature fractionation factor, the parental

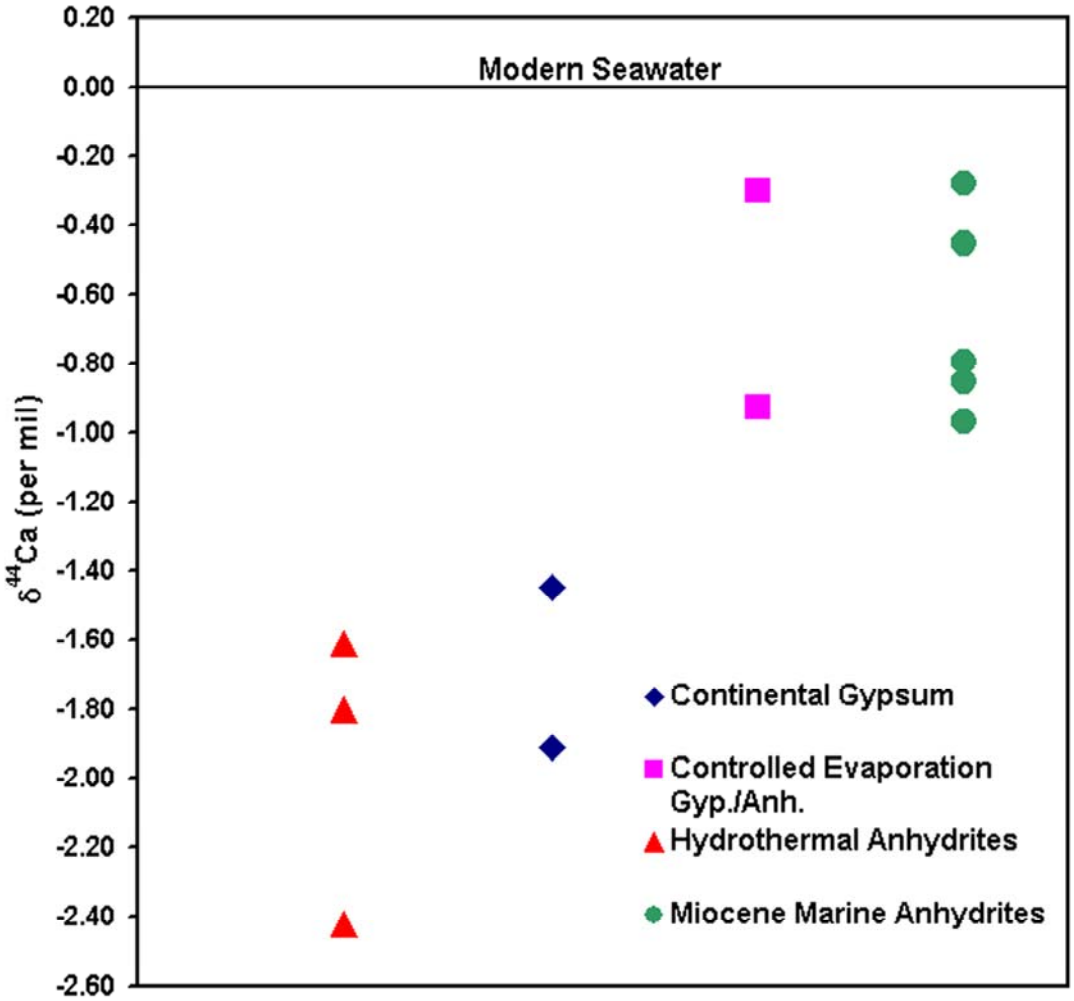

Figure 2.3.3 δ^{44}Ca data for 12 gypsum and anhydrite samples. Hydrothermal anhydrites and continental gypsums have lighter δ^{44}Ca values than marine derived gypsum and anhydrite. Miocene marine anhydrites are explored further in Section 3.1.4 of Chapter III. The isotopic range is larger for data in Chapter III; only selected samples were graphed in this figure to give a general idea of Miocene anhydrite isotopic range.

seawater for the Sylvester sample (δ^{44}Ca –2.48 per mil) must have been highly enriched with light calcium from the surrounding sediments and basalts and was likely precipitated from altered seawater with a value of around –1.48 per mil. Dissolved carbonates could have contributed calcium to the hydrothermal fluid, since carbonates are lighter than MORB and have an average value of –1.45 per mil. The same case could be made for the 9N Stockwork sample which has a δ^{44}Ca value of –1.80 ± 0.17 per mil. The anhydrite from the Sojourn chimney is heavier at –1.61 ± 0.01 per mil, and seems to have a parental fluid which is a combination of seawater and additional calcium from a MORB source.

The two continental evaporite samples are also isotopically light compared to most carbonates, river water, and MORB. The sample from the Anza Borrego Desert is from a large gypsum deposit located in the Imperial Formation of the Fish Basin. These large gypsum beds were deposited 4-5 million years ago from the evaporation of a shallow inland sea (Remeika and Lindsay 1992). As the small sea regressed and the increasingly isolated basin deepened, gypsum precipitated from the waters, which were a combination of Pliocene seawater and freshwater contributions from the Colorado River. The δ^{44}Ca value is –1.45 ± 0.06 per mil, only slightly different than that of the average carbonate value of –1.3 per mil. Using a fractionation factor of –1 per mil, the parental brine had a value of –0.45 per mil and supports the stratigraphic evidence that suggests a growing contribution of freshwater to the initial basin of Pliocene seawater. River water contains light calcium from weathering of old carbonates and igneous rocks exposed on the continents. Thus the world average river

water value (-1.07 per mil) is more negative than seawater but not as negative as carbonates.

The sample from the evaporative rim of Lake Meade is completely continental in nature because the lake results from the damming of the Colorado River, a freshwater source. Its $\delta^{44}Ca$ value of –1.91 ± 0.07 per mil reflects a strong continental influence of light calcium in the source waters with an inferred $\delta^{44}Ca$ value of –0.91 per mil. This value is within error of the average river water value, –1.07 per mil (Schmitt et al. 2003b). Gypsum precipitated as an evaporative rim of a freshwater lake is less likely to experience large fluctuations in calcium isotopes. The gypsum is not precipitating from a quickly concentrating saline lake, but as a result of tiny quantities of lake water splashing on rocks producing droplets which then evaporate to completion. Lake Meade does incur large evaporative losses as a result of its arid location, but the lake is still characterized as freshwater.

The late Miocene samples from the Red Sea and the Mediterranean all have similar $\delta^{44}Ca$ values. Red Sea samples are from DSDP Leg 23 Sites 225 and 227 and the Mediterranean sample is from DSDP Leg 13 Site 124 in the Balearic Basin. These massive salt deposits result from the late Messinian Salinity Crisis 5.5 million years ago, which will be discussed in depth in Chapter III. Their $\delta^{44}Ca$ values range from –0.97 to –0.28 per mil, with the Red Sea samples heavier than the one Mediterranean sample. All are considerably heavier than continental gypsums or hydrothermal anhydrites, but their $\delta^{44}Ca$ values overlap the lab precipitated anhydrite and saltworks gypsum samples. Data in Chapter III focuses solely on samples of the Messinian

evaporite and show a larger range of $\delta^{44}Ca$ (up to –1.71 per mil). As discussed in Section 2.2.3 of this chapter, a brine will undergo Rayleigh Fractionation of calcium throughout evaporation and become heavier with time as light calcium is sequestered in precipitated calcium-sulfate minerals. With little to no new addition of calcium to the brine or significant back reactions, the end result is brine with a $\delta^{44}Ca$ value of about 2.0 per mil and crystals with 1.0 per mil.

The intervals sampled in the Red Sea sediments are the heaviest naturally occurring evaporites measured in this dissertation and represent derivation from a brine that has fractionated considerably from initial seawater values. Chapter III contains more data from the late Messinian Mediterranean deposits, but the heavy values (>0 per mil) expected in evaporitic sediments are not found in those sampled intervals either. Apparently this is due to the highly dynamic and open nature of brines in nature; replenishment of the brine is a frequent phenomenon. Gypsum/anhydrite saturation of brines is common in most marine evaporative settings because new calcium is added to the system often, however this resets the calcium isotopes and erases any extremely heavy values that may have accumulated as a result of Rayleigh fractionation. Calcium sulfate minerals precipitated from a brine could produce heavier $\delta^{44}Ca$ values if deep fluids from buried ancient evaporites dissolved and migrated upwards to the sediment-water interface of a modern brine pool. These old brines could then contribute isotopically heavy calcium to an already fractionated brine. From the samples measured in this section, that scenario does not seem to be the case.

2.3.4 Conclusions

The calcium isotope fractionation factor for anhydrite precipitated in the laboratory under controlled conditions is, within measurement error, the same for 30°C and 40°C. The average of the two calculated fractionation factors is -0.95 ± 0.12 per mil. The first crystals to precipitate from an evaporating brine are generally 1 per mil lighter than the starting solution, in this case modern seawater (0 per mil). As expected, calcium isotopes follow a Rayleigh fractionation path, with the heaviest values of the brine reaching 1.15 ± 0.15 per mil and the corresponding crystals 0.10 ± 0.13 per mil. In nature, rejuvenation of the brine with calcium from continental or marine sources will reset $\delta^{44}Ca$ values and Rayleigh fractionation will start again from the new brine value. Repeating this replenishment process could lead to highly fractionated values, however data from gypsums and anhydrites in different geochemical settings is not consistent with this particular scenario.

A survey of naturally occurring gypsums and anhydrites shows a total $\delta^{44}Ca$ range of 2.18 per mil. This fairly large range of values for calcium isotopes is bounded by very light values from hydrothermal anhydrites and continental evaporites, and heavier values from late Messinian deposits in the Red Sea. This initial survey suggests that calcium sequestered in massive evaporite deposits could be significantly fractionated to light values only in continental settings where calcium from ancient carbonates and igneous rocks is incorporated into continental brines. Marine derived gypsum or anhydrite has $\delta^{44}Ca$ values between –1.0 per mil and 0 per mil (modern seawater). The marine evaporite $\delta^{44}Ca$ values are not significantly

different than the average carbonate value of –1.3 per mil. Fractionation to very heavy $\delta^{44}Ca$ values is not achieved within these brines, and these moderate values imply that the brine is continually rejuvenated with new calcium, mostly from ocean water replenishment, as the brine is kept within gypsum/anhydrite saturation. Further exploratory study into the $\delta^{44}Ca$ range of marine derived evaporitic sediments is continued in Chapter III.

Chapter III Application of Calcium Isotopes to Late Messinian Mediterranean Evaporites

The initial purpose of using calcium isotopes in relation to the Messinian Salinity Crisis was to investigate the role of saline giants in global calcium cycling as an additional sink for calcium in the oceans. These deposits have never before been investigated as potentially large sinks for calcium in the ocean. If marine basin-wide evaporites do sequester enough calcium with a unique isotopic composition, their effect must be taken into account for oceanic calcium budgets. The volume and distribution of calcium bearing sediments within the late Messinian deposits as well as the characteristic $\delta^{44}Ca$ values were needed to fit into a mass balance model. Additionally, an exploratory study into the extent of calcium isotope fractionation during gypsum/anhydrite precipitation in evolving marine brines was undertaken. The potential for large isotopic fractionation effects in these extreme environments is high and presents an opportunity to expand the limited range of calcium isotope values found on Earth.

3.1. Introduction to the Salinity Crisis

3.1.1 Timing and duration of the salinity crisis

The Messinian is the last stratigraphic stage of the Miocene on the geologic time scale, and it was during this time that the Mediterranean region experienced profound tectonic and glacio-eustatic changes, which caused complete isolation of the

Mediterranean Sea from the Atlantic Ocean. The initiation of the so-called Messinian Salinity Crisis (MSC) has been astronomically determined to be 5.96 ± 0.02 million years ago with total isolation from the Atlantic occurring between 5.59 and 5.33 Ma (Krijgsman et al. 1999). The total duration of the MSC is approximately 640,000 years. During this time massive evaporite deposits precipitated from isolated Mediterranean seawater, supplemented by water from large rivers in the region (Rhine and Nile Rivers) and also by occasional waterfalls of Atlantic seawater.

Two main salt units were deposited during the MSC in the Mediterranean, the Lower and Upper Evaporites. The high bromine content of salts from the Lower Evaporite Unit suggest that they were derived from seawater brines, implying a continuous partial connection with the Atlantic until 5.59 Ma (Hsu et al. 1977). The lower salts contain sequences of halite, anhydrite, polyhalite, and kainite and were deposited over 370 kyr (Krijgsman et al. 1999). They are restricted to the central part of each of the Mediterranean basins and are more than several thousand meters thick in some areas (Hsu et al. 1977). Once total isolation was achieved at 5.59 Ma, the solute source via Atlantic seawater ceased, and a period of erosion and non-deposition occurred. This unconformity represents the division between the Lower and Upper Evaporites. During this time local rivers cut steep canyons into the margins of the disappearing Mediterranean Sea. This time of erosion or “Messinian Gap” spanned 59 kyr from 5.59 to 5.50 Ma.

Deposition of the Upper Evaporite Unit followed the Messinian Gap at 5.50 Ma because of an inundation of Atlantic seawater, which probably filled the basin to

the brim once again (Hsu et al. 1977). Refilling and desiccation events were extremely fast, around 3-8 kyr or less, and required only a small connection with the Atlantic Ocean (Meijer and Krijgsman 2005). The upper salts are mostly halite, anhydrite, and anhydrite shales with low bromine content (less than 10 ppm) and were deposited in shallow brine pools located more than 1,000 meters below present day world sea level (Meijer and Krijgsman 2005). The 175 kyr sedimentary history of the upper salt unit is characterized by cyclical deposition of marls, gypsum, anhydrite, and stromatolitic carbonates due to numerous refilling and desiccation events (Krijgsman et al. 1999, Hsu et al. 1977).

The salinity crisis ended 5.32 Ma when the final deluge of the Atlantic filled the basin and a full and continuous connection with Atlantic seawater resumed exchange with the Mediterranean Sea. The transition to the latest Messinian flooding event is known as the Lago-Mare and is characterized by intercalation of the uppermost gypsum beds with carbonates, paleosols, and conglomerates, mostly in the sub-basins of the Eastern Mediterranean. The transition from hypersaline conditions to brackish and freshwater conditions is indicated by an increase in $\delta^{18}O$ values of the gypsums and carbonates, an increase in the carbonate fraction of the sediments, and the reappearance of brackish and fresh water organisms (Rouchy et al. 2001). Deposition of conglomerates implies rejuvenation of the fluvial system probably via reorganization of the drainage system in Europe and an inundation of Paratethyan water from Eastern Europe (Hsu et al. 1977). The Lago Mare event lasted less than 50

kyr and represents an increase of fresh water from rivers and continental runoff before the final deluge of the Atlantic.

The western Mediterranean basins may have experience limited Lago-Mare brackish water invasions over the Sicilian Channel, but sedimentary evidence suggests that restricted marine conditions dominated until the latest Messinian deluge (Hsu et al. 1977). Resumption to normal marine conditions indicating a continuous connection to the Atlantic is shown by a rapid decrease in $\delta^{18}O$ values and a sharp lithologic boundary between laminated brackish-water sediments in Eastern Mediterranean basins, laminated gypsum in the Western Mediterranean basins, and foraminifer-rich marls of the Early Pliocene (Rouchy et al. 2001).

3.1.2 Causes of the Messinian Salinity Crisis

Two main ideas have been put forward to explain onset of the MSC: Tectonic uplift of the Straits of Gibraltar and surrounding areas related to the collision of Africa and Eurasia, and/or a large global sea-level fall associated with expansion of the Antarctic Ice Sheet (Krijgsman et al. 1999). Exchange of Atlantic and Mediterranean seawater today occurs over the relatively shallow sill (600 m) at the Straits of Gibraltar. In late Miocene time (7-5.5 Ma), exchange occurred over the sill at Gibraltar and also through the Betic Straits, which are located in southern Spain along the Mediterranean coast (Weijermars 1988). Progressive uplift of the Arc of Gibraltar and folding in the Betic Straits caused the connection between the Atlantic and Mediterranean to diminish greatly at both of these seaways between 7-5.5 Ma. In

addition to the excess of evaporation over precipitation, this closure represents the beginning of the MSC because higher salinity Mediterranean seawater could not flush back out to the Atlantic Ocean, gradually increasing the salinity of the isolated seawater in the basin. At 5.59 Ma complete closure occurred because of continued uplift of the sill at Gibraltar totally isolating the Mediterranean Sea (Weijermans 1988).

The role of global sea level in isolation of the Mediterranean is tentative, with most researchers agreeing that sea level fall was not the sole cause of the MSC, but played a supporting role with regional tectonics. ODP Site 1085 in the southeastern Atlantic was used to create a high-resolution stable isotope record for global climate in the late Messinian (Vidal et al. 2002). A period of low amplitude changes in $\delta^{18}O$ ends by 6.3 Ma and is followed by a period of strong glacial events and sea level falls up until 5.57 Ma when a stage of global warming ensues (Vidal et al. 2002). The Site 1085 record shows a weak $\delta^{18}O$ increase at 5.96 Ma, with stronger events occurring at 6.05 and 6.1 Ma, predating deposition of evaporitic deposits in the Mediterranean. Paradoxically, the complete isolation event at 5.59 Ma appeared to have occurred during a period of global climate warming and sea level rise as deduced from oxygen isotopes. This timing suggests that glacio-eustatic factors did not cause the MSC, however high sea level conditions between 5.55 and 5.33 Ma could have fed seawater over the uplifted sill of Gibraltar supplying needed solutes for deposition of the Upper Evaporite Unit (Vidal et al. 2002, Clauzon et al. 1996). Termination of the MSC corresponds to a strong interglacial event, and reduced tectonic activity in the area

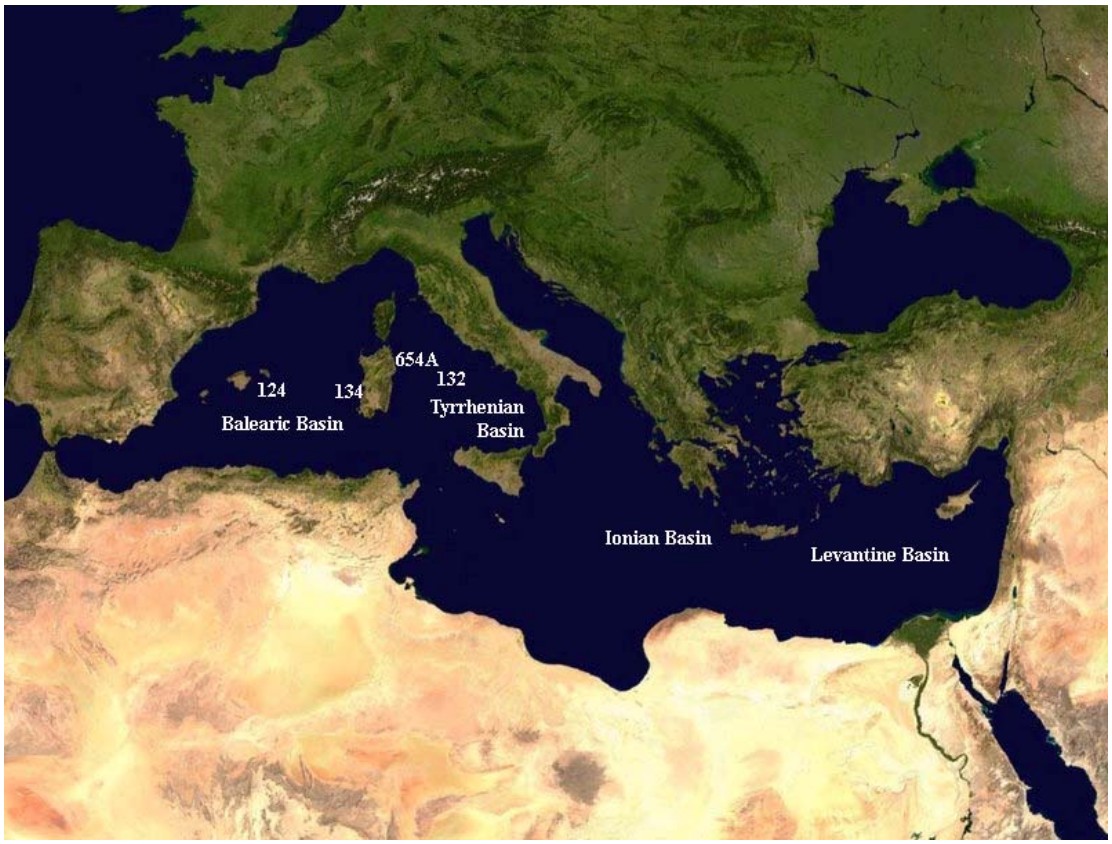

Figure 3.1.3 Satellite map of the Mediterranean region. Sites used in this study are labeled along with the deep basins where Messinian salts were discovered.

aided by this sea level high ended the 640,000-year salinity crisis.

3.1.3 Volume and distribution of salts

The Messinian Salinity Crisis in the Mediterranean resulted in the removal of at least 6% of all dissolved oceanic salts and deposited them as thick evaporite deposits with an estimated volume of one million cubic kilometers with up to two kilometer thick salts in the Balearic Basin alone (Ryan 1973). Several DSDP and ODP legs have visited the Mediterranean with the purpose of drilling into the Late Messinian salts. DSDP Legs 13 and 42 drilled salt in the Western Mediterranean in the Balearic and Tyrrhenian basins and the Eastern Mediterranean in the Ionian basin (Nesteroff 1973). Leg 42 revisited different areas of the same basins as Leg 13, but also drilled evaporites in the Antalya basin and Aegean Sea (Garrison et al. 1978). ODP leg 107 spent an entire cruise in the Tyrrhenian basin, and ODP Leg 161 visited the Alboran Sea and also drilled through Messinian salts.

Numerous land sections of evaporitic sediments also exist in Sicily, Cyprus, Spain, and Italy. These well-studied deposits represent marginal deposition during periods when sea level in the Mediterranean was slightly below present day levels. The deepest parts of the Mediterranean with the largest accumulation of salts are the Tyrrhenian, Balearic, Ionian, and Levantine sub-basins. These basins were probably not connected during extreme sea level lows in the region and represented individual saline lakes situated in the depressions of the Mediterranean seafloor (Warren 1999).

3.1.4 Summary of data from four Mediterranean sites

In order to fit evaporites into a mass balance budget for calcium in the oceans the average $\delta^{44}Ca$ value must be known. This study measured gypsum or anhydrite from four Mediterranean sites and two Red Sea sites and found the range of $\delta^{44}Ca$ values in the Late Messinian Mediterranean and Red Sea deposits to be from –0.28 to –1.72 per mil (total range 1.44 per mil) with an average value of -1.17 ± 0.40 ($2\sigma_m$) per mil. A summary of this data is found in Table 3.1.4 and Figure 3.1.4. Site 654 shows the widest variation in $\delta^{44}Ca$; however, most of the samples were taken from this site, therefore the others show much smaller variation.

Based on the survey of samples analyzed in this study, the average $\delta^{44}Ca$ for Messinian evaporites is -1.17 ± 0.40 per mil and very similar to the average $\delta^{44}Ca$ of –1.3 per mil for carbonates; however, the range of values is quite large and is larger than the range for carbonates. The average value will depend on what kind of evaporite is sampled (e.g. basin-wide vs. continental), or the geochemical conditions of the brine at any one time (freshening event vs. re-concentration of the brine). In the case of the Messinian data, deposition of evaporites will have the same effect on the calcium isotope value of seawater as carbonate sedimentation in the late Miocene; the two sink fluxes would be indistinguishable in the rock record because their characteristic average isotopic compositions are, within error, the same. If extremely rapid deposition occurred as it did during the MSC, there might be a corresponding change in the seawater value; however, residence time of calcium in the oceans is too long compared to mixing time to delineate these changes in the carbonate record (see

Table 3.1.4 $\delta^{44}Ca$ values for gypsum or anhydrite from DSDP and ODP sites 124 Balearic Basin, 132 Tyrrhenian Basin, 654A Tyrrhenian Basin, and 134 Sardinian Margin. Data is shown in Figure 3.1.4. Most Site 654A values are an average of 2 runs and standard deviation is given in $2\sigma_m$. $\delta^{44}Ca$ data for other sites only represents one TIMS run.

Sample	$\delta^{44}Ca$	$2\sigma_m$	n	Depth (mbsf)
Balearic 124-08-01	-0.8	--	1	392.59
124-09-01	-1.06	--	1	392.83
124-10-02	-0.75	--	1	395.88
124-11-02	-0.89	--	1	406.16
124-13-02	-0.89	--	1	415.25
Tyrrhenian 132-25-01	-1.72	--	1	207.16
132-27-01	-0.62	--	1	221.2
132-27R-01	-1.54	--	1	221.8
Sardinian Margin 134D-01-01	-1.61	--	1	175.93
134-10-01	-1.66	--	1	359.83
Tyrrhenian 654A-27-01-30	-1.3	0.07	2	242.7
654A-28-01-16	-1.59	0.13	2	252.14
654A-28-01-64	-1.37	0.25	2	252.64
654A-28-CCW-01	-0.53	0.03	2	261.7
654A-29-02-16	-1.59	0.19	2	263.36
654A-30-01-88	-1.44	--	1	272.18
654A-30-01-135	-1.59	0.16	2	272.64
654A-31-01-104	-0.94	0.19	2	277.34
654A-31-01-139	-1.71	--	1	277.69
654A-32-01-104	-1.06	--	1	282.22
654A-32-02-40	-1.46	--	1	282.8
654A-32-CCW-19	-1.31	0.02	2	287.6
654A-33-01-67	-0.92	0.01	2	288.26
654A-33-01-81	-1.31	0.21	2	288.4
654A-33-01-88	-1.28	0.21	2	288.49
654A-34-01-12	-1.18	0.23	2	290.71
654A-34-04-33	-1.69	--	1	295.43
654A-35-CCW-07	-1.31	0.08	2	310

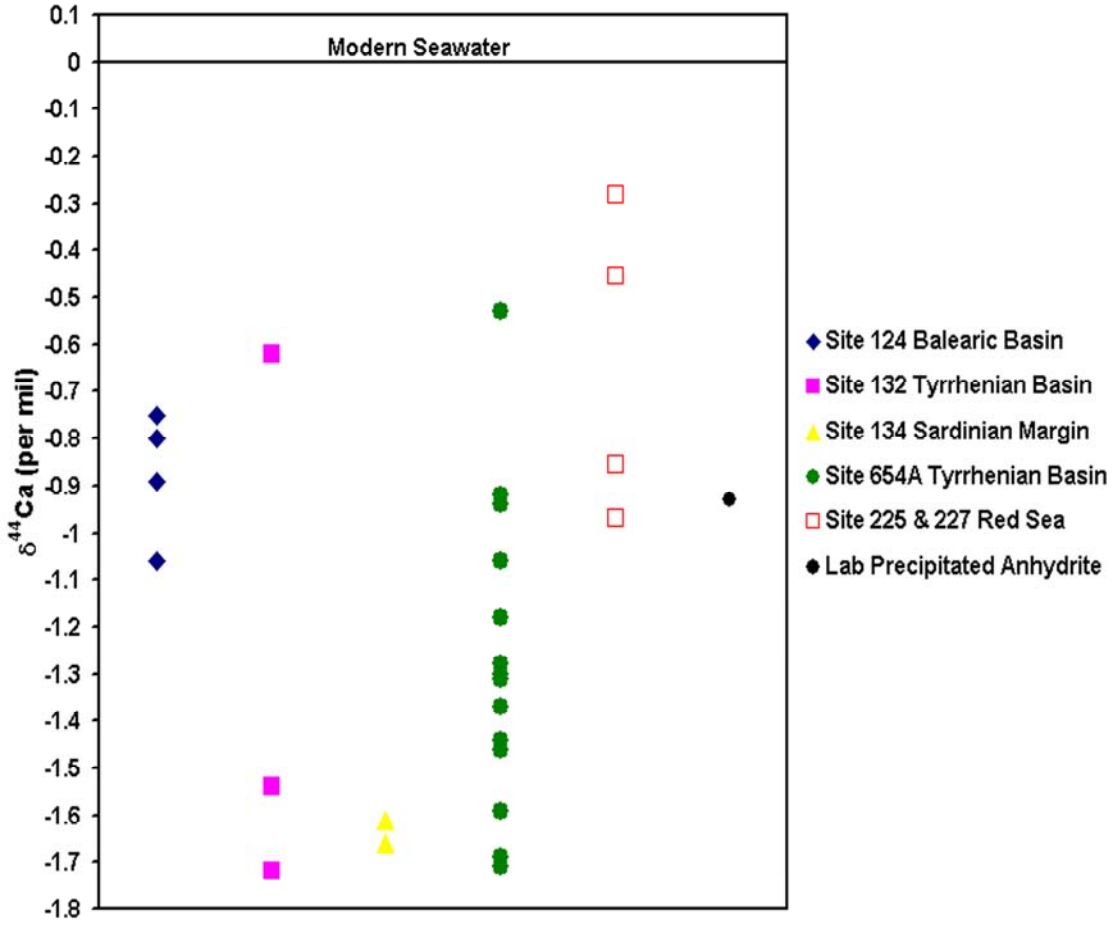

Figure 3.1.4 Summary of $\delta^{44}Ca$ values for various Mediterranean DSDP and ODP sites and two Red Sea sites 225 and 227 (data for the Red Sea samples located in Table 2.3.4). These analyses represent samples from the massive Late Miocene gypsum and anhydrite deposits of the Messinian Salinity Crisis.

Chapter IV for the late Miocene carbonate Ca isotope record). If the flux of calcium sequestered in evaporite deposits was sufficiently large and gradual as to affect the remaining pool of calcium in the oceans, a change in the seawater value might be observable, however a correspondingly large change of flux for carbonate sedimentation may also produce such a shift in the $\delta^{44}Ca$ of seawater. In the case of the MSC, 6% of the world ocean's calcium was sequestered in these large deposits in 280 kyr. The corresponding flux is $2.98 * 10^{8}$ moles/year. In contrast the average carbonate flux is $3.2 * 10^{13}$ moles/year (Milliman 1993). Five orders of magnitude separate the size of these two fluxes; combine this with the fact that evaporitic sediments have similar $\delta^{44}Ca$ values to carbonates and the possibility that the Late Messinian Salinity Crisis could affect the $\delta^{44}Ca$ value of seawater in the Late Miocene is small.

3.2 ODP Site 654 Tyrrhenian Basin: Calcium Isotopes and Brine Evolution

3.2.1 General geology and mineralogy of Site 654

The Ocean Drilling Program drilled through Messinian salts while investigating the basin evolution of the Tyrrhenian Sea during Leg 107. Gypsum deposits were found at sites 652, 653, and 654 with the largest section recovered at site 654. Total thickness of the drilled evaporite package at Hole 654A is 106 m, although the entire Messinian section was deemed incomplete as found from magnetostratigraphic studies (Pierre and Rouchy 1990). Stable isotope analyses ($\delta^{18}O$ and $\delta^{34}S$) were performed on the various gypsum deposits of Hole 654A. The same

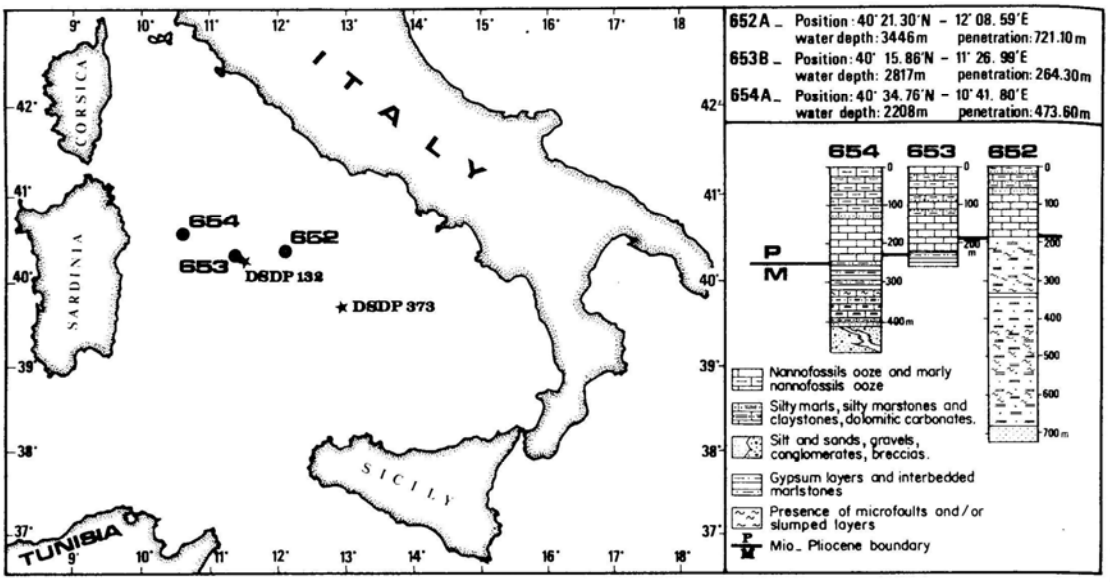

Figure 3.2.1 Map of the Tyrrhenian region taken from the Scientific Results of the Ocean Drilling Program for Leg 107 (Pierre and Rouchy 1990). Site 654 is located on the Sardinian margin in 2208 m of water. The entire core penetrated 473.6 m with 106 m of gypsum deposits drilled. During the MSC, the Tyrrhenian Sea may have been isolated from other Eastern and Western Mediterranean basins by extremely low water levels, and would have its own chemical evolution different than other bathymetrically deep, but shallow water basins in the region.

sample intervals used in the ODP study were analyzed for calcium isotopes in this dissertation with the aim of comparing/contrasting fractionation of calcium isotopes in precipitated gypsum with other more well known stable isotope systems. It is unknown how the two factors affecting calcium isotopes in precipitated minerals, initial brine isotopic chemistry plus Rayleigh fractionation, interact in a natural evaporative setting. In addition, Sr isotopes were measured on the same samples in order to shed light on the sources of water to the shallow Tyrrhenian basin during the MSC.

Several types of gypsum were found at site 654A, but the majority of the samples used in the study are regular laminated gypsum or wavy laminated gypsum. The regular laminated gypsum or "balantino"-type gypsum does not have a unique mode of deposition, but form by destruction of crystalline crusts that develop at the margins of evaporitic ponds, which are then locally reworked by currents or periodic flooding events, or could also form during seasonal concentration of marine waters (Pierre and Rouchy 1990). The laminations are millimeters thick and have alternating light and dark bands. Wavy laminated gypsum lacks algal relics, but the form suggests both depositional and diagenetic processes that include precipitation in the presence of an algal coating and overgrowths precipitated from an interstitial brine (Pierre and Rouchy 1990)

3.2.2 Previous isotope analyses for Hole 654A

Oxygen and sulfur isotopic analyses have been reported on the sediments from Site 654 Leg 107 (Pierre and Rouchy 1990). $\delta^{34}S$ data show a wide range from 20.3 to 23.4 and $\delta^{18}O$ data also exhibits a large range of values from 15.1 to 20.3. These values argue for a marine origin of the evaporites in the Tyrrhenian basin during the late Messinian; the basin was connected at times with the Atlantic through western Mediterranean basins and the water depth was shallow. High sulfur isotope values in the gypsum result from intense activity of sulfate-reducing bacteria, increasing the heavy component in the remaining sulfur pool from which gypsum will precipitate. Oxygen isotopes are also affected during sulfate reduction, with heavy oxygen expelled to the remaining pool. In addition oxygen isotopes record evaporation/dilution of the brine. Both of these stable isotopes systems are recording organic or inorganic processes and may even reflect reservoir effects because of massive gypsum precipitation (Pierre and Rouchy 1990).

In contrast to oxygen and sulfur isotopes, strontium isotopes do not fractionate due to temperature, salinity, biological activity, or reservoir effects. Leg 107 participants selected nine samples of Hole 654A for Sr isotope analysis with the hope of dating the deposits using the global seawater Sr isotope curve (Muller et al. 1990). Unfortunately this was not possible because the connection to the Atlantic was not continuous and originally marine waters were diluted significantly by continental runoff. The $^{87}Sr/^{86}Sr$ variation of Hole 654A gypsum is large (0.708866 to 0.708605) and lower than late Miocene seawater (0.70891 to 0.70902). The lower $^{87}Sr/^{86}Sr$

values are expected with increased riverine input since rivers draining the Northern Mediterranean region have less radiogenic Sr due to an abundance of mafic rocks and Mesozoic limestones (Muller et al. 1990). The strontium content of Hole 654A gypsum deposits is lower (410-902 ppm) than gypsum precipitated directly from seawater (1500-2300 ppm), which suggests that the gypsum has been chemically reworked in the presence of a fluid with changing Sr concentration and $^{87}Sr/^{86}Sr$ ratios (Muller et al. 1990). The authors of the Leg 107 strontium study prefer the term chemically reworked instead of diagenesis because gypsum can dissolve and re-precipitate very quickly after primary formation in a brine that is similar to the initial brine. Chemical reworking causes the deposits to undergo early lithification, after which the system becomes closed to new additions of less saline waters (Muller et al. 1990).

If strontium isotopes show regular and large variation, calcium isotopes should also exhibit wide variation since the $\delta^{44}Ca$ value of the brine will change with addition of new waters, either marine or fresh, following the behavior of strontium isotopes. In addition, Rayleigh fractionation will affect the calcium isotope values of the brine depending on the amount of gypsum or anhydrite precipitation. Neither Ca nor Sr isotopes are affected by biological activity or redox conditions as are O and S isotopes. Therefore it is not expected that $\delta^{44}Ca$ values will follow $\delta^{34}S$ changes in the sediments since the two systems do not share the same controlling factors. Similarly, $\delta^{44}Ca$ of the gypsum in Hole 654A should not closely follow $\delta^{18}O$ values since sulfate reduction influences oxygen isotopes. However the two isotope systems both track

Table 3.2.3 Hole 654A data for stable and radiogenic isotopes. ^{18}O and ^{34}S data are from Pierre and Rouchy (1990). Calcium and strontium isotope analyses are from this study.

MBSF	Sample	Lithologic Description	$\delta^{44}Ca$	$2\sigma_m$	n	$\delta^{18}O$	$\delta^{34}S$	$^{87}Sr/^{86}Sr$
242.7	654A-27-01-30	laminated gypsum	-1.30	0.07	2	18.1	22.4	0.708772
252.14	654A-28-01-16	wavy laminated gypsum	-1.59	0.13	2	17.7	22.4	0.708766
252.64	654A-28-01-64	wavy laminated gypsum	-1.37	0.25	2	18.3	22.1	0.708764
253.93	654A-28-02-43	selenite in siltstone	-1.59	0.15	2	--	--	0.708819
261.7	654A-28-CCW-01	laminated gypsum	-0.53	0.03	2	19.3	20.3	0.708777
263.36	654A-29-02-16	laminated gypsum	-1.59	0.19	2	20.3	22.9	0.708768
272.18	654A-30-01-88	laminated gypsum	-1.44	--	1	18.2	22.1	0.708789
272.64	654A-30-01-135	wavy laminated gypsum	-1.59	0.16	2	18.3	22.1	0.708766
277.34	654A-31-01-104	crystalline gypsum	-0.94	0.19	2	17.6	20.6	--
277.69	654A-31-01-139	laminated gypsum	-1.71	--	1	18	22.1	0.708784
282.22	654A-32-01-134	laminated gypsum	-1.06	--	1	18.7	22.2	0.708808
282.8	654A-32-02-40	laminated gypsum	-1.46	--	1	18.8	22.1	0.708802
287.6	654A-32-CCW-19	wavy laminated gypsum	-1.31	0.02	2	19.4	22.7	0.708814
288.26	654A-33-01-67	crystalline gypsum	-0.92	0.01	2	18.1	23.1	0.708800
288.4	654A-33-01-81	laminated gypsum	-1.31	0.21	2	17.8	21.3	--
288.49	654A-33-01-88	wavy laminated gypsum	-1.28	0.21	2	18	21.1	--
290.71	654A-34-01-12	saccharoidal gypsum	-1.18	0.23	2	18.3	22.9	0.708720
295.43	654A-34-04-33	laminated gypsum	-1.69	--	1	18	23.4	0.708804
310	654A-35-CCW-07	laminated gypsum	-1.31	0.08	2	15.1	22.3	0.708884

addition of new isotopically distinct waters to the brine, and at times of rejuvenation they may shift in unison.

3.2.3 $\delta^{44}Ca$ and $^{87}Sr/^{86}Sr$ data for Site 654

Calcium isotope data of evaporitic sediments at Hole 654A in the Tyrrhenian Sea show a total $\delta^{44}Ca$ variation of 1.18 per mil. The lightest value is –1.71 found at 277.69 mbsf, and the heaviest value is –0.53 per mil at 261.7 mbsf. The average value of 19 samples spaced over the entire interval of salt drilled at Hole 654A is –1.34 ± 0.32 per mil. The data are shown in Figure 3.2.3a and listed in Table 3.2.3. The $\delta^{44}Ca$ range is considerable and indicates that changes in brine chemistry are frequent and large, which is expected for a shallow body of water undergoing constant rejuvenation from either marine or freshwater. Shifts toward light values, as seen at 295.43 mbsf, indicate the intrusion of continental runoff or a riverine input, because light calcium concentrated in old, exposed carbonates is incorporated into runoff. Conversely, shifts toward heavier values indicate either an addition of late Miocene seawater or precipitation of calcium-sulfate minerals following a Rayleigh fractionation path during concentration of the brine. Using only calcium isotopes, it is impossible to tell if a shift toward heavy values is due to the presence of seawater or high precipitation rates, but if strontium isotopes are also used, the two processes may be separated.

Strontium isotope analyses were performed on 16 of the 19 samples from Hole 654A that were measured for Ca. Since there is no fractionation of strontium isotopes

during precipitation of minerals, the isotopic signature should reflect the composition of the brine, which is in turn affected by all sources of water to the pool. All $^{87}Sr/^{86}Sr$ values measured in this work are well below that of late Miocene seawater indicating a significant riverine dilution. The observed total range is from 0.708884 (more radiogenic) to 0.708720 (less radiogenic). In general, these data support the conclusions reached by Muller et al. (1990) although different samples were analyzed. Figures 3.2.3b and 3.2.3c display both the Sr and Ca isotope data. Figure 3.2.3c plots the two data sets together to illustrate agreement and disagreement between the behavior of Ca and Sr isotopes in order to determine if seawater intrusion or Rayleigh fractionation associated with rapid precipitation caused shifts to heavier $\delta^{44}Ca$ values.

The correlation between Ca and Sr isotopes is poor. There is no consistent trend correlating light $\delta^{44}Ca$ with less radiogenic $^{87}Sr/^{86}Sr$ values, indicative of a freshwater event. Similarly, heavy $\delta^{44}Ca$ and radiogenic $^{87}Sr/^{86}Sr$ values, suggesting a seawater incursion, generally do not coincide within the 106 m evaporite section. The r-value of correlation is a low 0.13. One way to illustrate this disagreement is by calculating the percentage river water/seawater contribution to the brine for each isotope system. Simple two-end-member mixing is assumed for both Ca and Sr isotopes (river water and seawater) with a fractionation factor of –1 per mil taken into account for the Ca analyses in order to determine the brine composition from which the Ca-sulfate precipitated. The weighted average of world river water for calcium isotopes is –1.07 per mil (Schmitt et al. 2003b) and this value is used in lieu of a Rhone river water value since this river has not been analyzed for Ca isotopes.

Seawater is assumed to be zero per mil. For Sr isotopes, the modern Rhone river water $^{87}Sr/^{86}Sr$ ratio is 0.70872 and the late Miocene seawater value is taken as 0.7091. Figure 2.3.2d shows the percentage riverine contribution to the brine for each isotope system.

The majority of the Sr isotope analyses indicate a greater than 50% riverine contribution to the brine throughout the entire section, and in most cases the Sr data indicate a higher percentage freshwater than the Ca isotopes suggest. The difference between the two estimates can be evaluated in terms of two groups: less than 30% disagreement and greater than 40% disagreement. The less than 30% group falls on both sides of the 1:1 agreement line, with Ca isotopes sometimes suggesting a greater riverine influence and other times Sr isotopes suggesting a larger freshwater contribution to the brine. If measurement error for both sets of analyses is considered, these differences are minimally significant.

There are six data points that show a significantly large disagreement (greater than 40%) between the Ca and Sr riverine percentage consistently biased toward a low riverine contribution for Ca isotopes and a high contribution for Sr isotopes: depths 290.71, 288.26, 282.22, 261.7, 252.64, and 242.7. The strontium isotopes indicate as much as 100% riverine contribution down to 50% during these intervals, whereas the Ca isotopes only suggest as much as 35% riverine contribution down to less than zero (an impossible scenario). One way to explain this large discrepancy is to invoke Rayleigh fractionation of calcium isotopes associated with rapid precipitation of gypsum during a freshwater event. The precipitation takes place at a rate that is equal

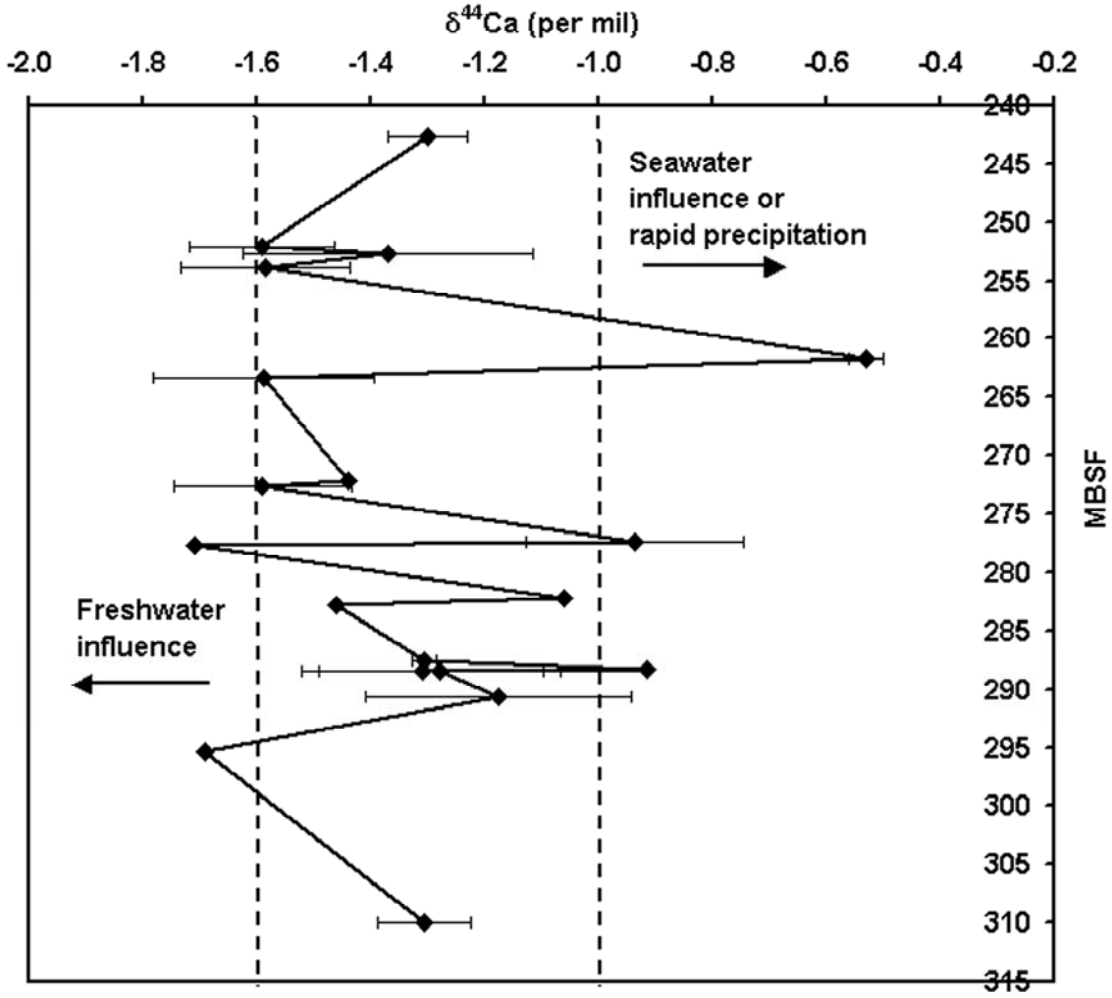

Figure 3.2.3a δ^{44}Ca data for Hole 654A Tyrrhenian Sea. Each data point represents the mean of at least two TIMS runs, with the exception of five samples where there is only one run, and the error bars represent $2\sigma_m$. The dashed vertical lines represent ± 0.32 per mil the standard deviation of the mean value of –1.34 per mil. Values around –1 per mil either represent direct precipitation from seawater or are the result of Rayleigh fractionation of the brine. Shifts to lighter values indicate addition of a freshwater continental influence.

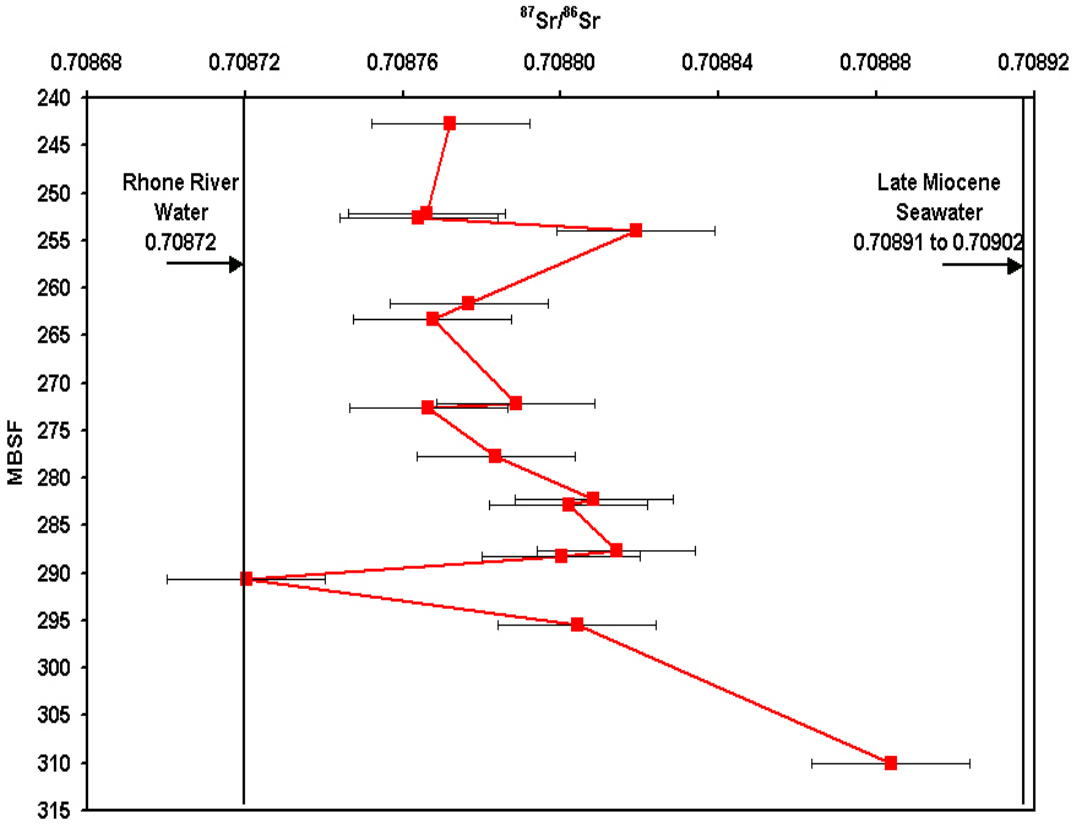

Figure 3.2.3b Strontium isotope data for 16 of the 19 samples from Hole 654A. All values are well below that of late Miocene seawater indicating a significant freshwater influence. Shift to less radiogenic (lower) values represent addition of freshwater. In the late Miocene the Rhone River would have been the most likely source for this water. Shifts to more radiogenic values indicate intrusion of seawater.

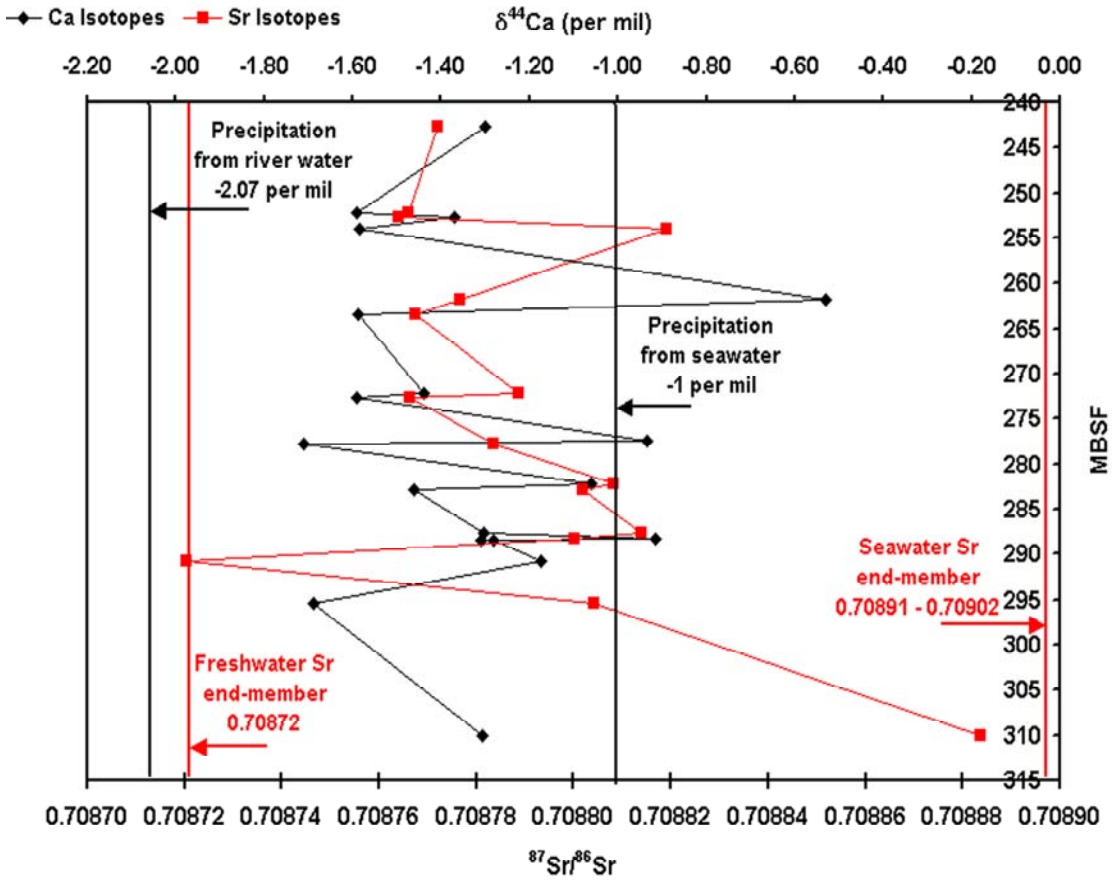

Figure 3.2.3c $\delta^{44}Ca$ and $^{87}Sr/^{86}Sr$ data for Hole 654A. A majority of the calcium analyses fall between precipitation from pure seawater (-1 per mil) and precipitation from pure river water (-2.07 per mil). Sr isotopes show a range of values between two end-members, late Miocene seawater and Rhone river water. The two isotopes systems show little correlation throughout the 106 m sampled interval (shifts toward lighter values are not correlated with shifts toward radiogenic values and visa versa). There are instances where the discrepancy between Ca and Sr isotopes is significantly large suggestive of a unique process. The strontium data at depths 290.71, 261.7, and 252.64 indicate either an influx of river water from the continent or do not change significantly, whereas the calcium data show a shift to heavy values characteristic of either a seawater incursion or Rayleigh fractionation associated with rapid precipitation of gypsum, or do not show a significant change at all.

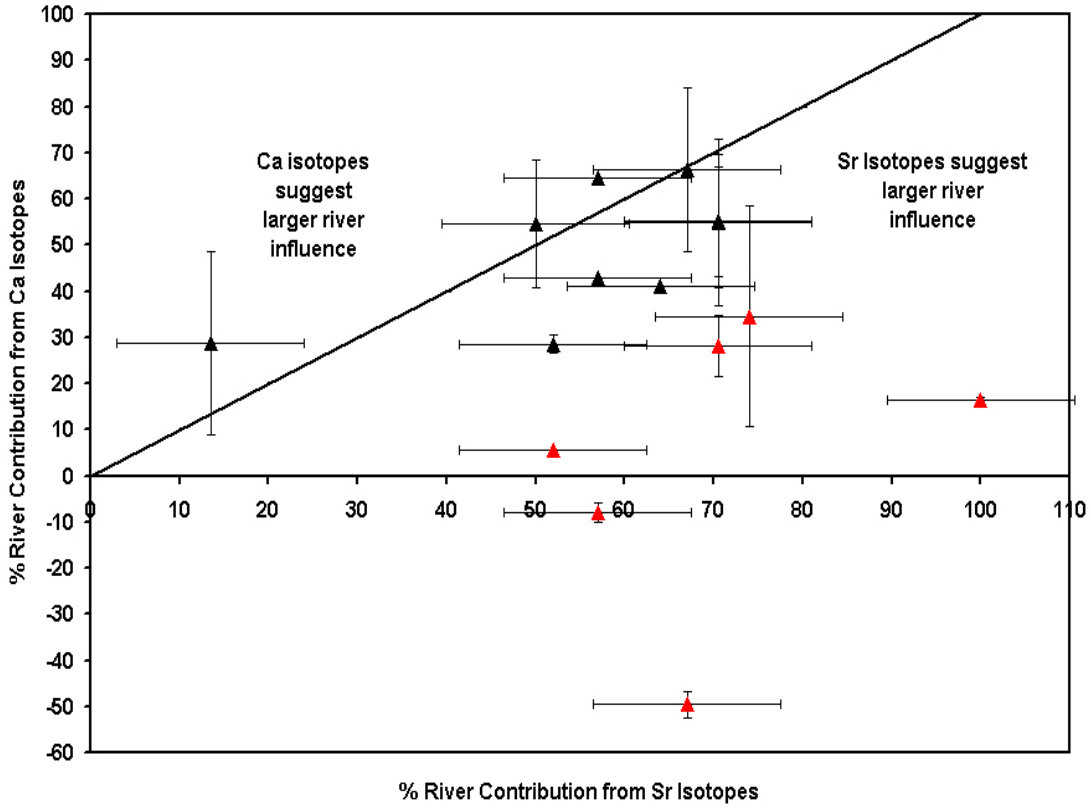

Figure 3.2.3d Sr and Ca isotopes are used to estimate the percentage of river water to the Tyrrhenian Basin during deposition of the upper evaporite. A majority of the time Sr isotopes suggest a larger riverine contribution than do Ca isotopes. With the exception of the red triangles, most of the samples fall close to (within 30%) of the 1:1 line. The samples denoted by red triangles reflect high disagreement between the two isotope systems (greater than 40%) with Sr isotopes suggesting 50-100% river water contribution and Ca isotopes suggesting little freshwater influence or impossible negative river water contributions. These discrepancies between the two isotope systems could be due to Rayleigh fractionation associated with rapid precipitation of gypsum that occurred at a faster rate than the influx of freshwater to the basin. Sr isotopes would not be affected by this process and thus would record the true isotopic composition of the brine, while Ca isotopes are actually recording a reservoir effect.

to or greater than the influx of new Ca^{2+} to the brine. This will push the $\delta^{44}Ca$ composition of the brine to heavier values because of the fractionation factor between precipitated gypsum/anhydrite and ambient water. Precipitation of gypsum preferentially removes ^{40}Ca from the evolving brine so quickly that even though new light calcium is injected into the system, it is not available fast enough to compensate for the rate of gypsum precipitation. As a result, precipitated gypsum progressed to heavier values. Strontium isotopes are not affected by mineral fractionation; therefore the Sr ratio recorded in the gypsum samples is the "true" isotopic composition of the brine, and the percentage of river water to the brine calculated from the $^{87}Sr/^{86}Sr$ ratios is the baseline for comparison to the Ca isotope based percentages. When the Ca isotopes suggest little to no riverine contribution and the Sr isotopes suggest large freshwater events, as is seen by the samples denoted with red triangles of Figure 3.2.3d, Rayleigh fractionation could explain the disagreement rather than an incursion of seawater which is not supported by the Sr isotopic evidence.

It is also possible that during chemical reworking, which may occur soon after gypsum formation, Sr isotopes experience alteration while Ca isotopes do not. This could explain disagreement between the two isotope systems. Strontium is a trace element in sulfate minerals that may be more susceptible to small changes in the isotopic composition of the interstitial brine. Calcium is a major element in sulfates and would be less sensitive to isotopic changes induced by chemical reworking. Unfortunately there is no lithologic indicator for rapid deposition of Ca-sulfate in these sediments as evidence for the Rayleigh fractionation hypothesis, and the

possibility of strontium's preferential alteration as an explanation for Ca-Sr isotope disagreement cannot be eliminated.

Rayleigh fractionation remains a convenient explanation for the disagreement between the two isotope systems. Although salinity drops during a freshwater event, as long as the salinity of the brine is maintained within gypsum saturation (4 to 11 times the concentration of seawater), gypsum will precipitate. Given the shallow nature of these brine pools, concentration of the brine could occur quickly after a freshening event, with the freshwater input supplying needed Ca^{2+} to the brine. Although this calcium would have a lighter isotopic signature initially, precipitation of gypsum will force the brine to heavier values. This is especially true since freshwater intrusions are probably periodic events, only supplying calcium for a limited time.

Oxygen isotopes of gypsum show almost no correlation with calcium isotopes at Hole 654A. Since $\delta^{18}O$ is affected by sulfate reduction, a process that has no influence on $\delta^{44}Ca$, it is not expected that the two records will correlate; however, oxygen isotopes record sources of new isotopically distinct waters to the brine similarly as calcium isotopes. There are intervals in the record where $\delta^{18}O$ and $\delta^{44}Ca$ show general agreement, but the calcium data usually exhibit shifts not mirrored in the oxygen data even within sections with correlation. For example, from 293 to 278 mbsf, both oxygen and calcium isotopes show a shift toward lighter values, with the exception of one data point at 282.2 mbsf where the calcium data shifts to a heavy value before shifting back to progressively lighter values. Again from 262 to 252 mbsf, oxygen and calcium isotopes show movement toward light values indicating an

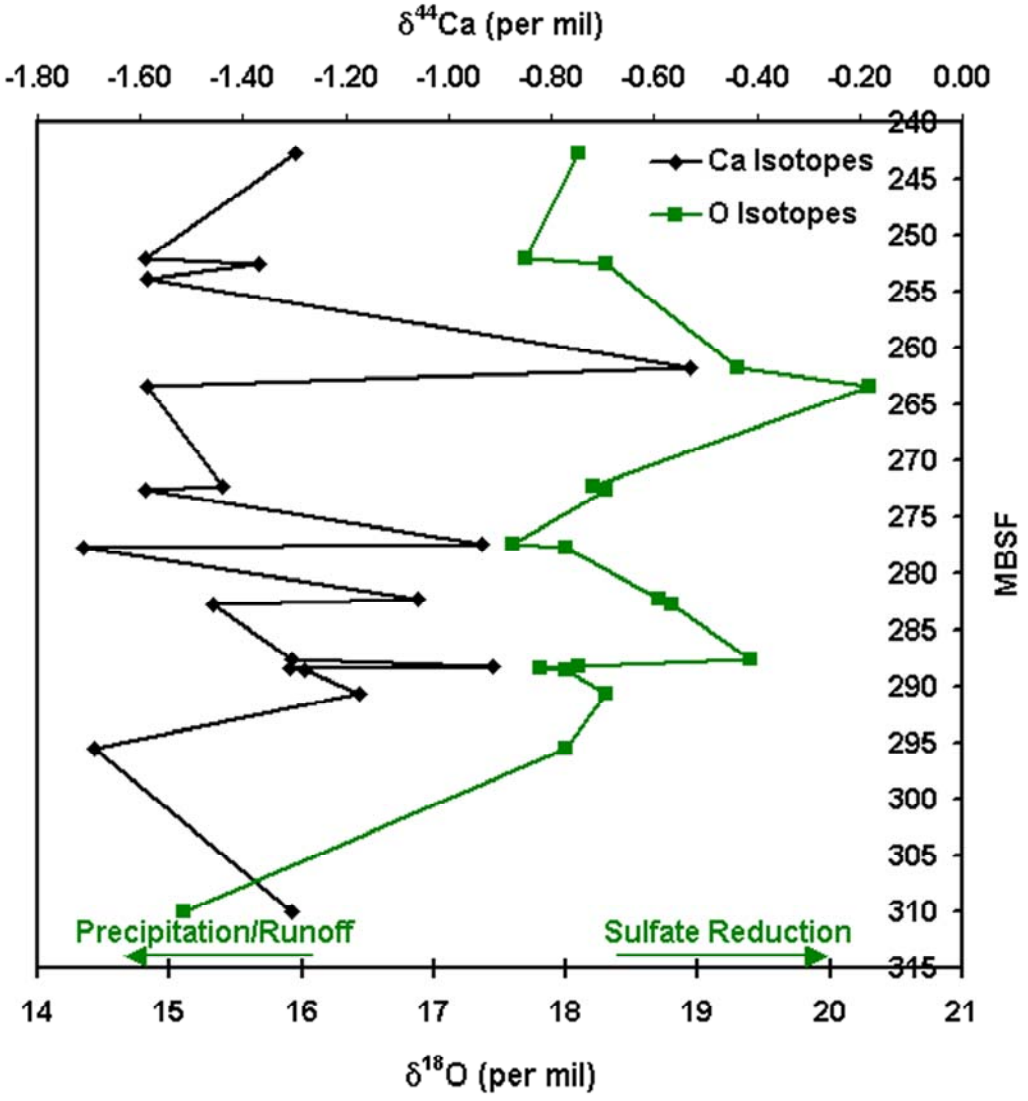

Figure 3.2.3e $\delta^{18}O$ and $\delta^{44}Ca$ data for Hole 654A. Lighter oxygen values suggest precipitation or continental runoff while heavier values indicate intense sulfate reduction within the brine. Correlation with the calcium record is weak, however there are intervals where the two roughly agree suggesting that both are sometimes recording introduction of continental waters to the brine.

addition of fresh or meteoric waters to the brine. The relationship between these two isotope systems is vague.

3.2.4 Testing external precision

The sample at 261.7 MBSF was processed three times in order to determine the external precision of this study. The initial value was –2.57 ± 0.16 per mil, a highly suspect value that indicated an impossibly large contribution of freshwater to the brine and was unsupported by Sr isotopic evidence. This anomalously light calcium value is difficult to explain in terms of Rayleigh fractionation since mineral precipitation should deplete the remaining brine in light calcium and minerals should show heavier values. Strontium isotopes do not indicate a freshwater event, but somehow the calcium in this sample, representing the δ^{44}Ca of the evaporating brine, is isotopically light. All other samples in the 654A section fell within reasonable limits of precipitation from seawater, river water, a mixture of the two, or indicated Rayleigh fractionation. This sample was chosen, first to check the anomalous value, and then also to test the external precision of the 654A exploratory study. The sample was re-processed from the beginning, starting with a new crushed sample and following through to dissolution, column elution, filament loading, and measurement. This re-processing was performed on two extra splits of the sample.

The results indicated that the initial sample was contaminated by intercalated dolomitic ooze thus giving the anomalously negative δ^{44}Ca value of –2.57 per mil. The two extra splits did not duplicate this very light value, but instead gave values of

–0.53 ± 0.03 and –0.58 ± 0.21 per mil. One explanation for the initial highly negative value is that during sampling in the lab, intercalated dolomitic ooze was incorporated into the gypsum sample. The wavy laminations within the samples are sometimes quite thick and these dark intervals have a higher concentration of carbonate in the form of inorganically precipitated dolomite. Several intercalated dolomitic oozes from DSDP Leg 13 Site 124 were sampled and measured for Ca isotopic composition in order to find the average dolomitic ooze δ^{44}Ca. These sediments had an average δ^{44}Ca of –2.02 per mil and the lightest sample measured was –2.60 per mil, considerably lighter than the δ^{44}Ca range of marine gypsum/anhydrite values. It is possible that the sample from 654A 261.7 MBSF contained a small quantity of dolomitic ooze thus lowered the δ^{44}Ca value. The light value of –2.57 per mil is very unusual in context of other δ^{44}Ca data on gypsum at Hole 654A and in terms of measured marine gypsum or anhydrite data as discussed in Chapter II of this dissertation. Therefore it is likely that this sample had experienced some contamination, and of course was not reflective of the true chemistry of the brine.

As for external precision of the 654A study, the two additional splits of the sample at 261.7 MBSF show high agreement (-0.53 and –0.58 per mil). These samples show no contamination by dolomitic carbonates and are firmly in the range of δ^{44}Ca for all measured gypsum and anhydrites in this study. As long as contamination by dolomitic carbonates when sampling is avoided, the processing of 654A samples appears to be robust. This new value actually suggests considerable Rayleigh fractionation of the brine, as the $^{87}Sr/^{86}Sr$ ratio for this sample is 0.70878 and indicates

a 67% river water contribution to the brine, but the Ca isotopic estimate for river water contribution is an impossible –50%.

3.2.5 Conclusions for Site 654

Gypsum deposits have never before been analyzed for calcium isotope variation. This study used the massive late Messinian salt deposits of the Mediterranean to explore calcium isotope fractionation in precipitated gypsum and anhydrite as a brine chemically evolves through time. The range of δ^{44}Ca data is large (1.63 per mil) as compared to the total known variation of calcium isotopes in nature (3-4 per mil), but not as large as would be expected for such an extreme geochemical environment. The average value of all Hole 654A sediments analyzed is –1.44 per mil, very similar to the average carbonate value of –1.3 per mil, although the total range of δ^{44}Ca is larger than for carbonates, and the average will depend on type and particular interval of evaporites that are measured. In this case, deposition of large evaporite deposits will have the same affect as carbonate deposition on the δ^{44}Ca value of seawater. In terms of Ca fluxes, evaporite deposition during the late Miocene is five orders of magnitude smaller than carbonate deposition, suggesting this saline giant, in spite of the massive size of the deposits, had little observable effect on calcium cycling in the world's oceans. Other saline giants deposited throughout the Phanerozic had larger accumulations of gypsum/anhydrite than the late Miocene Mediterranean deposits, therefore it is possible that deposition of these massive salts

could have equaled or exceeded carbonate sedimentation at a particular time (e.g. the Permian).

In general, calcium isotopes are poorly correlated with strontium isotopes at Hole 654A. This disagreement is best illustrated by calculating the percentage riverine contribution to the brine for each isotope system using assumed characteristic end-members for river water and seawater. Strontium isotopes predict larger freshwater additions to the brine than do calcium isotopes in most samples. For samples with very large disagreement between Ca and Sr freshwater estimates (Ca indicating low freshwater percentage and Sr indicating high freshwater percentage), Rayleigh fractionation associated with rapid deposition of gypsum during a freshwater event could explain the usually heavy $\delta^{44}Ca$ values (thus low riverine percentage). The precipitation of gypsum during these intervals occurs at the same rate or faster than delivery of new isotopically light calcium to the brine, thus pushing the $\delta^{44}Ca$ of the brine to unexpected heavier values. The relationship between calcium and oxygen isotopes is less clear than with strontium isotopes. Biological processes as well as evaporation/precipitation and addition of isotopically distinct water sources to the brine affect oxygen isotopes. These processes obscure any detailed relationship between calcium and oxygen isotopes and only general similarities in geochemical trends are seen in the record.

The use of calcium isotopes as a geochemical tool for understanding large saline deposits is promising, however they should be used in conjunction with other isotope systems or chemical proxies to support conclusions. Calcium isotopes could

be used in the future, in conjunction with Sr isotopes, to evaluate the rate of gypsum precipitation in basin-wide evaporites. Periods of very rapid deposition as indicated by Ca isotopes could provide information on basin subsidence or rapid localized climate changes.

The potential for large fractionation effects or extremely heavy $\delta^{44}Ca$ values in evaporite deposits is small given the continuous, but possibly pulsed, nature of rejuvenation needed for large accumulation of salts. Small deposits in isolated basins or coastal settings may be more likely to have unusually heavy values, but large deposits, which are constantly isotopically reset, have little potential to exhibit anomalous values. High-resolution sampling may reveal more extreme values. In the future, improvements in measurement precision will compensate for the small range of calcium isotope fractionation in nature as compared to other stable isotope systems, expanding its use in geochemical studies.

Chapter IV A Calcium Isotope Record for Bulk Carbonates, 0-12 Ma Eastern Equatorial Pacific

4.1 Introduction

One of the several applications of calcium isotopes to the field of geochemistry is their use in examining the marine biogeochemical budgets of calcium. Such studies, probing the strength of calcium fluxes into and out of the ocean, can shed light on global weathering trends, average carbonate sedimentation rates, and the range of seawater calcium concentration in the geologic past. There are few proxies available to earth scientists that can approximate these relatively unconstrained fluxes. Calcium isotope records of carbonate sediments may be valuable tools to investigate the intersection between global weathering input of major elements to the ocean and the response by calcifying organisms.

Similar to osmium or strontium isotopes, the calcium isotopic record of carbonates should reflect the strength of the weathering flux of calcium to the oceans. However, two important differences separate calcium isotopes from strontium and osmium isotopes: calcium isotopes will not significantly reflect the selective weathering of lithologies with different isotopic signatures, and calcium has an oceanic sink, marine carbonate sedimentation, with a significant isotope fractionation effect that works to buffer the $\delta^{44}Ca$ of the oceans through time. These differences have both advantages and disadvantages for global element cycling studies and will be discussed later in more detail.

The purpose of this study was to measure bulk carbonates samples spaced evenly every 500 kyr through the late Miocene, Pliocene, and Pleistocene to fill a gap in the calcium isotopic record of carbonates/seawater. Previous studies have focused on longer time scales, but with sparse sampling that gave a highly generalized record of $\delta^{44}Ca$ through geologic time (De La Rocha and DePaolo 2000, Schmitt et al. 2003a, Skulan et al. 1997, Zhu and Macdougall 1998b). One exception is Fantle and DePaolo (2005) who presented a 20 Ma Ca isotope curve for nannofossil oozes at DSDP 590B with a very high sampling resolution. This study will be discussed later in the chapter when new data for the past 12 Ma is presented. Other studies have zeroed in on interesting biogeochemical events, such as extreme climate change following the Ghaub Glaciation in the Neoproterozoic (Kasemann et al. 2005), but the Ca isotopic record for the last 15 Ma has been poorly represented. The residence time of Ca in the oceans is long (1 Ma) compared to the mixing time of the ocean (1 kyr), therefore sampling spaced much closer than one million years may actually measure local excursions, not the desired global record. This study sampled bulk carbonates at 500 kyr intervals for the last 12 Ma to examine changes (or lack thereof) of the calcium isotopic composition of seawater even though the residence time is 1 Ma in order to verify any sustained global changes. Calcium carbonate isotopic variation should be the result of changes in the strength of Ca fluxes into and out of the ocean (De La Rocha and DePaolo 2000, Fantle and DePaolo 2005). Complications to this model will be discussed in later sections.

Significant cooling of the Earth's climate has occurred over the past 50 Ma, for the most part gradually but with a sharp temperature drop in the early middle Miocene (Miller et al. 1987). Some researchers have suggested that late Cenozoic cooling (40 Ma to present) was caused by tectonic uplift of the Tibetan Plateau (Raymo and Ruddiman 1992). Reactions involving chemical weathering of Ca-silicates from increased mechanical erosion rates drew down CO_2 in the atmosphere and pumped large amounts of calcium (and other important elements like Si and P) into rivers that drained the region. Lowered atmospheric CO_2 sustained the cooling trend and ever since the collision of India with Eurasia the climate has continued to exhibit global cooling from this positive feedback cycle. Pulses of rapid tectonic activity are seen superimposed on the overall uplift in the Tibetan region, for example at 8 Ma initiation of the Indian Monsoon indicates an increase in the elevation of the Tibetan Plateau (Molnar et al. 1993). Calcium loads in local rivers should have increased in response to the uplift and initiation of strong seasonal rains. Given that calcium isotopes of carbonates reflect the strength of sources and sinks of Ca to seawater, a calcium isotope record for the past 12 Ma would encompass several hotly debated controversies in paleoceanography. Comparing a calcium isotope record to previously published Os and Sr isotopic data not only illuminates current questions in the weathering history of the past 12 Ma, but also adds knowledge to an isotopic system (calcium) that is not entirely understood.

4.2 ODP Leg 138 Site 850 Eastern Equatorial Pacific

4.2.1 Overview

Ocean Drilling Program Leg 138 drilled in the eastern equatorial Pacific with the primary goal of collecting information on the ocean's response to global climate change in the Neogene (Pisias et al. 1995). One of the major accomplishments of this leg was the development of a very high-resolution late Neogene geologic time scale, which supported tight stratigraphic age control for the other paleoceanographic objectives of Leg 138 (Shackleton et al. 1995). Although high-resolution sampling for Ca isotopes was not needed in this study because of the long residence time of Ca in the oceans, the tight age control was helpful in determining consistent spacing of carbonate samples for analysis. Also, the geochemical and paleoceanographic findings of Leg 138 formed a basis for comparison to a Ca isotopic study. Two interesting intervals were found in the stratigraphic record of Leg 138 sites: a decline in carbonate fluxes and concentrations from 11.2 to 9.8 Ma with a pronounced "carbonate crash" and almost complete loss of carbonate at most sites from 9.8 to 9.0 Ma, and an extremely large increase in carbonate accumulation, a "biogenic bloom", from 6.7 to 4.5 Ma (Pisias et al. 1995). Both events appear to have counterparts in other oceans such as the Indian, Atlantic, and central, north, and western equatorial sites in the Pacific and therefore may signal global changes in oceanic Ca fluxes.

4.2.2 The carbonate crash

The dissolution event centered at 9.5 Ma at Leg 138 sites was perhaps the strongest dissolution event in the entire late Neogene (Farrell et al. 1995). The Calcite Compensation Depth (CCD) was thought to shoal by more than 1400 m causing all of the sites, except for 850 and 851, which were the shallowest of the sites, to experience severe dissolution. The carbonate crash is identified in the sediments by extremely low calcium-carbonate percentages and MARs (Mass Accumulation Rates) (Lyle et al. 1995) and from poor nannofossil preservation (Farrell et al. 1995). Interestingly, the opal MARs remained the same before, increased during, and returned to pre-crash levels after the crash indicating a change in ocean alkalinity rather than a change in productivity. Recovery from the crash is seen from 8.9 to 7.5 Ma by gradually increasing calcium-carbonate percentages.

The causes of this event are still debated, but two mechanisms have emerged as likely candidates for the crash: constriction of the Panamanian seaway or onset of North Atlantic Deep Water (NADW) formation that reorganized abyssal global circulation. Both ideas hinge on the same mechanism, increased corrosivity of bottom waters characterized by low $[CO_3]^{2-}$. Formation of NADW should actually increase the $[CO_3]^{2-}$ of bottom waters, however the response in the Pacific is complicated and NADW formation may actually enhance the export of Antarctic Bottom Water (ABW), which is highly corrosive to carbonates, to the Eastern Pacific. This could have caused the carbonate crash, but other isotopic evidence for enhanced export of

ABW is lacking and the chronology of the crash is not tightly constrained by the NADW production history (Lyle et al. 1995).

The cause preferred by the authors of Leg 138 studies is constriction of the Panamanian seaway, first initiated from 13-12 Ma (Farrell et al. 1995). Before the initial restriction of the seaway, high $[CO_3]^{2-}$ waters from the Atlantic flowed to the eastern Pacific. As the sill depth shoaled, less and less of this water bathed the Leg 138 sites leading to increased corrosion of carbonate sediments. The spatial pattern of the crash is the best evidence supporting this theory (Lyle et al. 1995). Eastern Pacific sites were more affected than other areas of the Pacific, with some sites never fully recovering from the late Miocene crash (e.g. Site 844), suggesting the cause may have been locally derived. Lyle et al. (1995) calculates that constriction of the seaway producing 2 Sv less flow could account for the changes in preservation.

Since the carbonate crash identified in sites of Leg 138 is also seen in other ocean sites (particularly the central, western, and north Pacific) and is likely global in extent, the calcium isotope record of carbonates may have changed in response to this drastic event. The $\delta^{44}Ca$ of seawater should lighten, and the concentration of Ca increase, as the result of dissolution of large quantities of isotopically light calcium carbonate. As described in Chapter I, biogenic calcium carbonate is light because organisms discriminate against the heavy isotope during precipitation, thus maintaining seawater at isotopically heavy values. Because the preferred cause of the crash is increased corrosivity of bottom waters and not an increase in productivity leading to a more acidic bottom water environment (Lyle et al. 1995), carbonate

sedimentation flux and weathering flux need not have changed through this interval, but it is possible that the sedimentation flux may have changed to balance an injection of light calcium into seawater from dissolution. In order to change (lighten) the $\delta^{44}Ca$ of seawater by 0.20 per mil, $2.43 * 10^{18}$ moles of calcium with an isotopic signature of –1.36 per mil must be dissolved. The observed change from 11.1 ($\delta^{44}Ca = -0.23$) to 10.5 Ma (($\delta^{44}Ca = -0.12$) is 0.11 per mil. By 9.1 Ma the $\delta^{44}Ca$ of seawater had returned back to a value of 0.02 per mil and continued on in an upward trend to 0.50 per mil by 8.79 Ma.

4.2.3 The carbonate sedimentation maximum

A "biogenic bloom" or carbonate sedimentation maximum occurred in the eastern equatorial Pacific sediments of Leg 138 following recovery from the carbonate crash. This maximum in sedimentation began at 6.7 Ma and lasted until 4.5 Ma; again, this phenomenon was not strictly local, but has been observed in sediments of the low-latitude Indo-Pacific, all equatorial Pacific regions, and the North Pacific (Farrell et al. 1995). Pisias et al. (1995) suggest that the accumulation rate maximum in both $CaCO_3$ and opal, if global in extent, can be attributed to an increased flux of Ca and Si to the oceans. One possible way to increase the dissolved element flux is by invoking increased chemical weathering associated with a pulse of tectonic uplift of the Tibetan Plateau. Assuming that the ocean carbonate and silica systems are in steady state, any increase in sedimentation would be the result of an increase in the flux of these elements to the ocean. This idea can be tested with Ca isotopes: if the

weathering flux is dominant during this period the isotopic signature of seawater should reflect the increased input of Ca from the continent to the ocean.

On the other hand, the sedimentation maximum may not actually represent a global increase. The biogenic bloom could represent a fractionation of $CaCO_3$ and Si between and within ocean basins (Farrell et al. 1995), and may only signal a redistribution of these sediments. Although a causative link remains vague, a change in deep ocean circulation or trade wind fluctuations may lead to fractionation in Ca, Si and other nutrients in the tropics (Peterson et al. 1992). The lack of sedimentation maximum in several ocean basins, such as the Kerguelen Plateau (southern Indian Ocean), the Atlantic, and some high latitude regions, doesn't support an event that is global in extent. At some of these sites in the southern Indian Ocean a hiatus in sedimentation actually occurred (Peterson et al. 1992). Even at the Leg 138 sites there is a strong equatorial gradient in the sedimentation maximum; equatorial sites experienced significant increases in $CaCO_3$ and opal MARs, whereas off equatorial sites in both the central and eastern Pacific actually show declines (Farrell et al. 1995). If this is the case, and fractionation of $CaCO_3$ and Si occurred between and within ocean basins, no increase in the net flux of Ca or Si is needed to explain the sedimentation maximum. If no increase of Ca flux to the ocean occurred, then the calcium isotopes will not show an excursion to lighter values, but should stay relatively constant during the biogenic bloom since there was no net change of Ca into or out of the ocean, merely a redistribution of sedimentation.

4.3 Calcium Isotope Data for Leg 138 Site 850 and Comparisons to Other Isotope Systems

4.3.1 Sample selection and Ca budget relationships

This study used bulk carbonate samples at regular time intervals to obtain the $\delta^{44}Ca$ of carbonate and thus seawater for the last 12 Ma. A bulk sample was chosen instead of a particular species of foraminifera or cocolithophorid because the nature and consistency of Ca isotope fractionation with temperature remains contentious (Sime et al. 2005, Gussone et al. 2003, Lemarchand et al. 2004). Other researchers have circumvented the problem of species-specific effects in foraminifera by using an inorganically precipitated Ca-bearing mineral, either phosphorite peloids or barite, to obtain the $\delta^{44}Ca$ of seawater (Schmitt et al. 2003a, Morris et al. 2005 respectively). With the exception of Schmitt et al. (2003a), all previously published records of calcium isotope variation through time have also used bulk samples. Presumably any diagenetic or species related vital effects would be averaged out when all components of the sample are dissolved. Because the total range of $\delta^{44}Ca$ among marine carbonates is much smaller than the overall range of Ca isotopes in nature (Schmitt et al. 2003b), the possibility that a highly fractionated component of marine bulk carbonates has biased previous results is minimized.

One clear exception is the analyses from Zhu and Macdougall (1998a) for Holocene cocolithophorid and carbonate oozes from both the Pacific and Atlantic. These very negative values (ranging from –2.64 to –1.88 per mil) have not been reproduced in other studies of bulk carbonates, and researchers have not been able to

fit these values into models of weathering/sedimentation fluxes with reasonable results. Schmitt et al. (2003a) suggests that the fine-grained cocolithophorids re-crystallize more easily during diagenesis and therefore may record post-depositional fractionation effects, not primary fractionation from seawater. This explanation may only apply to the Zhu and Macdougall (1998a) analyses since other studies of bulk carbonates, including this one, have not measured such anomalously negative values despite a fine-grained fraction present in the sample. Until a *widely available* inorganic Ca-bearing alternative is discovered or the temperature dependant fractionation issue is fully understood, using a bulk carbonate sample for calcium budget studies remains the most convenient approach.

De La Rocha and DePaolo (2000) originally used the $\delta^{44}Ca$ of carbonates (and thus seawater) to investigate the balance of Ca sedimentation (F_{sed}) and Ca weathering fluxes (F_w) for the past 80 Ma. All of the variables and values in the budget are found in Table 4.3.1. The rate of change of $\delta^{44}Ca_{sw}$ is given by the following equation (from DePaolo 2004):

$$N_{Ca} (d\delta_{sw}/dt) = F_C (\delta_c - \delta_{sw}) + F_H (\delta_H - \delta_{sw}) - F_{sed}\Delta_{sed}$$

The flux of Ca from the continent (F_C) and the flux from hydrothermal activity (F_H) are combined as $F_{w,}$ the overall weathering flux to the oceans. The relationship between $\delta^{44}Ca$ of sediments (denoted as δ_{sed}) and the F_{sed}/F_w ratio is given by the following equation:

$$\delta_{sed} (t) = \delta_w (t) - \Delta_{sed} [F_{sed}/F_w (t) – 1]$$

Table 4.3.1 Summary of calcium budget variables and $\delta^{44}Ca$ values.
[1] Schmitt et al. (2003b), [2] De La Rocha and DePaolo (2000), [3] Milliman (1993)

Calcium Budget Variable	**$\delta^{44}Ca$ (per mil) or Flux (moles Ca/yr)**
Weighted average river value δ_C	**-1.07** [1] (-0.63 to –1.71 total range, only 8 world rivers included in weighted average)
Hydrothermal value δ_H	**-0.96** [1]
Combined weathering value δ_w	**-1.04** (hydrothermal 25% of river)
Biologic Fractionation Δ_{sed}	**-1.30** [2]
Carbonate value δ_{sed}	**Measured from sediments**
Weathering flux F_w	**Calculated from F_{sed}/F_w ratio**
Sedimentation flux F_{sed}	**$3.2 * 10^{13}$ moles Ca/yr** [3]
Number of moles N_{Ca}	**$1.411 * 10^{19}$ moles Ca** (current ocean inventory)

Where δ_{sed} is the measured $\delta^{44}Ca$ of a bulk carbonate sample, δ_w is the combined weathering Ca flux to the ocean via rivers and hydrothermal fluids from alteration of ocean crust, Δ_{sed} is the fractionation associated with biological precipitation of calcium carbonate (-1.3 per mil), and F_{sed}/F_w represents the balance of the input and output fluxes of Ca to or from the ocean. The hydrothermal input of Ca to the ocean is taken as 25% of the riverine Ca input although estimates for the percentage of hydrothermal to river input range from 0.1% - 28% (Schmitt et al. 2003b, Elderfield and Schultz 1996). The $\delta^{44}Ca$ of hydrothermal fluids and rivers was measured by Schmitt et al (2003b) and is -0.96 ± 0.19 per mil for hydrothermal fluids and the current discharge weighted average of eight world rivers is –1.07 per mil. The total range of 16 major rivers is 1.08 per mil (-0.63 to –1.71 per mil) (Zhu and Macdougall 1998, Schmitt et al. 2003b). Both MORB (-0.81 ± 0.26 n=5) and hydrothermal fluids (-0.96 ± 0.19 per mil n=3) show little $\delta^{44}Ca$ variation as compared to the range seen in world rivers. The value of Δ_{sed} (-1.3 per mil) is the same value used by De La Rocha and DePaolo (2000); Δ_{sed} ranges from –1.2 to –1.5 per mil and varies based on temperature and type of calcifying organism. If the above equation is rearranged the F_{sed}/F_w is defined as:

$$F_{sed}/F_w = [\ \delta_{sed}(t) - \delta_w(t) - \Delta_{sed}\ ] / -\Delta_{sed}$$

Using the F_{sed}/F_w ratio calculated above and holding either F_{sed} or F_w constant, one can also find the change in concentration of calcium through time:

$$dN_{Ca} / dt = F_w - F_{sed}$$

On long time scales it is expected that the Ca concentration of seawater will change as a result of varying strengths of weathering or sedimentation fluxes (changes

in F_{sed}/F_w). Evidence for changes in Ca with time is seen in the distribution of different carbonate mineralogies throughout the Phanerazoic. Predominance of aragonite and high-Mg calcite or pure calcite in the geologic record reflects changes in the Mg/Ca ratio of seawater controlled by the rate of seafloor spreading (Stanley and Hardie 1998). These "calcite or aragonite seas" also correspond to changes in evaporite mineralogy with "calcite seas" correlating to periods of KCl type evaporites and "aragonite seas" corresponding to deposition of $MgSO_4$ evaporites (Hardie 1996). Change in Ca concentration seen throughout the Phanerozoic ranges from the current value of 10.3 mmol to 40 mmol, four times the current concentration (DePaolo 2003, Hardie 1996). The Ca concentration for the time scale encompassed in this study is not significantly affected by changes in the seafloor spreading rate, but it is highly probable that the strength of the weathering flux has changed in the last 12 Ma given the pulsed uplift of the Tibetan Plateau (Molnar et al. 1993, Raymo and Ruddiman 1992, Richter et al. 1992). Fantle and DePaolo (2005) found changes in the concentration of Ca from 0.5 to 1.7 times the present value during the last 20 million years, suggesting that the weathering flux of Ca to the oceans has influenced concentration.

4.3.2 Sources of variability in the Ca budget

Three variables in the Ca budget can change through time and produce a corresponding change in $\delta^{44}Ca$ of carbonates/seawater: δ_w, Δ_{sed}, and F_{sed}/F_w. The value of δ_w is a combined term describing the average $\delta^{44}Ca$ value of river water and

hydrothermal fluids, the two sources of Ca to the marine system. As discussed above, the range of hydrothermal fluids δ^{44}Ca values is small and suggests that this source term is relatively constrained and only slightly varies, although the strength of this flux may have been stronger in the early history of the Earth. The range of δ^{44}Ca values for river water however is larger than for hydrothermal fluids. The calcium isotope value for river water is affected by two variables, the amount of continental weathering and the lithology weathered. In other isotope systems such as Os and Sr, the isotopic difference between select lithologies is large, such that preferential weathering of a particular rock type, such as black shales or granitic plutons, will significantly change the isotopic value of river water. This is not the case for Ca isotopes. The ratio of silicate to carbonate weathering on the continent may change, but the average δ^{44}Ca values of Ca-silicates and marine carbonates are similar enough that changes in lithology weathered do not largely change the δ^{44}Ca of river water. The difference between silicates and carbonates is around 0.40 per mil, which limits variation in δ_w due to changes in weathered lithology to 0.20 per mil, only slightly different than the current precision of Ca isotopes of around 0.10 per mil (De La Rocha and DePaolo 2000). Schmitt et al. (2003b) confirmed this when they found that the δ^{44}Ca variability of river water values was 0.50 to 1.0 per mil, and even though the rivers studied were found in very different climates and various continents, no relation to drainage lithology or climate was found. With mineral weathering δ^{44}Ca values relatively well described, the slightly larger variability seen in world rivers than would be expected may be explained by biological activity in the surficial soil horizon which

enriches the soil in the heavy isotope (Schmitt et al. 2003b) or by specific processes during continental weathering that preferentially enrich the light isotope in runoff and are currently unknown (Fantle and DePaolo 2005). On the whole, changes in the weathering ratio of silicates to carbonates will only slightly affect δ_w; it is the overall strength of the weathering flux (F_w) that will largely affect the $\delta^{44}Ca_{sw.}$

The relative strength of the weathering or sedimentation flux is the most likely candidate for $\delta^{44}Ca_{sw}$ variation. Although a constant fractionation factor is assumed for precipitation of carbonate (Δ_{sed} -1.3 per mil), changes in this term due to changes in temperature or precipitating species can be rapid and will likely be averaged out over the long residence time of Ca (1 Ma). Given the shallow slope of temperature dependence (0.019 per mil/°C), a 5°C change in temperature would only change the $\delta^{44}Ca$ of precipitated carbonates by about 0.1 per mil (Fantle and DePaolo 2005). If a sustained shift in temperature were to occur, the oceans will reach a new steady state by adjusting $\delta^{44}Ca_{sw}$ to any long-term change in Δ_{sed}. Fantle and DePaolo (2005) modeled diagenetic effects on $\delta^{44}Ca$ in Site 590 carbonate sediments and only found a 0.02 per mil variation with depth/age, ruling out significant diagentic effects on carbonate calcium isotopic variation, at least for Site 590.

Milliman (1993) estimated the late Holocene carbonate flux (accumulated in marine sediments) to be $3.2 * 10^{13}$ moles of $CaCO_3$ per year, which at steady state will be offset by an equal input of calcium and carbonate. Although much debated, the variance of the carbonate flux to marine sediments is probably small. For example, there is no evidence for an increase in deep-sea carbonate accumulation to offset a

decrease in shallow water carbonate accumulation during glacial intervals. Increased flux of Ca to the oceans during the last glacial lowstand was not balanced by increased carbonate sedimentation in the deep sea, suggesting that the oceans were out of steady state during the last low stand of sea level (Milliman 1993). This does not mean that over the course of millions of years encompassing numerous glacial-interglacial cycles, the sedimentation flux has not adjusted to sustained increases or decreases in the flux of Ca to the oceans. However, since it is well known that the input flux of elements to the ocean has varied considerably with changes in both tectonics and global climate, it is easiest to assume a constant Ca sedimentation rate and model the weathering flux of Ca to vary with F_{sed}/F_w. Fantle and DePaolo (2005) calculated Ca concentrations holding the residence time constant, which requires that the weathering flux follow changes in dissolved Ca in the oceans, by holding F_w constant, and by constraining F_{sed} and found no great difference in calculated Ca concentrations between methods.

In this study the F_{sed}/F_w ratio is used to obtain the concentration of calcium in the oceans at any time assuming the carbonate sedimentation rate is constant and the weathering flux follows changes in F_{sed}/F_w. As stated above, the current carbonate sedimentation flux to the oceans is $3.2 * 10^{13}$ moles Ca/year and the current inventory of Ca in the oceans is $1.411 * 10^{19}$ moles (volume of the ocean taken as $1.37 * 10^{21}$ liters and the Ca concentration as 0.0103 moles/liter). The simple relationship between the F_{sed}/F_w ratio derived from the $\delta^{44}Ca$ of carbonate sediments and the absolute weathering flux F_w is then:

$$F_w\,(t) = 3.2 * 10^{19} / F_{sed}/F_w\,(t)$$

Assuming linear increase or decrease in concentration, the moles change of Ca between two sample times will be the difference in average F_w and the constant F_{sed} rate multiplied by the sample time interval. The data for these calculations are found in Table 4.3.4a and illustrated in Figure 4.3.4b, and a summary of all the variables and values used is in Table 4.3.1.

4.3.3 Site 850 δ^{44}Ca data

In order to get a more complete picture of the geochemical conditions in the past, it is useful to examine data from several isotope systems describing elemental mass balances in seawater. Previously published data for Sr and Os isotopes from marine sediments are used to illuminate the Ca isotope data from this study. The strontium isotope record of seawater is well established (Burke et al. 1982, Richter and DePaolo 1988, Palmer and Edmond 1989, Veizer 1989, Richter et al. 1992,). For the past 40 Ma, the $^{87}Sr/^{86}Sr$ ratio of seawater has been steeply increasing; the rise has largely been attributed to the exhumation, increased chemical erosion, and denudation of the Tibetan Plateau, with some researchers using the Sr isotope curve to infer increased chemical weathering resulting in CO_2 drawdown and a progressively cooling Cenozoic climate (Raymo and Ruddiman 1992).

One caveat of the Sr system is that rapid change in the $^{87}Sr/^{86}Sr$ of seawater can be caused by either a change in the source of dissolved Sr or an increase in weathering intensity (Derry and France-Lanord 1996). Because the $^{87}Sr/^{86}Sr$ ratio of

river water is highly influenced by its drainage lithology, an increase in this ratio may spuriously indicate an increase in chemical weathering, when in reality the dominant source of dissolved Sr to the river has merely changed from carbonate Sr to highly radiogenic muscovite and biotite Sr. The $^{87}Sr/^{86}Sr$ ratio of river water is affected by the relative amounts of dissolved Sr from carbonate weathering and incongruent weathering of silicate minerals (e.g. feldspar versus mica dissolution) (Derry and France-Lanord 1996). The ratio of silicate to carbonate weathering is critical for determinations of CO_2 drawdown, as only silicate weathering acts as a sink for CO_2 from the atmosphere. Several studies have questioned the simplified relationship between increased $^{87}Sr/^{86}Sr$ and increased silicate weathering (Krishnaswami et al. 1992, Quade et al. 1997, Blum et al. 1998). Because of extensive metamorphism in the Tibetan region, highly radiogenic Sr from granites and gneisses may have partially equilibrated with marble bands resulting in calcite veins and marbles with highly radiogenic Sr ratios. Weathering of these carbonate and meta-carbonate minerals would increase the $^{87}Sr/^{86}Sr$ of rivers draining the Tibetan Plateau without drawing down CO_2 (Blum et al. 1998, Quade et al. 1997). Calcium weathered from these meta-carbonates and granitic rocks have similar $\delta^{44}Ca$ values. Hence, in this case a change in weathered lithology would not significantly affect the $\delta^{44}Ca$ of river water and would not provide information regarding the proportion of silicate to carbonate weathering, only the overall strength of the Ca weathering flux.

The Osmium isotope record of seawater has been used in conjunction with the Sr record because similar processes influence both systems: continental weathering

and oceanic crust alteration (Ravizza 1993). These records should co-vary if they are each accurate proxies for continental weathering. Highly radiogenic values of $^{187}Os/^{186}Os$ are found most commonly in old black shales due to their high Re/Os ratios and rapid ingrowth of ^{187}Os. Weathering of these sediments would force large amplitude changes in the $^{187}Os/^{186}Os$ ratio of seawater without corresponding change in $^{87}Sr/^{86}Sr$. By comparing and contrasting the record of Sr and Os isotopes in seawater, one could deduce the type of lithology dominating the weathering flux to the oceans. Ravizza (1993) reported both Sr and Os data for the past 28 Ma and concludes the two systems are decoupled. Prior to 15 Ma, Sr isotopes show large steady increases in $^{87}Sr/^{86}Sr$ while the $^{187}Os/^{186}Os$ ratio varies little. After 15 Ma, the situation is reversed, with Os isotopes contributing more radiogenic isotopes to seawater. This change is due to a switch in the types of lithologies weathered: for the past 15 Ma, organic rich black shales and marine carbonates were dominant, and from 28 to 15 Ma, granites and other igneous rocks were more important.

Because the isotopic difference between the average $\delta^{44}Ca$ of silicate and carbonate rocks is small, the calcium isotope variation in seawater should reflect the overall weathering flux of Ca to the oceans regardless of type of lithology weathered. Figure 4.3.3a plots Os, Sr, and Ca isotopes together for the last 12 Ma. Data for these analyses are found in Table 4.3.3a and Table 4.3.3b with Os and Sr isotopic data taken from Richter and DePaolo (1988), Peucker-Ehrenbrink et al. (1995), and Ravizza (1993). Sr isotopes exhibit the largest increase over the last 12 Ma, with Os isotopes also increasing but at a much slower rate. The difference between the rates of increase

is misleading because the range of variation for Os spans 60% of the range between continental and mantle end-members, whereas the range for Sr spans only 12% of this range (Ravizza 1993). Therefore the more dramatic increase is really the Os record; the increase is attributed to weathering of old black shales as discussed above. Weathering of organic matter from black shales actually consumes O_2 and releases CO_2 to the atmosphere. Therefore, increased $^{187}Os/^{186}Os$ in seawater may be related only to preferential weathering of black shales, and not to enhanced chemical weathering on the continents (Peucker-Ehrenbrink and Ravizza 2000).

In stark contrast to the Os and Sr data is the Ca isotope record from this study. The $\delta^{44}Ca$ record of seawater has short-term fluctuations on the period of 1-2 million years but no long-term trend towards increasing or decreasing $\delta^{44}Ca$ over time. This implies that there has been no sustained increase in the weathering flux of Ca over this time period, only short term pulses of increased Ca to the oceans. The record implies no increase in weathering intensity over the last 12 Ma and therefore no enhanced drawdown of CO_2 or cooling of the climate from this mechanism. Figure 4.3.3b shows the Ca record on a larger scale for a sampling interval of approximately 500 kyr. Transient changes in F_w or F_{sed} (or the value of δ_w limited to $\pm$ 0.20 per mil) may have caused the higher frequency fluctuations of $\delta^{44}Ca_{sw}$ seen in Figure 4.3.3b. The total range in $\delta^{44}Ca$ is 0.86 per mil, very similar to the total $\delta^{44}Ca$ range of 0.70 per mil for the last 20 Ma published in Fantle and DePaolo (2005). The heaviest seawater value in their study for the past 12 Ma is 0.16 at 1.76 Ma and the lightest –0.48 per mil at 8.22 Ma, and for this study the lightest value is –0.36 at 0.99 Ma and the heaviest is

Table 4.3.3a $\delta^{44}Ca$ data for Leg 138 Site 850 carbonates. Each sample value is the average of two TIMS runs and the error is given as $2\sigma_m$. In order to get the $\delta^{44}Ca_{SW}$, a constant 1.3 per mil is added to the carbonate value. The modern carbonate value is defined by assuming that the $\delta^{44}Ca_{SW}$ is currently zero as discussed in Chapter I. The formula for F_{sed}/F_w is described in the text. Three different δ_w values are used to obtain three different F_{sed}/F_w ratios to illustrate the range and sensitivity of the flux ratio to chosen δ_w. Ages were obtained from the age model of Shackleton et al. (1995).

Age (Ma)	Sample Name	$\delta^{44}Ca_{carb.}$	$2\sigma_m$	$\delta^{44}Ca_{SW}$	F_{sed}/F_w	F_{sed}/F_w	F_{sed}/F_w
		per mil		per mil	δ_w = -0.848	δ_w = -1.048	δ_w = -1.248
0	Assumed	-1.30	0.00	0.00	0.65	0.81	0.96
0.504	2H-01	-0.85	0.21	0.45	1.00	1.15	1.31
0.999	3H-01	-1.66	0.11	-0.36	0.37	0.53	0.68
1.504	4H-01	-1.26	0.02	0.04	0.68	0.84	0.99
2.052	5H-01	-1.03	0.03	0.27	0.86	1.02	1.17
2.438	6H-01	-1.32	0.05	-0.02	0.64	0.79	0.95
2.969	7H-01	-1.35	0.05	-0.05	0.61	0.77	0.92
3.496	7H-06	-1.33	0.00	-0.03	0.63	0.78	0.94
3.96	8H-07	-1.09	0.04	0.21	0.81	0.97	1.12
4.49	9H-06	-1.53	0.15	-0.23	0.47	0.63	0.78
5.055	12X-1	-1.18	0.05	0.12	0.74	0.89	1.05
5.507	14X-04	-1.02	0.06	0.28	0.87	1.02	1.18
6.003	17X-05	-1.40	0.02	-0.10	0.57	0.73	0.88
6.501	20X-05	-1.21	0.03	0.09	0.72	0.87	1.03
6.999	24X-04	-1.32	0.03	-0.02	0.64	0.79	0.95
7.474	26X-06	-1.55	0.04	-0.25	0.46	0.62	0.77
7.993	28X-02	-1.31	0.04	-0.01	0.64	0.80	0.95
8.796	31X-01	-0.80	0.01	0.50	1.04	1.19	1.34
9.107	32X-03	-1.28	0.01	0.02	0.67	0.82	0.97
10.51	36X-04	-1.53	0.13	-0.23	0.48	0.63	0.79
11.154	39X-06	-1.42	0.00	-0.12	0.56	0.71	0.87
11.547	41X-01	-1.34	0.00	-0.04	0.62	0.78	0.93
11.95	42X-03	-0.94	0.03	0.36	0.93	1.08	1.24

Table 4.3.3b Published osmium and strontium isotopes for the last 12.6 Ma. These data are illustrated graphically along with δ^{44}Ca data in Figure 4.3.3a.

Age (Ma)	$^{87}Sr/^{86}Sr$*
0.1	0.709256
1.8	0.709161
2.1	0.709149
2.3	0.709112
3.1	0.709126
3.6	0.709121
3.8	0.709102
4.3	0.709116
4.6	0.709096
5.6	0.70908
6	0.709031
6.4	0.709024
6.9	0.709016
7.4	0.708992
7.9	0.708978
8.4	0.708975
8.9	0.70898
9.9	0.708958
10.7	0.70896
11.2	0.708926
11.4	0.708895
11.8	0.708892

Age (Ma)	$^{187}Os/^{186}Os$**
0.104	7.886
1.06	8.12
1.5	7.675
3.6	7.503
3.7	7.285
3.8	7.381
6.34	7.203
8.1	6.933
12.6	6.592

*** $^{87}Sr/^{86}Sr$ data from Richter and DePaolo (1988)**
**** $^{187}Os/^{186}Os$ data from Peucker-Ehrenbrink et al. (1995) and Ravizza (1993)**

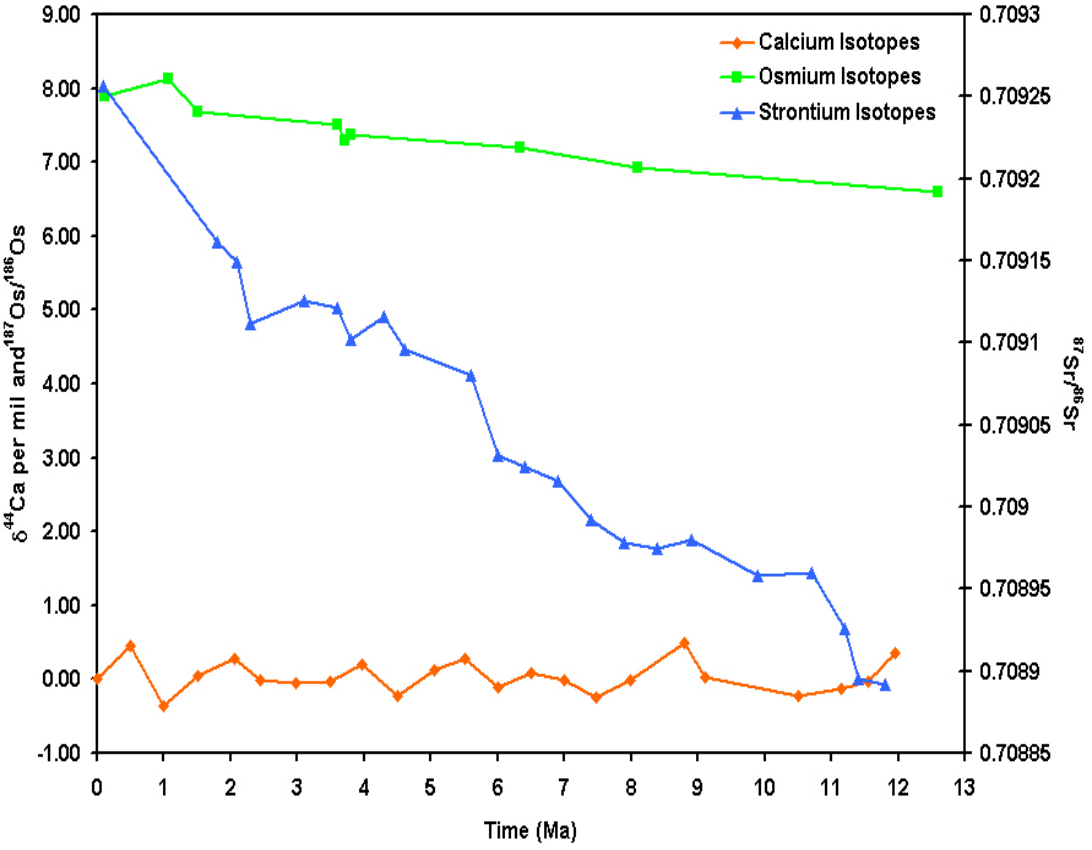

Figure 4.3.3a Osmium, strontium, and calcium isotopic records for the past 12 Ma. Os and Sr data are from Richter and DePaolo (1988) (Sr) and Peucker-Ehrenbrink et al. (1995) and Ravizza (1993) (Os). Ca data is from this study. Both Os and Sr isotopes increase to more radiogenic ratios from 12-0 Ma indicating either an increase in weathering intensity or preferential weathering of radiogenic lithologies. In contrast, Ca isotopes show no overall trend towards increasing or decreasing δ^{44}Ca indicating no consistent bias towards increased carbonate sedimentation (increase δ^{44}Ca) or an increased weathering Ca flux (decrease δ^{44}Ca). The calcium isotope record suggests that Os and Sr isotopes may actually record preferential weathering of radiogenic lithologies and not an increase in weathering intensity.

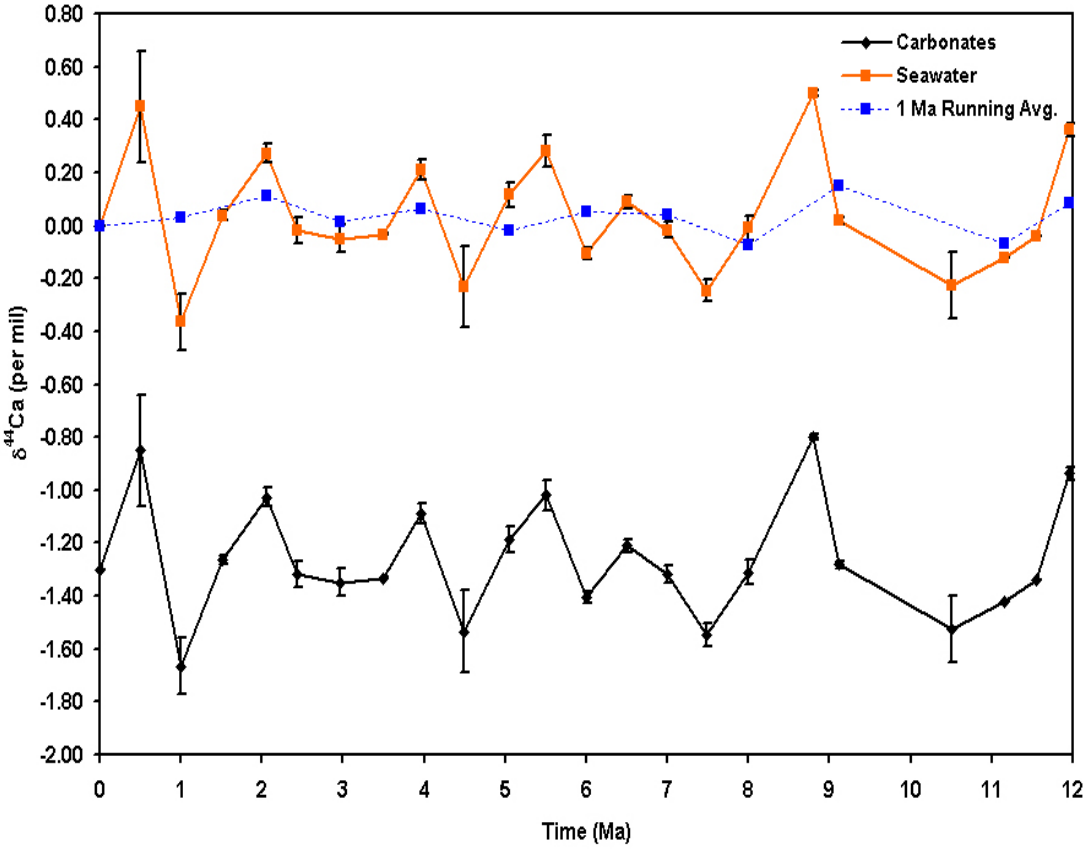

Figure 4.3.3b Calcium isotope data for bulk carbonate samples from Site 850 Leg 138 Eastern Equatorial Pacific. A 1.3 per mil biological fractionation factor was added to the carbonate data to get the δ^{44}Ca of seawater for the past 12 Ma. The average value of seawater is 0.04 ± 0.22 per mil with a total range of 0.86 per mil (carbonate average is –1.26 ± 0.22 per mil). The bright blue dashed curve represents a 1 Ma running average of the δ^{44}Ca of seawater for the past 12 Ma. Total range for the 1 Ma average data set is only 0.22 per mil.

0.50 at 8.79 Ma. The 20 Ma data set overlaps, within error, with the majority of data from this study, however there are several instances where they do not agree. For example, one large disagreement occurs around 8.7 Ma where the Fantle and DePaolo (2005) record indicates a small drop in the $\delta^{44}Ca$ of seawater while the data for this study show the largest increase in $\delta^{44}Ca$ and heaviest value achieved of the entire record. A similar disagreement occurs around 4 Ma and again at 0.5 Ma. This could be due to differences in mineralogy or species composition of the bulk samples which may alter the original signal recording the Ca isotopic composition of seawater. The two study sites are in different areas of the Pacific Ocean. The Fantle and DePaolo (2005) study samples DSDP Site 590 on the Lord Howe Rise in the southwest Pacific and data for this study are from the eastern equatorial Pacific ODP Site 138. There is one interval that is highly correlated in both records. From 6 to 4.5 Ma both records exhibit an increase in the $\delta^{44}Ca$ of seawater on the order of 0.35 per mil suggesting a sedimentation maximum, centered on the same time period as the "biogenic bloom" in Leg 138 sediments, lending support to globally increased carbonate sedimentation during this time. The data in Figure 4.3.3b show a broad minimum in $\delta^{44}Ca$ from 11.5 to 9 Ma followed by the heaviest value of the data set at 8.79 Ma. The record after this point is marked by excursions to both light and heavy values on the scale of 1-2 million years. Linking these changes to global oceanographic events, such as the mid-Miocene carbonate crash or initiation of the Indian Monsoon, proves to be elusive as discussed below.

Using Sr isotopes from pedogenic clay minerals as a proxy for weathering intensity in the Ganges-Brahmaputra Basin, Derry and France-Lanord (1996) published a record of Sr flux and $^{87}Sr/^{86}Sr$ ratios for the Ganges-Brahmaputra river system over the last 16.4 Ma. They found a late Miocene to mid-Pleistocene interval of high weathering intensity (shown through very radiogenic Sr ratios indicative of mica weathering) and low Sr flux, bracketed by intervals of low weathering intensity (less radiogenic Sr ratios implying feldspar or carbonate weathering) and high Sr flux. Because Sr and Ca fluxes generally correlate in rivers, the period between 7 and ca. 1 Ma should also show a decrease in the flux of Ca to the ocean via the Ganges-Brahmaputra River (Derry and France-Lanord 1996). This suggestion is different from that of Pisias et al. (1995) who invoke increased flux of Ca and Si from rivers draining the Himalayan Plateau to explain the biogenic bloom and sedimentation maximum from 6-4.5 Ma in the Leg 138 sediments. The Ca isotope record from this study does not support a sustained decrease in flux of Ca to the oceans from 7 to 1 Ma.

The calcium isotope data in Figure 4.3.3b from 6-2 Ma show three excursions to heavier $\delta^{44}Ca$ at 5.5, 4, and 2 Ma, suggesting a possible increase in Ca sedimentation around the time period of the sedimentation maximum, in support of Pisias et al (1995). However the equally large maxima at 0.5 and 8.7 Ma in $\delta^{44}Ca$ is not supported by an increase in carbonate concentration in the late Pliocene sediments of Site 850, casting doubt on the uniqueness of the 4 Ma maximum in particular and the validity of *globally* increased Ca sedimentation from 6-4.5 Ma. If the 1 Ma running average of $\delta^{44}Ca$ of seawater is considered, the previously discussed maxima

and minima are damped significantly. The change in the isotopic composition of seawater for this curve is mostly within the error of the measurements or is within range of a change in weathered lithology.

4.3.4 The F_{sed}/F_w ratio and Ca concentration of the ocean

Figure 4.3.4a illustrates the F_{sed}/F_w ratio with time discussed in Section 4.3.1 and 4.3.2. Throughout the entire interval the ratio suggests a bias towards excess weathering flux of Ca to the oceans for the past 12 Ma ($F_{sed}/F_w < 1$, for δ_w = -1.048 per mil). There are some short-term fluctuations towards a steady state scenario (e.g. at 2, 4, 5.5, and 9 Ma) when flux of Ca to the oceans is equally balanced by flux of Ca out of the oceans into the sediment ($F_{sed}/F_w = 1$). The choice of the weathering flux $\delta^{44}Ca$ (δ_w) value predictably affects the value of F_{sed}/F_w. Three different values for δ_w were chosen to illustrate the range of F_{sed}/F_w: -0.848, -1.048, and –1.248 per mil. δ_w is a combination of the average $\delta^{44}Ca$ of hydrothermal fluid and global river water with the weight of the hydrothermal variable as 25% of the river water value. For each scenario, the same hydrothermal $\delta^{44}Ca$ was used, but three different river water $\delta^{44}Ca$ values were modeled: –0.82, –1.07, and –1.32 per mil. As discussed in Section 4.3.1, Schmitt et al. (2003b) estimated a global river water value of –1.07 per mil and the average hydrothermal value as –0.96 per mil. The three river water values were chosen based on the –1.07 average value ± 0.25 per mil, the suggested variation in $\delta^{44}Ca$ due to a change in the carbonate to silicate ratio of weathered sediments.

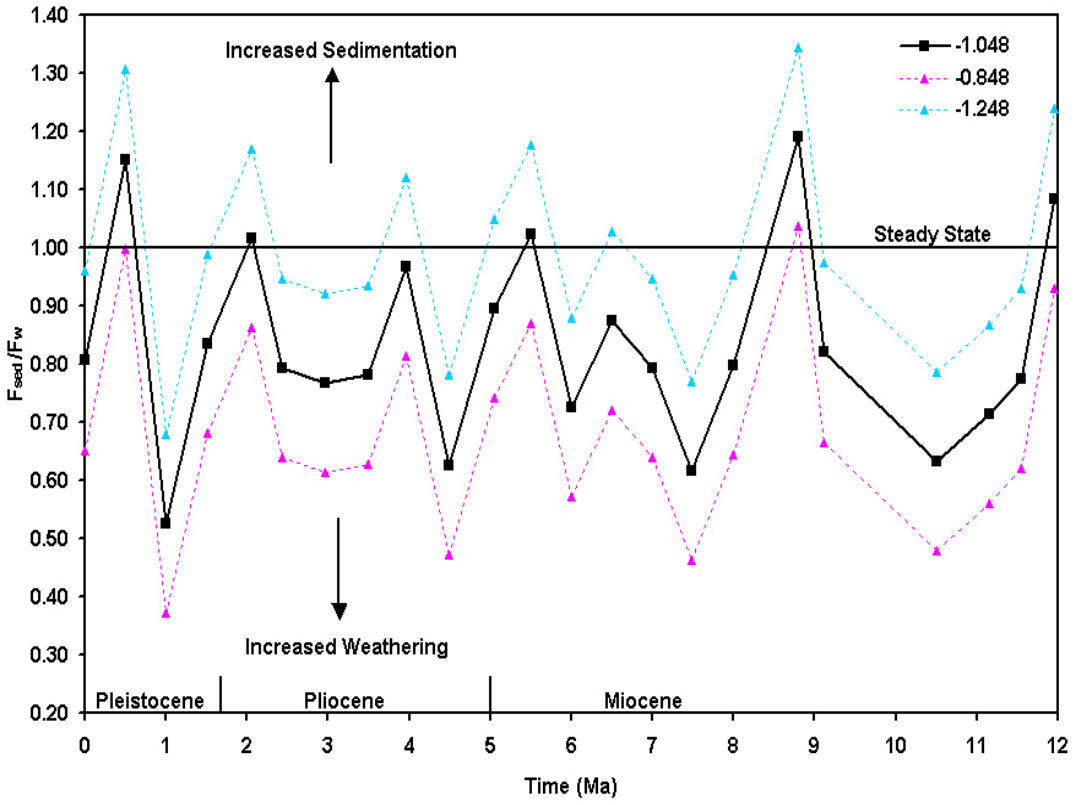

Figure 4.3.4a The F_{sed}/F_w ratio illustrates the balance (or imbalance) of Ca input and output fluxes through time. If both fluxes are changing at the same rate, the ratio will equal one. If an imbalance occurs and one flux exceeds the other, a ratio greater than one indicates a higher output flux and a ratio less than one indicates a greater input flux. Three values of δ_w (-1.248, -1.048, -0.848)are used to show the variation of the F_{sed}/F_w ratio with changes in the weathering flux δ^{44}Ca. The curve describing δ_w = -1.248 is the closest to a steady state scenario, whereas the two higher values show a bias toward the weathering flux at all of the sample times. There is no consistent trend throughout the record towards gradually increasing/decreasing sedimentation or weathering flux.

In Figure 4.3.4a, if –1.248 is used as the average weathering value, the system is closer to steady state throughout the majority of the record but punctuated by several excursions to excess sedimentation (F_{sed}/F_w = 1 or >1). This is higher than the average estimated by Schmitt et al. (2003b), but is plausible give the large range (about 1.0 per mil) of $\delta^{44}Ca$ exhibited in world rivers (from –0.63 for the Yangtze at its mouth, to –1.71 for the Pilang gad at its mouth) (Zhu and Macdougall 1998, Schmitt et al. 2003b). If -1.048 is used for δ_w, the F_{sed}/F_w record is biased towards increased weathering flux over the last 12 Ma at all times and this situation is only intensified if the heaviest value of –0.848 is used. The total change in F_{sed}/F_w is about 67% between times of greatest weathering flux and greatest sedimentation flux for all values of $\delta_{w,}$ confirming that the shape of each curve is unaffected by choice of δ_w. The average river water value calculated by Schmitt et al. (2003b) (-1.07 per mil) accounts for 16% of the Ca flux to the oceans and 30% of total discharge to the oceans. The total range of all rivers previously analyzed for calcium isotopes is biased toward $\delta^{44}Ca_R$ greater than 1.15 per mil. Only a few rivers have $\delta^{44}Ca$ around –0.80 per mil. For the sake of discussion it is reasonable to exclude the heaviest δ_w value of –0.848 per mil and consider only –1.048 and –1.248 per mil. The heavy value may be more valid during times of much larger hydrothermal input, for example when the rate of seafloor spreading was greater in the Cretaceous. Using the lighter values (–1.048 and –1.248 per mil), the Ca isotopic system for the last 12 Ma is rarely in steady state, which is similar to the conclusions of Fantle and DePaolo (2005) with their 20 Ma record. Spikes in excess sedimentation occur at 1, 4.5, 7.5, and 10.5 Ma.

Hodell et al. (1989) published a detailed Sr isotope stratigraphy for 9-2 Ma where they found three distinct changes in slope of the $^{87}Sr/^{86}Sr$ ratio of seawater: near zero change from 9-5.5 Ma, steep slope from 5.5-4.5 Ma, and near zero slope from 4.5-2 Ma. They conclude that a pulse-like increase in dissolved riverine Sr created the steep slope seen from 5.5-4.5 Ma. The calcium record at 4.5 Ma does show an excursion to excess weathering in agreement with the sharp increase in slope of Sr. However, the magnitude of this change is similar to the excursion from 1.5-1 Ma, and this excursion cannot be compared to the Hodell et al (1989) record which ends at 2 Ma. The sedimentation maximum seen in the F_{sed}/F_w ratio at 2 Ma does not seem to be in response to an influx of dissolved Ca via rivers since there is no evidence for a pulsed increase in dissolved Sr in the Hodell et al. (1989) study, and it is not supported by an increase in calcium carbonate concentration in the Leg 138 sediments. This is similarly true for spikes in excess sedimentation at 0.5 and 8.7 Ma.

The mid-Miocene carbonate crash from 11.2-9.0 Ma identified in several ocean basins, in particular the Eastern Equatorial Pacific Leg 138 sediments, has been attributed to increased corrosivity of bottom waters due to changes in ocean circulation, not increased productivity, causing acidic bottom water conditions (Lyle et al. 1995). The Ca isotopic record shows a significant increase in weathering (over the rate of Ca sedimentation) from 11.5 to 9 Ma. By 8.7 Ma the Ca isotopic composition of seawater has reached the heaviest value and largest excess of sedimentation over weathering in the entire 12 Ma record. This is inconsistent with the slow and steady recovery from the crash seen in Leg 138 sediments. The changes in the Ca isotopic

record are not uniquely correlated with stratigraphic evidence, which compounds the problem that the magnitude of these changes are not generally correlated with estimates of changes from other isotopic proxies such as Sr and Os.

The F_{sed}/F_w ratio can be used to obtain the concentration of calcium in the oceans for the past 12 Ma as discussed in Section 4.3.1 and 4.3.2. The data for calcium concentration are found in Table 4.3.4a and 4.3.4b. Since the F_{sed}/F_w ratio is affected by the choice of δ_w, the calculated concentration is also affected by this variable. For the two previously discussed values for δ_w (-1.248 and –1.048 per mil), the concentrations range from the modern value to 1.79 times modern concentration. The lighter δ_w has a smaller range of variability (modern to 1.32). It is important to remember that the F_{sed} variable is held constant throughout the record at $3.2 * 10^{13}$ moles/year Ca in order to calculate F_w. Therefore the calculated concentration, in reality, may be damped by the buffering influence of carbonate sedimentation if the strength of this flux has actually varied in the last 12 Ma. This record provides an idea of the maximum change of Ca concentration based only on changes in the input flux. For example the large increase in Ca concentration estimated from 3-1 Ma might actually be smaller, or even change direction, if carbonate deposition increased in response to a sustained increase in the weathering flux.

The range in calcium concentration is highly influenced by the choice of $\delta_{w,}$ with the largest range associated with the heaviest weathering value and the smallest with the lightest value. This is expected since the average output value of –1.3 per mil is much lighter than the heaviest value of –0.848 per mil. When the input and output

Table 4.3.4a Ca concentrations for three different δ_w calculated from a 1 Ma running average of F_{sed}/F_w described in the text. The data are illustrated in Figure 4.3.4b.

Age (Ma)	Sample Name	F_{sed}/F_w	Avg. F_w (lin.)	Moles Change	# Moles Ca	Times Modern Ca Conc.
		δ_w = -0.848				
0	Modern	0.65	4.91E+13	--	1.41E+19	1.00
0.504	2H-01a	1.00	4.06E+13	4.31E+18	1.84E+19	1.31
0.999	3H-01a	0.37	5.91E+13	1.37E+19	2.78E+19	1.97
1.504	4H-01a	0.68	6.65E+13	1.89E+19	3.30E+19	2.34
2.052	5H-01a	0.86	4.20E+13	3.87E+18	1.80E+19	1.27
2.438	6H-01a	0.64	4.36E+13	6.16E+18	2.03E+19	1.44
2.969	7H-01a	0.61	5.11E+13	1.01E+19	2.42E+19	1.71
3.496	7H-06a	0.63	5.16E+13	9.07E+18	2.32E+19	1.64
3.96	8H-07a	0.81	4.52E+13	6.97E+18	2.11E+19	1.49
4.49	9H-06a	0.47	5.35E+13	1.22E+19	2.63E+19	1.86
5.055	12X-1a	0.74	5.54E+13	1.06E+19	2.47E+19	1.75
5.507	14X-04a	0.87	4.00E+13	3.97E+18	1.81E+19	1.28
6.003	17X-05a	0.57	4.64E+13	7.17E+18	2.13E+19	1.51
6.501	20X-05a	0.72	5.02E+13	9.05E+18	2.32E+19	1.64
6.999	24X-04a	0.64	4.72E+13	7.23E+18	2.13E+19	1.51
7.474	26X-06a	0.46	5.96E+13	1.43E+19	2.84E+19	2.01
7.993	28X-02a	0.64	5.94E+13	2.20E+19	3.61E+19	2.56
8.796	31X-01a	1.04	4.02E+13	2.56E+18	1.67E+19	1.18
9.107	32X-03a	0.67	3.95E+13	1.05E+19	2.46E+19	1.74
10.51	36X-04a	0.48	5.74E+13	1.64E+19	3.05E+19	2.16
11.154	39X-06a	0.56	6.20E+13	1.18E+19	2.59E+19	1.84
11.547	41X-01a	0.62	5.43E+13	8.99E+18	2.31E+19	1.64
11.95	42X-03a	0.93	--	--	--	--

Age (Ma)	Sample Name	F_{sed}/F_w	Avg. F_w (lin.)	Moles Change	# Moles Ca	Times Modern Ca Conc.
		δ_w = -1.048				
0	Modern	0.81	3.97E+13	--	1.41E+19	1.00
0.504	2H-01a	1.15	3.38E+13	8.87E+17	1.50E+19	1.06
0.999	3H-01a	0.53	4.43E+13	6.24E+18	2.03E+19	1.44
1.504	4H-01a	0.84	4.96E+13	9.64E+18	2.37E+19	1.68
2.052	5H-01a	1.02	3.49E+13	1.12E+18	1.52E+19	1.08
2.438	6H-01a	0.79	3.59E+13	2.09E+18	1.62E+19	1.15
2.969	7H-01a	0.77	4.10E+13	4.75E+18	1.89E+19	1.34
3.496	7H-06a	0.78	4.13E+13	4.32E+18	1.84E+19	1.31
3.96	8H-07a	0.97	3.70E+13	2.66E+18	1.68E+19	1.19
4.49	9H-06a	0.63	4.21E+13	5.69E+18	1.98E+19	1.40
5.055	12X-1a	0.89	4.34E+13	5.16E+18	1.93E+19	1.37
5.507	14X-04a	1.02	3.35E+13	7.57E+17	1.49E+19	1.05
6.003	17X-05a	0.73	3.77E+13	2.83E+18	1.69E+19	1.20
6.501	20X-05a	0.87	4.03E+13	4.15E+18	1.83E+19	1.29
6.999	24X-04a	0.79	3.85E+13	3.07E+18	1.72E+19	1.22
7.474	26X-06a	0.62	4.61E+13	7.32E+18	2.14E+19	1.52

Table 4.3.4a Continued

Age (Ma)	Sample Name	F_{sed}/F_w	Avg. F_w (lin.)	Moles Change	# Moles Ca	Times Modern Ca Conc.
		δ_w = -1.048				
7.993	28X-02a	0.80	4.60E+13	1.12E+19	2.53E+19	1.79
8.796	31X-01a	1.19	3.35E+13	4.60E+17	1.46E+19	1.03
9.107	32X-03a	0.82	3.30E+13	1.35E+18	1.55E+19	1.10
10.51	36X-04a	0.63	4.48E+13	8.25E+18	2.24E+19	1.58
11.154	39X-06a	0.71	4.77E+13	6.17E+18	2.03E+19	1.44
11.547	41X-01a	0.78	4.30E+13	4.45E+18	1.86E+19	1.32
11.95	42X-03a	1.08	3.54E+13	--	--	--

Age (Ma)	Sample Name	F_{sed}/F_w	Avg. F_w (lin.)	Moles Change	# Moles Ca	Times Modern Ca Conc.
		δ_w = -1.248				
0	Assumed	0.96	3.33E+13	--	1.41E+19	1.00
0.504	2H-01a	1.31	2.89E+13	-1.55E+18	1.26E+19	0.89
0.999	3H-01a	0.68	3.58E+13	1.92E+18	1.60E+19	1.14
1.504	4H-01a	0.99	3.97E+13	4.23E+18	1.83E+19	1.30
2.052	5H-01a	1.17	2.98E+13	-8.30E+17	1.33E+19	0.94
2.438	6H-01a	0.95	3.06E+13	-7.55E+17	1.34E+19	0.95
2.969	7H-01a	0.92	3.43E+13	1.19E+18	1.53E+19	1.08
3.496	7H-06a	0.94	3.45E+13	1.14E+18	1.53E+19	1.08
3.96	8H-07a	1.12	3.14E+13	-3.31E+17	1.38E+19	0.98
4.49	9H-06a	0.78	3.48E+13	1.56E+18	1.57E+19	1.11
5.055	12X-1a	1.05	3.58E+13	1.70E+18	1.58E+19	1.12
5.507	14X-04a	1.18	2.89E+13	-1.56E+18	1.26E+19	0.89
6.003	17X-05a	0.88	3.18E+13	-1.05E+17	1.40E+19	0.99
6.501	20X-05a	1.03	3.37E+13	8.70E+17	1.50E+19	1.06
6.999	24X-04a	0.95	3.24E+13	2.13E+17	1.43E+19	1.02
7.474	26X-06a	0.77	3.76E+13	2.93E+18	1.70E+19	1.21
7.993	28X-02a	0.95	3.76E+13	4.46E+18	1.86E+19	1.32
8.796	31X-01a	1.34	2.87E+13	-1.03E+18	1.31E+19	0.93
9.107	32X-03a	0.97	2.83E+13	-5.15E+18	8.96E+18	0.64
10.51	36X-04a	0.79	3.68E+13	3.07E+18	1.72E+19	1.22
11.154	39X-06a	0.87	3.88E+13	2.67E+18	1.68E+19	1.19
11.547	41X-01a	0.93	3.57E+13	1.47E+18	1.56E+19	1.10
11.95	42X-03a	1.24	--	--	--	--

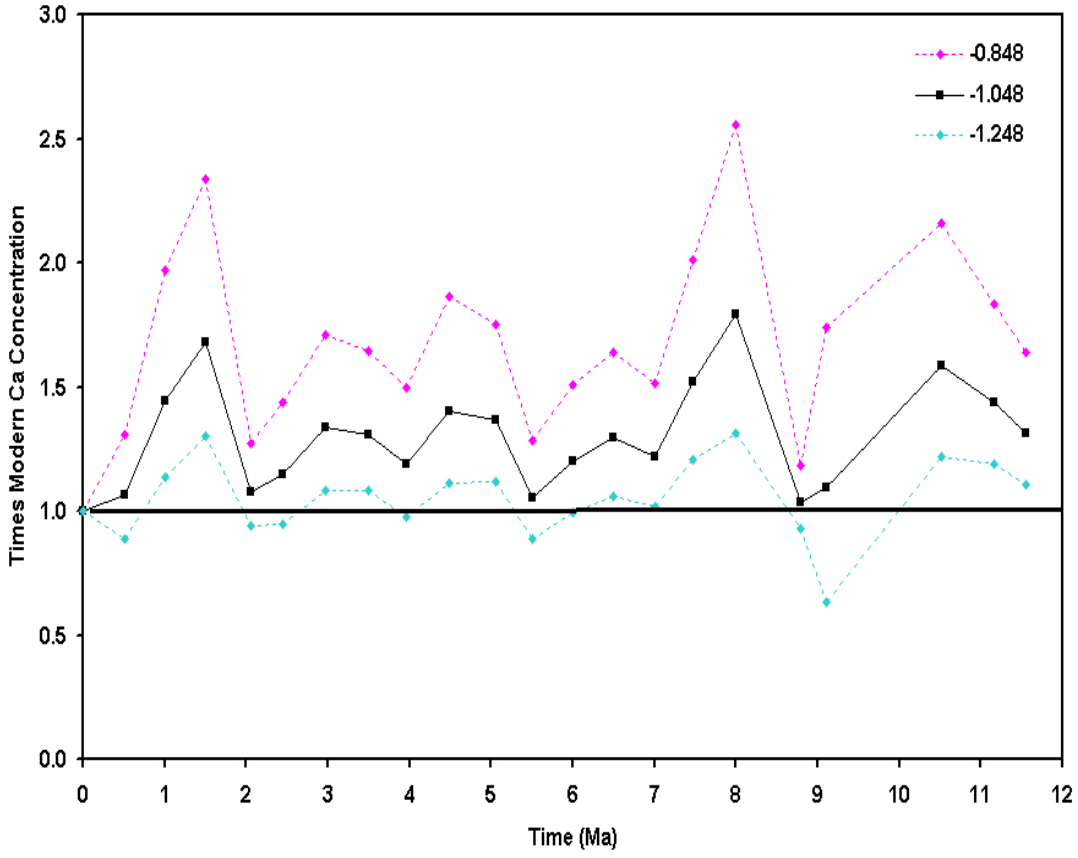

Figure 4.3.4b Calculated Ca concentrations from the F_{sed}/F_w ratio obtained from the $\delta^{44}Ca$ of carbonates. For δ_w of –1.048, the total range in Ca concentration for the last 12 Ma is 1.79 (present concentration to 1.79 times the present value). Choice of δ_w affects the shape of the concentration curve. The concentration of calcium in the oceans is highly variable for the last 12 Ma.

$\delta^{44}Ca$ values are closer, the imbalance between the fluxes is minimized, hence the range in concentration is smaller and vice versa. This record suggests that the calcium concentration of the oceans has not been constant at least for the last 12 Ma. The carbonate crash could be reflected by the large increase in concentration from 11.5 to 9 Ma, either as the result of an increase in the weathering flux of Ca or a dissolution event that injected Ca into the oceans. Neither can be ruled out based on Ca isotopes alone. The highest peak in concentration occurs at 7.99 Ma and the lowest concentration is the same as present day. Equally low concentrations also occurred at 8.7, 5.5, 2, and 0.5 Ma. Presumably these minima were due to excess sedimentation removing Ca from the oceanic pool and depositing it as carbonate rock on the ocean floor.

4.3.5 Site 850 Conclusions

A new calcium isotope record for the last 12 Ma was generated for sediments in the Eastern Equatorial Pacific on 500 kyr intervals. This study filled a gap in calcium isotope literature regarding the mass balance of Ca in the oceans. Previous studies, with the exception of Fantle and DePaolo (2005), focused on longer time scales with very wide sample spacing and showed a lack of data for the past 12 Ma. The ratio of Ca fluxes into and out of the ocean (F_{sed}/F_w) will remain constant if both fluxes are changing at the same rate, but will be greater or less than one if one flux exceeds the other. The data from this study show several trends that can be very loosely correlated to global oceanographic events in the Late Neogene and

Quaternary. There is no sustained increase or decrease in the $\delta^{44}Ca$ of seawater during the last 12 Ma, only short-lived excursions on the scale of 1-2 Ma towards lighter or heavier values with a total range in $\delta^{44}Ca$ of 0.86 per mil. This is in contrast to Sr and Os isotope data, which show a steady increase in the radiogenic isotope (^{87}Sr or ^{187}Os) in seawater for the last 12 Ma. The evolution to more radiogenic values in these other isotope systems could be due to weathering of radiogenic lithologies, not an overall increase in weathering intensity. Conversely, Sr and Os isotopes may actually record increased weathering intensity and flux of Sr, Os, and Ca to the oceans. However, Ca isotopes will not record this increased flux if they are sufficiently buffered by the carbonate sedimentation sink, such that no sustained increase in the concentration of Ca in the oceans can occur because of increased weathering input. If the Ca data are averaged on a 1 Ma interval, the total change in seawater isotopic composition is only 0.22 per mil, very close to the range of ± 0.20 per mil for a change in the lithology weathered on the continent. In this case, the small changes in the isotopic composition of seawater could be due to changes in the value of the weathering flux alone or a combination of a change in the weathering flux and δ_w. It is impossible to know based solely on Ca isotopes.

Throughout the entire record F_{sed}/F_w is biased towards values < 1.0 for δ_w < -1.048 per mil. For a weathering flux value greater than –1.048 per mil the system reaches or exceeds steady state (Fsed/Fw = 1) at 8.7, 5.5, 4, 2, and 0.5 Ma. The F_{sed}/F_w ratio for the last 12 Ma has a total range of 67%, with the largest excursion at 7.99 Ma indicating a short lived excess in carbonate sedimentation flux lasting less

than 1 Ma. The second largest excursion occurs from 2-0.5 Ma, but this time indicates excess weathering over sedimentation. The Ca data do not strongly support an influx of Ca (among other elements) to the oceans around the time of the sedimentation maximum in the latest Miocene and earliest Pliocene as is suggested by Pisias et al. (1995) and by Sr isotopic data from Hodell et al. (1989). The record does show a spike towards heavier values suggesting that the sedimentation maximum may have had a significant isotopic effect on the oceans, although Ca isotopes do not record an initial weathering pulse, only the sedimentation response. The δ^{44}Ca data from this study neither confirm nor contridict the conclusions of Derry and France-Lanord (1996), who used Sr isotopes in pedogenic clays as a proxy for weathering intensity and found an increase in weathering intensity but decrease in dissolved riverine Sr (and thus Ca) from 7-1 Ma in Tibetan rivers. No sustained decrease is seen in the Ca isotopic record from 7-1 Ma, however three spikes suggesting less weathering input occur during this interval.

Using the F_{sed}/F_w ratio, the concentration of Ca through the last 12 Ma was calculated for this study. For a δ_w –1.048 per mil, the range extends from the present day concentration to 1.79 times modern concentration. The curve is highly variable and suggests that over this time period the Ca concentration has rarely been stable. An increase in concentration occurs during the time of the late Miocene carbonate crash and could reflect either an increase in riverine Ca flux or an injection of light Ca to the oceans from massive dissolution of seafloor carbonates. Ca isotopes alone cannot distinguish between these possibilities. Ca concentrations calculated in this way

represent a maximum range, because the sedimentation flux is held constant at 3.2 * 10^{13} moles/year Ca and only the weathering flux is allowed to vary in response to changes in F_{sed}/F_w. Changes in the sedimentation flux would buffer the changes in the weathering flux and work to damp overall changes in concentration or isotopic composition of seawater. This is different from other isotopic proxies such as Os and Sr because there is no fractionation associated with deposition in marine sediments for those systems. Fractionation introduces an additional variable in mass balance calculations using Ca isotopes. In this record, variation in $\delta^{44}Ca$ is loosely correlated to the sedimentation maximum from 6.7-4.5 Ma and the carbonate crash from 11.2-9.0 Ma. However, excursions of similar magnitude are seen at times when there is no stratigraphic evidence for large changes in sedimentation. The use of calcium isotopes as a paleo-proxy for weathering intensity may be limited by the buffering effect of carbonate sedimentation in the oceans.

References

Birck, J.L. 1986. Precision K-Rb-Sr isotopic analysis: Applications to Rb-Sr chronology. Chemical Geology 56 pp.73-83

Blum, J.D., Gazis, C.A., Jacobson, A.D., Chamberlain, C.P. 1998. Carbonate versus silicate weathering in the Raikhot watershed within the High Himalayan Crystalline Series. Geology 26 (5) pp. 411-414

Braitsch, O. 1971. Salt deposits: their origin and composition. Springer-Verlag

Burke, W.H., Denison, R.E., Hetherington, R.B., Koepnick, R.B., Nelson, H.F., Otto, J.B. 1982. Variation of seawater $^{87}Sr/^{86}Sr$ throughout Phanerozoic time. Geology 10 pp. 516-519.

Clauzon, G., Suc, J-P., Gautier, F., Berger, A., Loutre, M-F. 1996. Alternate interpretation of the Messinian salinity crisis: Controversy resolved? Geology 24 (4) pp. 363-366

Compton, W., Oversby, V.M. 1969. Lead isotopic analysis using a double spike. Journal of Geophysical Research 74 (17) pp. 4338-4348

De La Roche, C., DePaolo, D. 2000. Isotopic evidence for variations in the marine calcium cycle over the Cenozoic. Science 289, 1176-1178

DePaolo, D. J. 2004 Calcium isotopic variations produced by biological, kinetic, radiogenic, and nucleosynthetic processes. Reviews in Mineralogy and Geochemistry, v.55, pp.255-288

Derry, L.A., France-Lanord, C. 1996. Neogene Himalayan weathering history and river $^{87}Sr/^{86}Sr$: impact on the marine Sr record. Earth and Planetary Science Letters 142 pp. 59-74

Elderfield, H., Schultz, A. 1996. Mid-ocean ridge hydrothermal fluxes and the chemical composition of the ocean. Annual Reviews of Earth and Planetary Science 24 pp. 191-124

Eugster, O., Tera, F., Wasserburg, G.J. 1969. Isotopic analyses of barium in meteorites and in terrestrial samples. Journal of Geophysical Research 74 (15) pp. 3897-3908

Eugster, H.P. 1971. The beginnings of experimental petrology. Science 173 pp. 481-489

Fantle, M.S., DePaolo, D.J. 2005. Variations in the marine Ca cycle over the past 20 million years. Earth and Planetary Science Letters 237 pp.102-117

Farrell, J.W., Raffi, I., Janecek, T.R., Murray, D.W., Levitan, M., Dadey, K.A., Emeis, K-C., Lyle, M., Flores, J-A., Hovan, S. 1995. Late Neogene sedimentation patterns in the eastern equatorial Pacific Ocean. Proceedings of the Ocean Drilling Program, Scientific Results, 138 pp. 717-756

Gale, N. H. 1970. A solution in closed form for lead isotopic analysis using a double spike. Chemical Geology 6 pp. 305-310

Garrels, R.M., Lerman A. 1981. Phanerozic cycles of sedimentary carbon and sulfur. Proceedings of the National Academy of Sciences, USA 78 (8) pp. 4652-4656

Garrison, R.E., Schreiber, B.C., Bernoulli, D., Fabricius, F.H., Kidd, R.B., Melieres, F. 1978. Sedimentary petrology and structures of Messinian evaporitic sediments in the Mediterranean Sea, Leg 42A, Deep Sea Drilling Project. Initial Reports of the Deep Sea Drilling Project 42 pp. 571-611

Gopalan, K., Macdougall, J.D., MacIsaac, C. 2006. Evaluation of a 42-43 double-spike for high precision Ca isotope analysis. International Journal of Mass Spectrometry 248 pp. 9-16

Gussone, N., Eisenhauser, A., Heuser, A., Dietzel, M., Bock, B., Bohm, F., Spero, H., Lea, D., Bijma, J., Nagler, T. 2003. Model for kinetic effects on calcium isotope fractionation (δ^{44}Ca) in inorganic aragonite and cultured planktonic foraminifera. Geochimica et Cosmochimica Acta 67 (7) pp.1375-1382

Hardie, L.A. 1967. The gypsum-anhydrite equilibrium at one atmosphere pressure. American Mineralogist 52 pp. 171-200

Hardie, L.A. 1996. Secular variation in seawater chemistry: an explanation for the coupled secular variation in the mineralogies of marine limestones and potash evaporites over the past 600 m.y.. Geology 24 (3) pp. 279-283

Harvie, C.H., J.H. Weare, L.A. Hardie, and H.P. Eugster. 1980. Evaporation of seawater: calculated mineral sequences. Science 208 pp. 498-500

Haymon, R.M., Fornari, D.J., Von Damm, K. L., Lilley, M.D., Perfit, M.R., Edmond, J.M., Shanks III, W.C., Lutz, R.A., Grebmeier, J.M., Carbotte, S., Wright, D., McLaughlin, E., Smith, M., Beedle, N., Olson, E. 1993. Volcanic eruption of the mid-ocean ridge along the East Pacific Rise crest at 9° 45-52'N: direct submersible

observations of seafloor phenomena associated with an eruption event in April, 1991. Earth and Planetary Science Letters 119 pp. 85-101

Heuser, A., Eisenhauer, A., Gussone, N., Bock, B., Hansen, B.T., Nagler, Th.F. 2002. Measurement of calcium isotopes ($\delta^{44}Ca$) using a multicollector TIMS technique. Journal of Mass Spectrometery 220 pp. 385-397

Hirt, B., Epstein, S. 1964. A search for isotopic variations in some terrestrial and meteoritic calcium. Transactions of the American Geophysical Union 45 p. 113

Hodell, D.A., Mueller, P.A., McKenzie, J.A., Mead, G.A. 1989. Strontium isotope stratigraphy and geochemistry of the late Neogene ocean. Earth and Planetary Science Letters 92 pp. 165-178

Hsu, K.J., Montadert, L., Bernoulli, D., Cita, M., Erickson, A., Garrison, R.E., Kidd, R.B., Melieres, F., Muller, C., Wright, R. 1977. History of the Mediterranean salinity crisis. Nature 267 pp. 399-403

Kasemann, S.A., Hawkesworth, C.J., Prave,A.R., Fallick, A.E., Pearson, P.N. 2005. Boron and calcium isotope composition in the Neoproterozoic carbonate rocks from Nambia: evidence for extreme environmental change. Earth and Planetary Science Letters 231 pp. 73-86

Kinsman, D.J.J. 1976. Evaporites: relative humidity control of primary mineral facies. Journal of Sedimentary Petrology 46 pp. 273-279

Krijgsman, W., Hilgen, F.J., Raffi, I., Sierro, F.J., Wilson, D.S. 1999. Chronology, causes and progression of the Messinian salinity crisis. Nature 400 pp. 652-655

Krishnaswami, S., Trivedi, J.R., Sarin, M.M., Ramesh, R., Sharma, K.K. 1992. Strontium isotopes and rubidium in the Ganga-Brahmaputra river system: Weathering in the Himalaya, fluxes to the Bay of Bengal and contributions to the evolution of oceanic $^{87}Sr/^{86}Sr$. Earth and Planetary Science Letters 109 pp. 243-253

Lemarchand, D., Wasserburg, G.J., Papanastassiou, D.A. 2004. Rate-controlled calcium isotope fractionation in synthetic calcite. Geochimica et Cosmochimica Acta 68 (22) pp. 4665-4678

Lyle, M., Dadey, K.A., Farrell, J.W. 1995. The late Miocene (11-8 Ma) eastern Pacific carbonate crash: evidence for the reorganization of the deep-water circulation by the closure of the Panama gateway. Proceedings of the Ocean Drilling Program, Scientific Results138 pp.821-838

Meijer, P.Th., Krijgsman, W. 2005. A quantitative analysis of the desiccation and re-filling of the Mediterranean during the Messinian Salinity Crisis. Earth and Planetary Science Letters 240 (2) pp. 510-520

Miller, K.G., Fairbanks, R.G., Mountain, G.S. 1987. Tertiary oxygen isotope synthesis, sea level history, and continental margin erosion. Paleoceanography 2 (1) pp. 1-19

Milliman, J.D. 1993. Production and accumulation of calcium carbonate in the ocean: budget of a non-steady state. Global Biogeochemical Cycles 7 (4) pp. 927-957

Molnar, P., England, P., Martinod, J. 1993. Mantle dynamics, uplift of the Tibetan Plateau, and the Indian Monsoon. Reviews of Geophysics 31 (4) pp. 357-396

Morris, E.J., Paytan, A., Bullen, T.D. 2005. Seawater calcium isotopes from marine barite: a potential record of carbonate deposition in the oceans. Geochimica et Cosmochimica Acta 69 (10) pp. 546

Nagler, T., Eisenhauer, A., Muller, A., Hemleben, C., Kramers, J. 2000. The δ^{44}Ca-temperature calibration on fossil and cultured globigerinoides sacculifer: new tool for reconstruction of past sea surface temperatures. Geochemistry Geophysics Geosystems 1 paper number 2000GC000091.

Nesteroff, W.D. 1973. Mineralogy, Petrology, Distribution, and Origin of the Messinian Mediterranean Evaporites. Initial Reports of the Deep Sea Drilling Project 13 pp. 673-694.

Nurnberg, D., Bijma, J., Hemleben, C. 1996. Assessing the reliability of magnesium in foraminiferal calcite as a proxy for water mass temperatures. Geochimica et Cosmochimica Acta 60 (5) pp. 803-814

O'Neil, J.R., Clayton, R.N., Mayeda, T.K. 1969. Oxygen isotope fractionation in divalent metal carbonates. Journal of Chemical Physics 51(12) pp. 5547-5558

Palmer, M.R., Edmond, J.M. 1989. The strontium isotope budget of the modern ocean. Earth and Planetary Science Letters 92 pp. 11-26

Peterson, L.C., Murray, D.W., Ehrmann, W.U., Hempel, P. 1992. Cenozoic carbonate accumulation and compensation depth changes in the Indian Ocean. *In* Duncan, R.A., Rea, D.K., Kidd, R.B., von Rad, U., Weissel, J.K. (Eds.), Synthesis of Results from Scientific Drilling in the Indian Ocean. Geophysical Monographs, American Geophysical Union, 70 pp. 311-333

Pisias, N.G., Mayer, L.A., Mix, A.C. 1995. Paleoceanography of the eastern equatorial Pacific during the Neogene: synthesis of Leg 138 drilling results. Proceedings of the Ocean Drilling Program, Scientific Results 138 pp. 5-21

Pierre, C., Rouchy, J.M. 1990. Sedimentary and diagenetic evolution of Messinian evaporites in the Tyrrhenian Sea (ODP LEG 107, Sites 652, 653, and 654): Petrographic, Mineralogical, and Stable Isotope Records. Proceedings of the Ocean Drilling Program, Scientific Results 107 pp. 187-201

Peucker-Ehrenbrink, B., Ravizza, G., Hofmann, A.W. 1995. The marine $^{187}Os/^{186}Os$ record of the past 80 million years. Earth and Planetary Science Letters 130 pp. 155-167

Quade, J., Roe, L., DeCelles, P.G., Ojha, T.P. 1997. The late Neogene $^{87}Sr/^{86}Sr$ record of lowland Himalayan rivers. Science 276 pp. 1828-1831

Ravizza, G. 1993. Variations of the $^{187}Os/^{186}Os$ ratio of seawater over the past 28 million years as inferred from metalliferous carbonates. Earth and Planetary Science Letters 118 pp. 335-348

Raymo, M.E., Ruddiman, W.F., Froehlich, P.N. 1988. Influence of late Cenozoic mountain building on ocean geochemical cycles. Geology 16 pp. 649-53

Remieka, P., Lindsay, L. 1992. Geology of Anza-Borrego: Edge of Creation. Sunbelt Publications Inc., San Diego

Richter F.M., DePaolo, D.J. 1988. Diagenesis and Sr isotopic evolution of seawater using data from DSDP 590B and 575. Earth and Planetary Science Letters 90 pp. 382-394

Richter, F.M., Rowley, D.B., DePaolo, D.J. 1992. Sr isotope evolution of seawater: the role of tectonics. Earth and Planetary Science Letters 109 pp. 11-23

Rouchy, J.M., Orszag-Sperber, F., Blanc-Valleron, M.M., Pierre, C., Riviere, M., Combourieu-Nebout, N., Panayides, I. 2001. Paleoenvironmental changes at the Messinian-Pliocene boundary in the eastern Mediterranean (southern Cyprus basins): significance of the Messinian Lago-Mare. Sedimentary Geology 145 pp. 93-117

Russell, R. D. 1971. The systematics of double spiking. Journal of Geophysical Research 76 (20) pp. 4949-4955

Russell, W., Papanastassiou, D., Tombrello, T. 1978. Ca isotope fractionation on the earth and other solar system materials. Geochimica et Cosmochimica Acta 42 pp. 1075-1090

Ryan, W.B.F. 1973. Geodynamic Implications of the Messinian Crisis of Salinity. in Drooger,C.W., ed., Messinian Events in the Mediterranean: Amsterdam, North Holland, pp. 26-38

Schmitt, A-D., Stille, P., Vennemann, T. 2003a. Variations of the 44Ca/40Ca ratio in seawater during the past 24 million years: Evidence from δ44Ca and δ18O values of Miocene phosphates. Geochimica et Cosmochimica Acta 67 (14) pp. 2607-2614

Schmitt, A-D., Chabaux, F., Stille, P. 2003b. The calcium riverine and hydrothermal isotopic fluxes and the oceanic calcium mass balance. Earth and Planetary Science Letters 213 (3-4) pp. 503-518

Shackleton, N.J., Crowhurst, S., Hagelberg, T., Pisias, N.G., Schneider, D.A. 1995. A new late Neogene time scale: application to Leg 138 sites. Proceedings of the Ocean Drilling Program, Scientific Results 138 pp. 73-101

Sime, N.G., De La Rocha, C., Galy, A. 2005. Negligible temperature dependence of calcium isotope fractionation in 12 species of planktonic foraminifera. Earth and Planetary Science Letters 232 (1-2) pp. 51-66

Skulan, J., DePaolo, D., Owens, T. 1997. Biologic control of calcium isotopic abundances in the global calcium cycle. Geochimica et Cosmochimica Acta 61 (12) pp. 2505-2510

Sonnenfeld, P. 1984. Brines and Evaporites. Harcourt, Brace, Jovanovich

Stahl, W., Wendt, I. 1968. Fractionation of calcium isotopes in carbonate precipitation. Earth and Planetary Science Letters 5 pp. 184-186

Stanley, S.M., Hardie, L.A. 1998. Secular oscillations in the carbonate mineralogy of reef-building and sediment-producing organisms driven by tectonically forced shifts in seawater chemistry. Palaeogeography, Palaeoclimatology, Palaeoecology 144 pp. 3-19

Steiger, R.H., Jaeger E. 1977. Subcommission on geochronology: convention on the use of decay constants in geo- and cosmochronology. EPSL 36 pp. 359-362

Veizer, J. 1989. Strontium isotopes in seawater though time. Annual Review of Earth and Planetary Science 17 pp. 141-167

Vidal, L., Bickert, G., Wefer, G., Rohl, U. 2002. Late Miocene stable isotope stratigraphy of SE Atlantic ODP Site 1085: Relation to Messinian events. Marine Geology 180 pp. 71-85

Warren J. 1999. Evaporites: Their Evolution and Economics. Blackwell Science Ltd., 438 p.

Weijermars, R. 1988. Neogene tectonics in the Western Mediterranean may have caused the Messinian Salinity Crisis and an associated glacial event. Tectonophysics 148 pp. 211-219

Yechieli, Y., W.W. Wood 2002. Hydrogeologic processes in saline systems: playas, sabkhas, and saline lakes. Earth and Planetary Science Letters 58 pp. 343-365

Zhu, P. 1999. Calcium isotopes in the marine environment. Doctoral Dissertation University of California San Diego

Zhu, P., Macdougall, J.D. 1998a. Calcium isotopes in the marine environment and the oceanic calcium cycle. Geochimica et Cosmochimica Acta 62 pp. 1691-1698

Zhu, P., Macdougall, J.D. 1998b. Variation of marine carbonate $^{44}Ca/^{40}Ca$ ratio from c.a. 3.4 Ga ago to the present. EOS Trans. AGU 79 F413